A.Yu.Manakov, A.S.Stoporev
Russ. Chem. Rev., 2021, **90** (5) 566 – 600

https://doi.org/10.1070/RCR4986

Physical chemistry and technological applications of gas hydrates: topical aspects

Andrey Yu. Manakov,[a, b] Andrey S. Stoporev [a, b, c]

[a] *Nikolaev Institute of Inorganic Chemistry, Siberian Branch, Russian Academy of Sciences, prosp. Akademika Lavrentieva 3, 630090 Novosibirsk, Russian Federation*
[b] *Novosibirsk State University, ul. Pirogova 2, 630090 Novosibirsk, Russian Federation*
[c] *Kazan (Volga Region) Federal University, ul. Kremlevskaya 18, 420008 Kazan, Russian Federation*

The review considers the research and engineering works in selected fields of the physical chemistry of gas hydrates and gas hydrate technologies, mainly performed over the last 10 – 15 years. Data on the hydrate structures are given, including the structures formed during phase transitions at low temperatures, and on new hydrate structures that are formed under ultra-high pressures. The dynamics of guest and host subsystems is considered in brief. Phase diagrams of systems involving hydrate formation (in particular, in some porous media) and methods for calculating phase equilibria and compositions of hydrates in these systems are analyzed. Data on the hydrates formed by 'non-classical' hydrate formers (alcohols, amines, ammonia, *etc.*) studied in the last decade and on some of their properties are presented. The Section devoted to hydrate formation kinetics addresses the effect of compounds dissolved in water (surfactants, low-dosage inhibitors) and catalysts on this process. The hydrate growth dynamics on the water surface and hydrate decomposition-formation processes in disperse systems are discussed. Among technological applications, the attention is focused on gas storage and transportation in the hydrate form. Methods for the preparation of hydrates are considered.
The bibliography includes 618 references.

Contents

1. Introduction 566
2. The structure of gas hydrates 569
   2.1. Structural types of gas hydrates 569
   2.2. Dynamics of host and guest subsystems in hydrates 571
   2.3. Compositions of gas hydrates and occupancies of hydrate cavities 571
   2.4. Gas hydrates at high pressure 572
3. Phase equilibria of hydrate-forming systems 573
4. Properties of hydrates 577
5. Hydrates formed by 'non-classical' hydrate formers 578
6. Hydrate formation kinetics 579
   6.1. Catalysts for hydrate formation 579
   6.2. Formation of hydrates from water dispersed in various media 580
   6.3. Effect of admixtures dissolved in water on the growth of gas hydrates 580
   6.4. Some features of hydrate growth and morphology 581
   6.5. Gas hydrate dynamics in systems containing liquid hydrocarbons 582
7. Technological applications of gas hydrates 586
   7.1. Natural gas storage and transportation 586
   7.2. Separation of mixtures using gas hydrates 587
   7.3. Other gas hydrate technologies 588
   7.4. Preparation methods of gas hydrates 589
   7.5. Formation of hydrates from amorphous layers under cryogenic conditions 590
8. Note added in proof 590
9. Conclusion 590
10. List of acronyms and designations 591

1. Introduction

The structure of gas hydrates (GHs) consisting of two subsystems, the host and guest ones, represents a framework of hydrogen-bonded water molecules with internal cavities of up to 10 Å in size, which can be completely or partly filled with guest atoms (molecules) of inert gases or lower hydrocarbons, Freons, some organic solvents, *etc.* Host framework water molecules and guest atoms (molecules) interact mainly *via* van der Waals forces. In appearance, gas hydrates resemble ice. Most often, gas hydrates exist below room temperature and at pressures above several megapascals. The formation/dissociation of one hydrate volume is accompanied by absorption/release of up to 170 volumes of the gas (under standard conditions). Several publications [1 – 6] summarize a large array of information on GHs.

Gas hydrates were discovered by Humphry Davy in 1810, who obtained chlorine hydrate. Also, it is quite likely that sulfur dioxide hydrate was prepared by Joseph Priestley back in 1777 – 1778. Practical interest in these compounds was expressed in the mid-1930s, when it was found that gas hydrates that formed in pipelines operating in Alaska can block up gas supply and give rise to emergency situations. At the end of the 20th century, gas hydrates were recognized as a promising source of hydrocarbons, on the one hand, but started to bring about more and more problems for oil and gas production and transportation (which still remain relevant) due to intensification of the production under conditions favourable for hydrate formation, on the other hand. All this resulted in the explosive growth of the number of publications on this subject (Fig. 1).

Received 25 July 2020
© 2021 Uspekhi Khimii, ZIOC RAS, Russian Academy of Sciences and IOP Publishing Limited

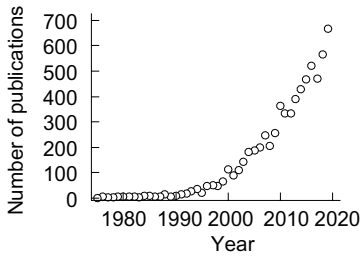


Figure 1. Change in the number of publications with time. The dependence was plotted on the basis of query 'Gas Hydrate' for the Web of Science Core Collection database. A considerable part of relevant publications are not found by this query; therefore, the actual number of publications may be ~1.5 times higher.

There are large natural accumulations of GHs.[2, 7, 8] They were discovered ~60 years ago. The first sample of natural gas hydrate was taken during an expedition to the Black Sea (1972). The history of the discovery and studies of gas hydrates was described in a number of publications.[9–12] Among the substances present in the upper layer of Earth's crust, GHs are most sensitive to pressure and temperature changes, and even minor variations of these parameters can affect the formation/dissociation of gas hydrates. Natural GHs exist at pressures and temperatures that ensure their stability and where water occurs in contact with a hydrate former, either free or dissolved in water. These conditions are met near the sea or ocean floor and at the bottom of deep lakes, and also in permafrost areas and adjacent cold rocks on land (Fig. 2). It is known that the pressure at a certain depth is close to (in the rock) or is equal to (in aquatic areas) the hydrostatic pressure, *i.e.*, to the pressure of a water column of the same height. In aquatic areas, the temperature always decreases from the surface towards the floor, while below the floor the temperature rises according to the geothermal gradient. On land, the temperature always increases with depth, but the absolute temperatures in permafrost areas are much lower than those without it. These features account for the presence of a range of depths in which the temperature and pressure conditions ensure stability of gas hydrates (see Fig. 2). This range of depths is referred to as the hydrate stability zone (HSZ). In water areas, this zone can cover some of the water layer, but hydrates can exist in water only at a sufficient concentration of the hydrate former.

Gas hydrates can be present at depths of >250 m in cold water areas if the near-bottom temperature is close to 0 °C and at depths of >500 – 700 m in warm waters. The height of the subaqueous hydrate existence zone reaches

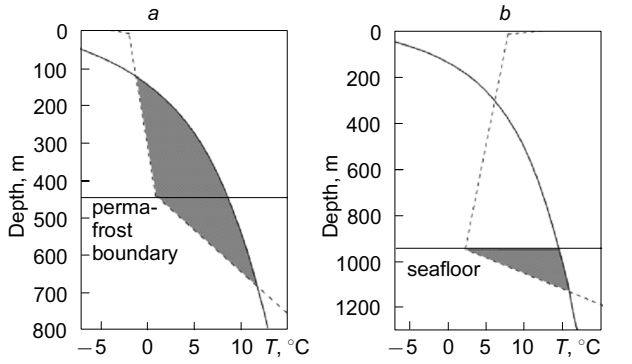


Figure 2. Examples of hydrate stability zones (HSZ) in permafrost (*a*) and in water areas (*b*). The dashed line corresponds to the temperature at the given depth. The continuous curve corresponds to the equilibrium temperature of hydrate formation at the hydrostatic pressure and at a given depth; HSZ is highlighted in dark. The Figure was prepared by the authors using the data of Refs 2 and 4.

1 km, while in permafrost, it can vary from 400 m to 1 km (and more); the upper boundary of HSZ occurs at a depth of ~250 m.[2, 4, 7, 8] The most gas-rich accumulations of hydrates are located at a rather large depth below the seafloor. In these accumulations, hydrates normally exist as 'cement' sticking together the sedimentary rock particles, which behaves, in this case, as a frozen rock even at temperatures above 0 °C.

The existence of hydrate accumulations at moderate depths below the seafloor requires constant supply of a gas that creates a sufficient gas concentration in the near-bottom layer of water and in interstitial water; therefore, near-bottom hydrates (located directly on the seafloor or several metres below the seafloor) are accumulated at the sites of discharge of gas-saturated fluids (mud volcanoes, gas seeps, *etc.*). If the gas supply ceases, the hydrate is dissolved in water because of gas diffusion to the water layer. Owing to low pressure of the overlying rocks in the near-bottom layers, the GH inclusions may have a variety of forms such as monolithic layers of various thickness and orientation, small lenses and intricately shaped inclusions. It is assumed that the permafrost above HSZ can accommodate relic gas hydrates, which appeared during the cold climate period and have been retained until now owing to the self-preservation effect.[2] Upon mechanical or thermal impact, they rapidly decompose to give off large gas volumes. This may give rise to unexpected gas seeps during drilling at small depth, heaving mounds and rock blow-outs (like the known Yamal crater †).[13] The major component of natural hydrates is methane (up to 98 – 99% for hydrate formation from biogenic gas). In the case of hydrate formation from the thermogenic gas, the hydrates can contain C_2H_6, C_3H_8, CO_2, H_2S, N_2 and some other components,[4] the total content of which can amount to several tens of percent.

Gas hydrate accumulations have been found in the continental shelves of all continents, in the permafrost regions of Eurasia and North America (see, for exam-

A.Y.Manakov. Doctor of Chemical Sciences, Chief Researcher at the NIIC SB RAS, Associate Professor at the NSU.
E-mail: manakov@niic.nsc.ru
Current research interests: structures, compositions, properties and applications of gas and clathrate hydrates, phase equilibria and transitions in hydrocarbon systems.
A.S.Stoporev. PhD, Senior Researcher at the NIIC SB RAS and the KFU, Assistant at the NSU.
E-mail: stopor89@bk.ru
Current research interests: study of the nucleation, growth and decomposition of gas and clathrate hydrates.

Translation: Z.P.Svitanko

† The Yamal crater is a round pit with a diameter of ~20 m and a depth of more than 50 m surrounded by ejected rock debris. The crater formed for no apparent cause at the central part of the Yamal peninsula in 2013 or 2014.

ple[8, 11, 14 – 18] and references cited therein) and in the sediments of the Baikal lake.[19] The amounts of hydrate gas estimated by various authors differ by five orders of magnitude.[17] Currently, a value of $\sim 10^{15}$ m^3 is the most realistic estimate for marine gas hydrates, which is an order of magnitude greater than the proven natural resources in traditional type deposits; the minimum value derived from the data on explored gas hydrate accumulations is 2×10^{14} m^3 (Ref. 20). Most of the gas occurs in deep-water accumulations; the gas volume in the near-bottom hydrates is estimated as $\sim 10^{13}$ m^3 (Refs 17, 20). The amount of gas in hydrates in the permafrost regions of Russia is estimated as 7.2×10^{12} to 1.7×10^{13} m^3 (Ref. 7), while the global amount of gas in permafrost-associated gas hydrates is $\sim 3.5 \times 10^{13}$ m^3 (Ref. 21). More recent estimates for Russia are markedly higher: 3.2×10^{14} m^3 for permafrost regions and 1.5×10^{14} m^3 for adjacent seas.[22] The natural GH accumulations occurring in Russia and in adjacent seas have been little studied; however, in recent years, research along this line has been in progress (see, for example, Refs 23 – 25).

Currently, four key methods are considered for gas production from hydrate accumulations:[26, 27]

— lowering of the reservoir pressure below the equilibrium value for GHs,

— heating of the reservoir above the GH equilibrium temperature,

— injection of thermodynamic inhibitors (brines, methanol, *etc.*), which cause gas hydrate decomposition, into the accumulation,

— replacement of methane in the hydrate by carbon dioxide.

Heating can be accomplished, for example, by injecting hot water into the hydrate reservoir. Methanol and salt solutions are injected into the hydrate reservoir as inhibitors. The depressurization method implies pumping-out of the gas, for example, from the gas permeable rock underlying the gas hydrate accumulation. The hydrate decomposes due to the pressure drop in the adjoining rocks below the equilibrium pressure. This method is considered as the most promising. Decomposition of the hydrate is accompanied by cooling of the reservoir; therefore, additional heating is required. In the replacement method, carbon dioxide, or a CO_2 mixture with nitrogen, is injected into the reservoir. After completion of the exchange reaction, the methane-rich gas can be extracted. An advantage of this method is the simultaneous disposal of considerable amounts of carbon dioxide.

It is recognized that gas production from natural gas hydrates started in the Messoyakha field in Western Siberia in 1972. Experiments on gas production from GH accumulations in permafrost rocks were carried out in 2002 – 2009 at the Mallik gas hydrate site in the Mackenzie river delta region (North Canada). Heating and depressurization methods were used. A pilot production of the gas from the submarine GHs by the depressurization method was carried out near the south-east coast of Japan (the eastern part of the deep-sea Nankai trough) in 2013 and 2017. The longest stable production time was 24 days; the experiments had to be stopped because the well was plugged with sand and/or the forming ice. In 2012, a successful field experiment on hydrate gas production by the replacement method in combination with the depressurization method was carried out in the USA. In 2017, the Geological Survey of China performed two successful tests in the South China Sea on gas production from GH accumulations in clay rocks, most difficult to develop. Original methods for the production were used:

— considerably modified depressurization method (no details were reported),

— crushing and carrying over of the hydrate-bearing rock from the formation.

The first method resulted in stable production for 60 days and the total amount of produced gas was 3.09×10^5 m^3. Detailed information on these tests can be found in a number of publications.[16, 17, 26, 28 – 32] It is noteworthy that a procedure similar to the latter one was first tested in the near-bottom hydrates of the Baikal lake during a Japanese – Russian expedition.[33] Currently, the gas production from gas hydrates is economically unprofitable. However, it can be assumed that gaining more in-depth knowledge about natural hydrates and improvement of production technology would change this situation in the foreseeable future.[17] This is especially likely for the countries that have no conventional hydrocarbon resources. For example, recently the results of implementation of the second gas hydrate program of India were released to the public. During implementation of this program, large GH accumulations suitable for industrial development were found (see Ref. 34 and other papers in this issue of the journal).

It is noteworthy that the areas of occurrence of natural gas hydrates are not limited to those considered above. For example, inclusions of GHs formed by air gases were found in the Antarctic ice sheet.[35 – 37] There are grounds to suggest the presence of GHs on some planets and satellites of the Solar System[8 – 40] and comets.[41] Apart from the resource aspect, the scientific community actively discusses the possible participation of natural GHs in global climatic processes.[42, 43] It was noted that the release of methane from natural gas hydrate accumulations that decompose due to global warming may lead to acceleration of the warming, but the magnitude and time period of this process are now difficult to evaluate. An interesting review of a broad range of issues related to possible risks of development of offshore gas hydrate fields was published by Wang *et al.*[44]

As noted above, in recent years, more than a thousand publications devoted to various gas hydrate issues have appeared annually. Therefore, writing of a review that would cover the whole research area of GHs in any detail is almost impossible. In the present review, the attention is focused on various aspects of physical chemistry and some of the developing industrial applications of gas hydrates. The appearance of a large number of reviews devoted to GHs in recent years allows the authors to choose new and the most interesting original publications. References to recent review publications are given for more in-depth acquaintance with one or another topic. Some important and intensively developing areas of gas hydrate research remain almost beyond the scope of this review. References to papers and monographs that are meant to fill this gap to some extent are given below. Molecular modelling studies and theoretical calculations of gas hydrates are integrated in Refs 45 – 49. The issues concerning thermodynamic simulation of gas hydrates are discussed in monographs[2, 4] and in some papers (*e.g.*, Ref. 50). We also do not consider the problems of preventing gas hydrate formation during oil and gas production,[1, 4, 51, 52] geophysics and geochemistry of GH-containing natural and artificial cores and physicochemical aspects of formation of natural GHs. Some infor-

mation on these subjects can be found in reviews.[53 – 57] We also do not consider the intensively developing physical chemistry of ionic clathrate and semiclathrate hydrates, which are related to gas hydrates. This subject is covered, for example, in Refs 12 and 58.

2. The structure of gas hydrates

2.1. Structural types of gas hydrates

The crystalline framework of GHs can be represented as a combination of face-sharing polyhedral cavities, with vertices being occupied by the oxygen atoms of water molecules and edges being formed by hydrogen bonds. The angles between hydrogen bonds can vary from 90 to 120°, but in most cases, they are close to tetrahedral angles. The cavities with 12 (*D* and *D′*), 14 (*T*), 16 (*H*) and 20 (*E*) faces are encountered most often (Fig. 3). Type *D* and *D′* cavities are usually called small, while *T*, *H* and *E* cavities are large. If the guest molecule located in a host cavity has polar groups, hydrogen bonds can arise between the guest and the host, which affects the dynamics of both guest and host molecules (see below). At moderate (up to 50 MPa) pressures, each cavity is normally occupied by a single guest molecule. The vast majority of GHs correspond to three types of structures: cubic I (sI), cubic II (sII) and hexagonal III (sH). The packings of polyhedral cavities and crystallographic parameters of hydrate frameworks are presented in Fig. 4 and in Table 1, respectively. The structures of GHs and ionic and semiclathrate hydrates have been described in detail.[4, 12, 59] The type of hydrate formed by single guest components (below referred to as simple GHs) is determined by the size of the guest molecule (see Table 1). The gas hydrates with two or more different guest molecules are called double or mixed, respectively. If components of a mixture form hydrates of the same structural type, a double or mixed hydrate may represent a continuous solid solution of this structural type. For example, mixtures of CH_4 and CO_2 form sI hydrates at any component ratio; the corresponding structural data were reported by Everett *et al.*[60] The structural type of hydrate formed from a mixture of methane and ethane depends on their ratio in the initial mixture. When the methane content is 61 – 93%, sII hydrates are formed, while other methane contents lead to sI hydrates.[61 – 63] It was found that the interconversion between double sI and sII methane – ethane hydrates occurs *via* their decomposition.[64]

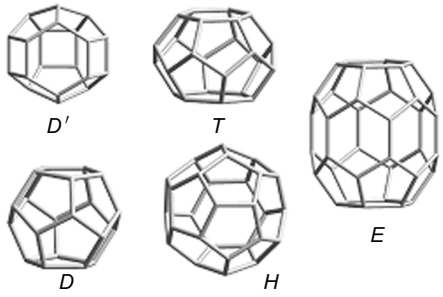


Figure 3. Typical cavities in the water clathrate frameworks. The space accessible for the inclusion of guest molecules for *D*, *D′* and *H* cavities is close to spheres with diameters of 5.3, 5.2 and 6.6 Å, respectively. In the case of the *T* cavity, the space is a flattened spheroid with diameters of 6.4 and 5.3 Å; for the *E* cavity, it is prolate spheroid with diameters of 9.6 and 7.3 Å. Adapted by the authors with the permission of Elsevier.[12]

Depending on the composition of a mixture the components of which form hydrates of different structures, double hydrates of various structural types are formed. For example, it was shown[65] that mixtures of carbon monoxide (sI hydrate) and nitrogen (sII hydrate) form sI hydrate when the CO content in the initial mixture is >35% and sII hydrate at lower CO content in the mixture. In sII hydrates with large guest molecules, all small cavities remain vacant (the size of guest molecules precludes filling these cavities, see Table 1). In this case, double hydrates with smaller molecules are easily formed. Depending on the conditions of hydrate preparation, some of small molecules can enter large cavities. For example, the addition of fractions of a percent of propane to methane results in the formation of double sII hydrate, instead of sI hydrate formed in the case of pure methane.[4] At moderate pressures, only double hydrates exist as the sH structural type (see Table 1);[4] in this case, large *E* cavities of the framework are occupied by large molecules (most often, those forming no simple hydrates by themselves). Small cavities accommodate molecules of so-called auxiliary components (H_2S, Xe, CH_4).

The unit cell parameters of GHs depend on the temperature, pressure and type of guest molecules. The compressibility[66] and thermal expansion[67, 68] coefficients of hydrates in the temperature and pressure ranges suitable

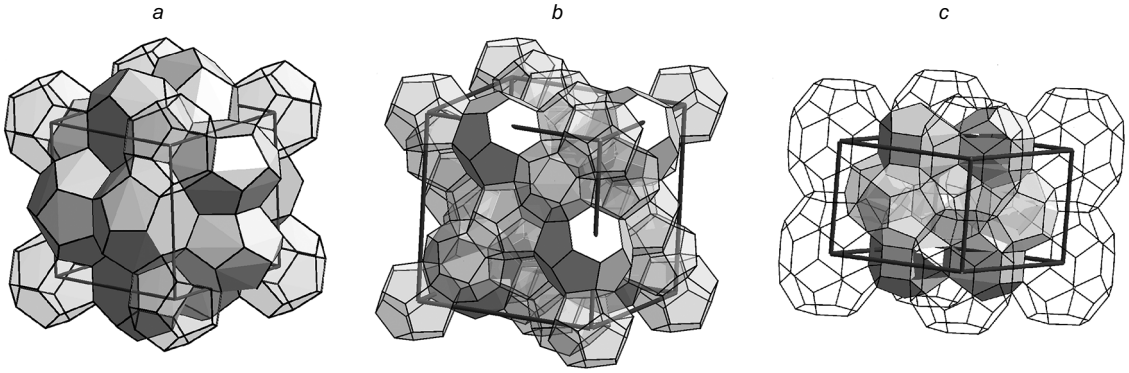


Figure 4. Schematic view of sI (*a*), sII (*b*) and sH (*c*) frameworks. The polyhedra in Figs *a* and *b* designate large cavities (*T* and *H*, respectively); in Fig. *c*, they mark small cavities (*D* or *D′*); parallelepipeds correspond to unit cells.[12] Adapted by the authors with the permission of Elsevier.

Table 1. Characteristics of the most frequent structures of water frameworks of gas hydrates.[2, 4, 12]

Structure	Unit cell			Size of the guest molecule, Å	Examples of guest molecules	*n* (see [c])
	space group	formula [a]	parameters, Å (see [b])			
sI	$Pm\bar{3}n$	$6\,T\cdot 2\,D\cdot 46\,H_2O$	$a = 12.0$	4.3 – 5.8	CO, CH_4, H_2S, CO_2, SO_2, Xe, C_2H_6 cyclo-C_3H_6, Cl_2, N_2O	form 5.75 (see [e]) to 7.67 (see [d])
sII	$Fd\bar{3}m$	$8\,H\cdot 16\,D\cdot 136\,H_2O$	$a = 17.1$	3.5 – 4.2 5.8 – 7.2	Ar, Kr, N_2, O_2 CCl_4, $CHCl_3$, CH_2Cl_2, cyclo-C_3H_6, cyclo-C_5H_{10}, C_3H_8, SF_6, CCl_2F_2, tetrahydrofuran, dioxolanes, dioxanes, acetone	to 5.67 (see [e]) 17 (see [d])
sH	$P6/mmm$	$E\cdot 2\,D'\cdot 3\,D\cdot 34\,H_2O$	$a = 12.3$, $c = 10.2$	7.2 – 9.0	adamantane + Xe, methylcyclohexane + CH_4, 2,2-dimethylpentane + H_2S	34 (see [f])

[a] The formula of the unit cell includes the number of cavities of different types and water molecules in one unit cell.
[b] The range of sizes of guest molecules that form this structure at moderate pressures. [c] The hydration number (*n*) is the number of water molecules per guest molecule. [d] Large cavities are singly occupied. [e] Large and small cavities are singly occupied. [f] At moderate pressures, they exist only as double hydrates with guest molecules of appreciably different sizes; the formula contains one large guest molecule per 34 water molecules; the occupancy of small cavities is variable and can reach 100% (5 per 34 water molecules).

for practical applications are rather similar, although the unit cell parameters differ. The unit cell parameters are mainly determined by the type of guest molecules in large framework cavities, *i.e.*, by the larger molecules. The variation of the size of cavities of sII framework as a function of the size of the cyclic guest molecule they accommodate was studied by Takeya *et al.*[69] A nearly linear increase in the size of the cavity with increasing unit cell parameters of the hydrate was found. Regarding the framework compressibility, at pressures up to 50 MPa, the V/V_0 ratio (V is the unit cell volume at a given pressure, V_0 is the unit cell volume at a 'zero' pressure) decreases, on average, by 0.11% upon pressure increase by every 10 MPa. The linear thermal expansion coefficients at -73 °C are 77×10^{-6} and 52×10^{-6} K^{-1} for the sI and sII frameworks, respectively.

Examples of clathrate hydrates with structures other than those considered above are rare. It was shown [70] that dimethyl ether clathrate hydrate has an unusual trigonal structure in which the ratio of the numbers of large and small cavities is the highest among hydrate structures. An sII hydrate is also formed in this system.[71] Apparently, the change in the structural type is due to the features of the host – guest interaction. In a very interesting structural study, Dobrzycki *et al.*[72] detected and structurally studied seven (!) *tert*-butylamine hydrates with hydration numbers from 1/4 to 17. This series of hydrates is a unique example demonstrating transition from typical lower hydrate structures, in which the organic molecules are hydrogen-bonded to the water framework, to a typical clathrate sII structure (heptadecahydrate) with weak host – guest hydrogen bonding. The intermediate structures are semi-clathrates, and the structure of the undecahydrate is similar to the structure of the dimethyl ether hydrate, which was previously considered unique. Bromine forms a tetragonal hydrate; this structure is often encountered among hydrates of tetra-n-butylammonium salts.[73] The presence of other hydrates, in particular sII, in the bromine – water system also cannot be ruled out.[74] Stabilization of the unusual hydrate structure was attributed to the specific oxygen – dihalogen interactions.[75, 76] Note that chlorine interacting in a similar way forms a usual sI hydrate.

The hydrate framework can adjust itself to a change in the external conditions (temperature and pressure). The effect of pressure is considered below. The change in the framework upon lowering the temperature has been rather little studied. Udachin *et al.*[77] detected a phase transition, taking place on lowering the temperature, of the cyclooctane hydrate with the sH structure to a hydrate with the sH superstructure and a lower symmetry. The double hydrate with the sII structure formed by propan-2-ol and methane is converted to a tetragonal structure upon the decrease in temperature.[78] It is of interest that an analogous hydrate formed by propan-1-ol does not show this phase transition.

It is known that only several types of molecules can be incorporated into the water frameworks of ices and hydrates; examples of such molecules are ammonium fluoride and hydrogen fluoride. In the last decade, quite a few studies have been devoted to modification of the hydrate framework with ammonium fluoride.[79, 80] Earlier, this type of inclusion was demonstrated for ionic hydrates.[81] In the case of a mixed water + ammonium fluoride framework, even the hydrates of pure methanol and diols were prepared, which is impossible in the case of a purely water framework.[79, 80] It is evident that the hydrate is no longer clathrate in this case; it should rather be classified as an ionic hydrate. Park *et al.*[82] succeeded in incorporating ammonium fluoride (ion pair) into the methane hydrate framework; this was accompanied by pronounced destabilization of the hydrate. The ammoniun cation was located in the cavity. Bando and Sugahara [83] reported the formation of an unusual double hydrate formed by ethane and ammonium bromide, and Seol *et al.*[84] described the incorporation of ion pairs of methanesulfonate and sodium sulfamate in propane hydrate cavities.‡

‡ In A.Yu.Manakov's opinion, the results of Refs 83 and 84 need to be verified and corrected.

2.2. Dynamics of host and guest subsystems in hydrates

The dynamics of reorientation of water molecules in the hydrates resembles that in the ice I_h § and is related to the formation of Bjerrum defects, *i.e.*, rotations of water molecules, resulting in either the absence of a proton or the presence of two protons in the hydrogen bond. When the guest molecules are nonpolar, the activation energy for the defect formation is about 50 kJ mol^{-1}; if the guest molecules are polar and can form hydrogen bonds with the water framework, the activation energy is 20–30 kJ mol^{-1} (see, for example, Ref. 85). When the temperature is below −163 °C, reorientation of water molecules in the framework is almost terminated. In conventional hydrates, the proton disorder of the framework is 'frozen' in this case; near the absolute zero, the framework has a high entropy. A different situation arises if the hydrate framework is doped with a minor ($\leqslant$0.1 mol.%) amount of KOH. The dopant catalyzes the phase transition, related to the proton ordering, which takes place at −200 °C;[86] this may be caused by the unusual mechanism of migration of hydroxide ions in the water framework.[87] In the tetrahydrofuran (THF) hydrate, the proton ordering in the framework is accompanied by ordering of the guest in the cavity;[88] a partial ordering of the guest at low temperatures is known only for the proton-disordered framework of the trimethylene oxide hydrate.[89] The effect of hydrogen bonding between the hydrate framework and the *tert*-butylamine and pinacolone guest molecules on the dynamics of water molecules in the framework is discussed, for example, in the study of Alavi *et al.*[90]

The dynamics of guest molecules in the hydrate cavities is studied by dielectric methods, NMR spectroscopy and X-ray diffraction. If the cavity is larger than the guest molecule, the molecule is almost free to move inside the cavity; this is the case for methane molecules in the sI structure cavities even at −271 °C.[91] If the size of the molecule approaches one of the characteristic dimensions of the cavity, the arrangement and movement of the molecule are subject to restrictions. In the case of a larger bromomethane molecule in the hydrate with the same structure, the guest reorientation in the cavity is activated only at −173 °C; the activation energy of reorientation is 4.2 kJ mol^{-1} (Ref. 92). The centre of mass of a carbon dioxide molecule in an ellipsoidal *T* cavity (a greater diameter is in the equatorial plane) is close to the centre of the cavity, the molecule is rotated around a fourfold axis somewhat inclined to the equatorial plane, while the axial position is free.[93] In sI hydrates, the CH_3F, CH_2F_2 and CHF_3 molecules are arranged in a similar way (near the equatorial plane of a large cavity).[94] The CF_4 molecule is located in the cavity isotropically, which leads to a stepwise increase in the unit cell parameter of the hydrate.[94] In a series of molecules of the same type, the activation energy for reorientation increases with increasing ratio between the sizes of the guest molecule and the occupied cavity. Indeed, in the sulfur hexafluoride–selenium hexafluoride–neopentane series (all molecules occupy the large cavity of structure II), the activation energies for reorientation are 0.56, 0.9, and 3.106 kJ mol^{-1}, respectively.[95]

Comparison of the dynamics of guest and host molecules depending on the size and polarity of cyclic guest molecules (trimethylene oxide, cyclopentane, tetrahydropyran, 1,3-dioxolane and 1,4-dioxane) was reported by Nelson *et al.*[96] In particular, it was shown that for polar guest molecules, the potential barrier for reorientation is proportional to the size of the molecule. The degree of effect of the host–guest hydrogen bond on the properties of the hydrate depends on the strength of this bond. Ahn *et al.*[97] reported a structural study of sII double hydrates formed by oxygen with THF or 3-hydroxytetrahydrofuran. In the case of pure THF, no indications of hydrogen bonding with the framework was detected down to −173°C, although it is known from earlier studies that 'instantaneous' hydrogen bonds are formed in this case. In the case of 3-hydroxytetrahydrofuran hydrate, the hydroxy groups are hydrogen bonded to the hexagonal faces of large cavities (apparently, the molecule is reoriented between several positions), which markedly distorts the framework. According to molecular dynamics, the lifetime of the host–guest hydrogen bonds in double hydrates of ethanol and propan-1- and -2-ols with methane is ~10 ps.[98] It was shown[99] that at sufficiently high temperatures, relatively large guest molecules (CH_4, CH_3F) may hop between the cavities. Monreal *et al.*[100] showed that polar guest molecules (SO_2 or HCN in a small cavity and THF or trimethylene oxide in a large cavity) in double hydrates form hydrogen bonds with the framework on lowering the temperature, thus converting the framework from a clathrate to a semi-clathrate one.

2.3. Compositions of gas hydrates and occupancies of hydrate cavities

For calculating the composition of GHs, it is necessary to know the structure of hydrate, the types of guest molecules and occupancy of the cavities. The software applicable for calculation of the composition of hydrates is considered below. In this Section, we briefly discuss the available experimental data. In the general case, the occupancy of large framework cavities by guest molecules differs little from 100%.[101] The occupancy of small cavities can vary from 0 to virtually 100% depending on the conditions of hydrate formation. The greatest deviations from 100% occupancy of large cavities are known for sI hydrate of carbon monoxide in which the large cavities have 90% occupancy, while the occupancy of small cavities is almost 100%.[102] It was shown[103] that the large cavities of sI have variable occupancy depending on the pressure of synthesis, while small cavities remain 100% filled. In other cases of sI hydrates, the deviation of the occupancy of large cavities from 100% does not exceed several percent.

In sII (Ref. 104) and, the more so, sH hydrates formed by large molecules, the occupancy of large cavities does not, most likely, differ significantly from 100%.[101] The occupancy of small cavities regularly increases with increasing pressure of hydrate synthesis and with decreasing temperature (Fig. 5).[104–106] In addition, the composition of the hydrate depends on the molar ratio of water and hydrate former in the initial mixture. At ~1.5°C, ethylene oxide hydrate synthesized from a solution with a low content of ethylene oxide had a hydration number of 7.46, while in the presence of an excess (relative to the hydrate composition) of ethylene oxide, the hydration number was 6.74.[107] The hydration numbers of methane hydrate at the same temperature and a pressure of 30 MPa were 6.19 and 5.80 for the initial compositions with excess water and methane, respectively.[108]

In the case of molecules able to occupy small cavities of the sI framework, the hydration numbers decrease with

§ Common designations of ice: I_h is hexagonal ice, I_c is cubic ice.

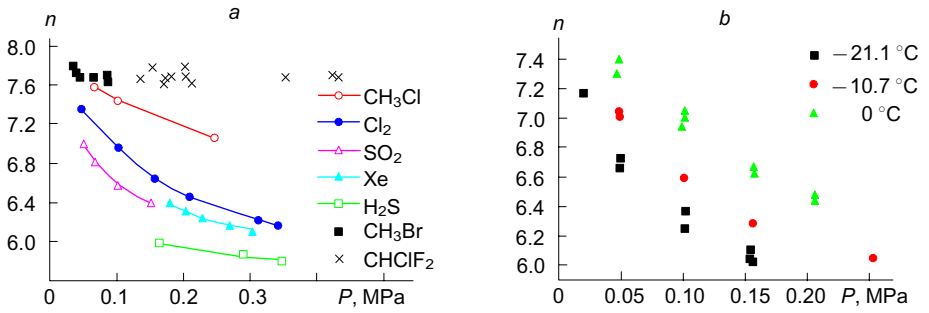


Figure 5. Dependences of hydrate numbers for various hydrates on the pressure (*a*)[104,105] and for chlorine hydrate (*b*)[106] on the pressure and temperature at which the hydrate was synthesized. Adapted by the authors with the permission of the American Chemical Society and Wiley.

increasing pressure to approach 5.75 (100% occupancy). For the CH_3Br and $CHClF_2$ molecules, which can fit only into a large cavity of sI hydrate, the hydration number corresponds to 7.67 to within the determination error, *i.e.*, this means that the large cavities of the hydrate are completely filled. All experiments were carried out at 0 °C. It can be seen that a temperature rise results in increasing hydration number, that is, decreasing cavity occupancy.

The limiting compositions of simple hydrates are summarized in Table 1. In double and mixed hydrates, large cavities in the framework tend to be mainly occupied by heavier molecules (with greater Langmuir constants, see below), while small cavities are mainly occupied by lighter molecules (with smaller Langmuir constants). According to Uchida *et al.*,[109] a methane–ethane mixture (2 mol.% ethane) gives an sI hydrate in which large cavities are 50% occupied by ethane molecules (the rest is methane), while small cavities in this hydrate are filled with methane. In sII hydrates obtained from initial mixtures with 10–20 mol.% ethane, the occupancy of large cavities by this component is 70–90%. When sI hydrate is formed from initial gas mixtures with higher ethane concentrations, the ethane content in large cavities reaches 90–100%, while the occupancy of small cavities by methane is low. At high concentrations of the auxiliary component in the initial mixture, this component can occupy a considerable part of large cavities. It is evident that a large molecule cannot occupy *D* cavities due to steric restrictions; therefore, the opposite situation is impossible.

We will consider the formation of double hydrates from THF and methane. The stoichiometric composition of the hydrate of pure THF corresponds to the composition $THF \cdot 17\,H_2O$ (5.6 mol.% hydrate former). When a double hydrate is formed from a 0.1 mol.% aqueous solution of THF and a large excess of methane, large cavities are occupied by methane by 30%.[110] In the case of a double propane and methane hydrate with a 1 mol.% propane concentration in the initial mixture, the occupancy of large cavities by methane does not exceed 30% (the content of propane in the hydrate is ~20 mol.%).[111] When the concentration of propane in the mixture is high, a hydrate with a low occupancy of small cavities is formed. If the propane : methane molar ratio in the starting mixture is 1 : 2, all large cavities in the resulting hydrate are occupied by propane and small cavities are occupied by methane.[112] The results of studies of the composition of hydrates formed by complex mixtures of C_1-C_4 hydrocarbons, nitrogen and carbon dioxide are fully in line with this trend.[113] Published data on the phase equilibria and compositions of hydrates and on the comparison of experimental and theoretical results have been considered in detail in reviews.[114,115]

2.4. Gas hydrates at high pressure

By high pressure, we will mean a pressure above 50–100 MPa where new structural and physicochemical features of hydrates start to appear. The studies on this topic published before 2007 have been covered in a number of reviews.[116–118] A pressure increase always results in compaction of crystal structures. In the case of gas hydrates, this occurs in three main ways:

— due to multiple (with several molecules) filling of cavities,

— due to the formation of new types of structures,

— due to a combination of the above ways.

In sII hydrates formed by nitrogen, oxygen and argon, multiple filling of large cavities takes place at elevated pressures.[119,120] At $P < 700$ MPa, new structures that formed under the action of high pressure correspond to the known structural types. Indeed, a pressure increase induces a sII to sI transition of the sulfur hexafluoride hydrate.[121] In this case, the hexafluoride molecule is literally embedded into the *T* cavity, which is too small for this molecule. The structures of low-pressure methane and argon hydrates, sI and sII, respectively, are transformed into sH in which the large *E* cavities are filled with five argon atoms[120] or with approximately three methane molecules.[122] Further compaction of the structure with retention of known hydrate frameworks is impossible; therefore, at pressures of ~800 MPa and above, hydrates of new structural types appear. They include hydrates with structures in which the cavities have a polyhedral shape (Fig. 6 *a*).[116,123,124] Hydrates of this type were found for argon, nitrogen and tetrahydrofuran.[12] Volume changes upon interconversion and the compositions of methane and argon hydrates existing below 1000 MPa were studied by Manakov and co-workers.[125,126] When the pressure is ⩾1000 MPa, diverse channel structures are formed. An interesting example of the channel system was found for high-pressure hydrates of methane, argon, krypton and nitrogen (Fig. 6 *b*). The water framework of these hydrates is composed of hexagonal layers and resembles the ice I_h framework.[118,127,128]

Hydrogen, helium and neon hydrates were the first channel structures to be discovered. At low pressures, these gases are dissolved in the ice I_h. Raising the pressure to 100–200 MPa results in the formation of sII hydrates with multiple occupancy of all cavities.[12,116,117,129] It is noteworthy that the small size of molecules allows these gases to diffuse across the hydrate framework.[130,131] Removal of the guest from the neon hydrate quenched to cryogenic temperatures resulted in the formation of an empty sII hydrate framework (ice XVI, Ref. 132), while absorption of helium by the empty framework at 300 MPa

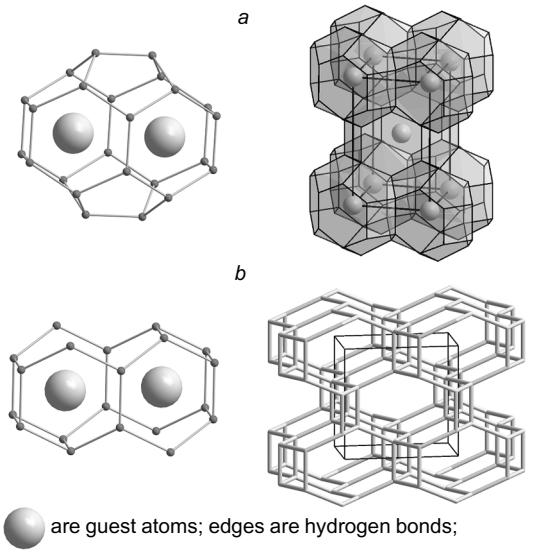


Figure 6. Shape of the polyhedral cavity (tetradecahedron filling the space) and packing of the polyhedra in the framework of high-pressure argon hydrate (*a*); the channel unit and general view of the channel framework of high-pressure hydrates of methane, argon, krypton and nitrogen (*b*).[12] Adapted by the authors with the permission of Elsevier.

and at cryogenic temperatures afforded sII hydrate of helium.[133] Higher pressures in the water – hydrogen system result in successive formation of new structures with helical chiral channels (Fig. 7),[134] hydrates based on an ice II framework and a hydrate based on an ice I_c framework.[12, 116, 117] It is of interest that the interaction of amorphous ice with hydrogen may give a hydrate based on ice I_c even at moderate pressures.[135] Like in the case of sII hydrates, an empty framework of this type can be prepared by pumping out of the guest at cryogenic temperatures (ice XVII);[136, 137] the empty framework can absorb other gases.[138, 139] The channel hydrate with a structure similar to the structure of hydrogen hydrate was detected in the CO_2 – water system.[134] Solving this structure and determination of the stability region of the corresponding hydrates required efforts of several research groups (see, for example, Refs 140 – 142). A good review of the current state of research on high-pressure channel hydrates was published by Bove and Raniery.[143] It is worth noting that the chemical behaviour of hydrate components at high pressures has been scarcely studied. An exception is a paper of Matsumoto *et al.*,[144] who demonstrated that at 80 MPa, bromocyclopentane within a hydrate did not undergo any changes, whereas in the liquid phase in equilibrium with the hydrate, a mixture of cyclopentene and cyclopentanol was formed.

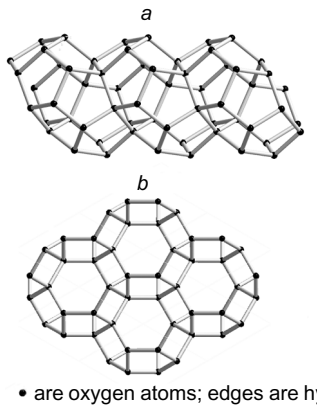


Figure 7. Shape of the helical channel (*a*) and packing of the channels (*b*) in high-pressure hydrates of hydrogen and carbon dioxide (the channel cross-section is shown). The Figure was prepared by the authors using the data of Ref. 134.

Hydrogen hydrates have long been considered as hydrogen storage materials. Since the pure hydrogen GH is formed at pressures of <100 MPa, numerous attempts were made to shift the hydrate formation conditions to a more favourable region by forming double hydrates (see, for example, Refs 145 – 147). A review of these studies has been reported.[148] A key issue concerning the applicability of hydrates for hydrogen storage is the attainable occupancy of small and large cavities of the sII framework with hydrogen molecules. The known limiting occupancies amount to four molecules per large cavity and two molecules per small cavity; however, other values have also been proposed. The conclusion drawn by Rasoolzadeh and Shariati[129] appears to be the most adequate. They believe that the real occupancy depends on the temperature and pressure used in the experiment. Due to the insufficient hydrogen content in the hydrate (it is easy to calculate that the limiting content of pure hydrogen even in sII hydrate does not exceed 5 mass %), the use of GHs for some practical applications, *e.g.*, hydrogen storage for vehicles, has no prospects. The possible application of hydrates for stationary hydrogen storage is somewhat more interesting.[149, 150]

3. Phase equilibria of hydrate-forming systems

The equilibrium conditions of existence represent the basic physicochemical information about gas hydrates That is why a great many experimental and theoretical calculation studies of the phase diagrams of hydrate-forming systems have been undertaken. The $P-T$ projections of the phase diagrams of typical methane – water, carbon dioxide – water and propane – water systems are presented in Fig. 8. In the vast majority of cases at 20 – 30 MPa pressure, one thermodynamically stable hydrate is formed in each system (the few exceptions include cyclopropane, which forms sI and sII hydrates,[2] and dimethyl ether, which forms hydrates with a new tetragonal structure and with sII structure[71]). Two types of hydrate former – water systems are distinguished (see Fig. 8):

— systems in which the guest component occurs in the gaseous state in the considered $P-T$ range (methane-containing system),

— systems with a liquefied guest (carbon dioxide- and propane-containing systems).

In the former case, the region of existence of hydrate is enclosed by univariant ihg and $l_1$hg curves, while in the latter case, it is confined by the ihg, $l_1$hg and l_1hl_2 lines. These lines determine the type of processes in which gas hydrates can be formed/decomposed with simultaneous presence of the water and a hydrate former. A large body of information on the phase equilibria of GHs formed by single components can be found in monographs.[1 – 4, 9]

In recent years, the interest in the GHs formed by single components has been focused on studying them under special conditions (low temperatures or the use of isotopomers). The equilibrium curves of the CH_4, C_2H_6,

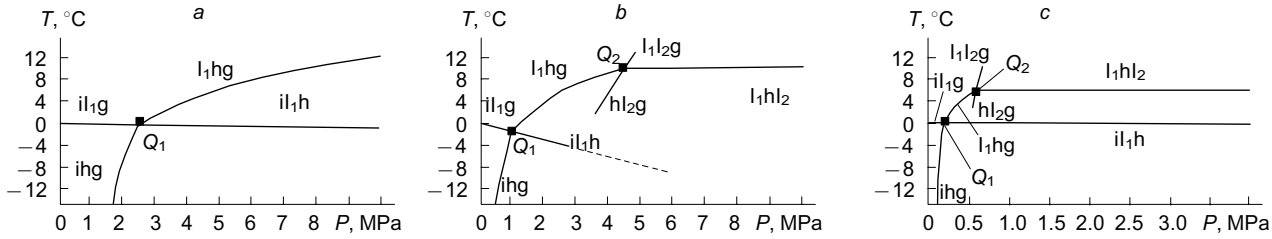


Figure 8. $P-T$ projections of phase diagrams of binary systems: methane – water (*a*), carbon dioxide – water (*b*) and propane – water (*c*). i is ice; l_1 is water saturated with the hydrate former; h is hydrate; l_2 is water-saturated liquid hydrate former; g is hydrate-forming gas with water vapour. Q_1 is the il_1hg quadruple point, Q_2 is the l_1hl_2g quadruple point. For explanations, see the text. The Figure was prepared by the authors using the data of Refs 2, 4. The quadruple point Q_1 for the system with carbon dioxide is given according to Ref. 151.

C_2H_2, CO_2, Xe and Kr hydrates were measured for temperatures below −43 °C;[152, 153] for a broad range of hydrate-forming molecules, the equilibrium curves were defined for temperatures up to −70 °C.[154–159] The equilibrium conditions of hydrate formation in D_2O have been investigated.[124, 160] As could be expected, the equilibrium temperatures for D_2O hydrates at a given pressure proved to be a few degrees higher than those for H_2O hydrates. Meanwhile, the replacement of a hydrogen atom with deuterium in the methane molecule leads to decreasing equilibrium temperature at a given pressure.[161] This result is quite unexpected and is at variance with the known trend for increasing temperature of hydrate decomposition with increasing weight of the guest molecule.

The $T-X$ section of the phase diagram of the methane – water system is depicted in Fig. 9. In this case, the hydrate-former-rich phase is gas g (methane with water vapour). Note that for systems in which the hydrate former is liquefied under pressure, the $T-X$ section would look qualitatively the same; however, phase g would be replaced with the liquid hydrate former l_2. Analysis of the $T-X$ section demonstrated that a hydrate can be formed not only in the reaction with water, but also in other cases:

— on cooling (freezing) of a gas solution in water (on crossing the contact line between the l_1 and l_1 + h regions and the univariant il_1h curve);

— on cooling of a water-saturated gaseous or liquid hydrate former (on crossing the boundaries between the g and h + g or between l_2 and h + l_2 regions, respectively).

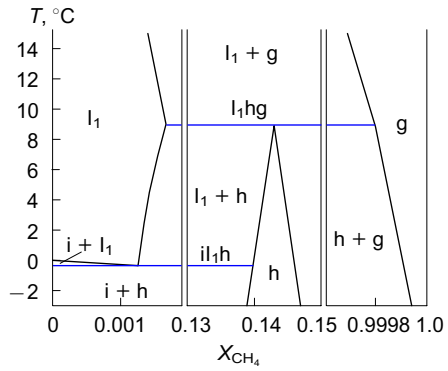


Figure 9. Characteristic fragments of the $T-X$ section of the phase diagram of the methane – water system at 6 MPa. For clarity, fragments are shown on different scales in the composition axis. X_{CH_4} is the mole fraction of methane in the methane – water system; other designations are given in the caption to Fig. 8. The Figure was prepared by the authors using published data.[2, 4, 108, 162, 163]

Certainly, the reverse hydrate dissolution and evaporation processes are also possible. The number of studies addressing the water content of liquid or gaseous hydrate formers occurring in equilibrium with hydrates is moderate. Chapoy *et al.*[164] studied the content of water in liquid CO_2 occurring in equilibrium with GHs at temperatures below −20 °C and pressure of 13.9 MPa. The change in the water content of methane and ethane in equilibrium with the hydrate was studied over broad temperature and pressure ranges.[162, 165] Much more publications are devoted to the solubility of hydrate formers in the liquid aqueous phase occurring in equilibrium with the hydrate: CH_4 in water,[163, 166] CO_2 in water and in brines,[167–170] CH_4 and C_2H_6 in water and salt solutions,[171, 172] mixtures of CH_4 and CO_2 in water,[173] C_3H_8 in water[174] and mixtures of N_2 and CO_2 in water.[175] If the hydrate former is an organic liquid immiscible with water (CCl_4, $CHCl_3$, CH_2Cl_2, *etc.*), then the quadruple point Q_2 shifts to pressures of <0.1 MPa. When the guest is infinitely soluble in water (THF, acetone, ethylene oxide, *etc.*), either congruent melting takes place with hydrate degradation to the liquid phase of the same composition (as in the case of THF hydrate), or peritectic melting occurs with decomposition to ice I_h and a saturated solution of water in the guest (as in the acetone – water system). Data on relevant phase diagrams can be found in the literature.[176–178]

At temperatures below 0 °C, GHs can exist, under certain conditions, at pressures lower than the pressures defined by the ihg curve (see Fig. 8). This can be caused by hydrate self-preservation (the self-preservation is considered in detail by Manakov *et al.*[179]) or by the presence of supercooled water in the system.[180, 181] In the phase diagram, the presence of supercooled water is indicated by the metastable continuation of the univariant l_1hg line directed towards negative temperatures. The hydrate can exist, for a long period of time, in the region enclosed by the metastable continuation of the l_1hg curve and by the ihg curve. After the supercooled liquid is frozen, the hydrate decomposes (hydrate self-preservation was not observed in these samples).

The graphical representation of the phase diagrams of systems comprising more than two components is fairly sophisticated. Khaldoyanidi[182] reported a detailed account of the phase diagrams of ternary hydrate-forming systems. The phase equilibria of the systems with several hydrate formers are represented, most often, as a set of $P-T$ curves for formation/decomposition of the hydrate obtained from various gas mixtures. In experiment, the mixture of hydrate formers acts as the only hydrate-forming component and the system is considered as a pseudo-double one. It is clear

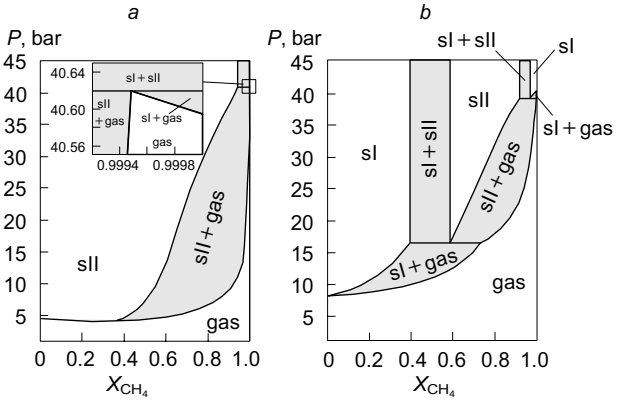


Figure 10. Simplified $P-X$ diagrams of the methane–propane–water (*a*) and methane–ethane–water (*b*) systems at 4.5 °C. In all $P-X$ phase fields, there is also a liquid phase (saturated solution of the corresponding gases in water). X_{CH_4} is the methane mole fraction in the initial gas mixture. The Figure was prepared by the authors using the data of Ref. 183.

that this approach is valid only if a small amount of the hydrate is formed, so that the composition of the mixture of hydrate formers can be considered invariable.

In some cases, simplified $P-X$ diagrams are used, demonstrating which phases are formed in the system at different temperatures, pressures and compositions of a hydrate former mixture. An example of such diagrams is shown in Fig. 10. It can be seen that in the methane–propane–water system, the sI to sII structural change takes place when <1% propane is added to methane, while in a methane–ethane–water mixture, the sII hydrate is formed only in a particular concentration range. In the case of double hydrates formed by large (propane, isobutane) and small (methane, nitrogen, *etc.*) guest molecules, the equilibrium curve of a double GH is usually located at a higher temperature than that for the hydrates of single components. To simplify the situation, one can state that the increased stability of the double GHs it attributable to filling of each type of cavity in the framework by the most suitable type of guest molecules.

Reviews of available data on the GH phase equilibria in multicomponent systems can be found in the literature.[4,184–186] Mention may also be made of a series of studies[187–190] describing an unconventional approach, in which the composition of the gas phase occurring in equilibrium with the hydrate was studied as a function of temperature and pressure for CO_2-N_2, CO_2-H_2, CO_2-CH_4 and $CO_2-N_2-CH_4$ mixtures. Bhawangirkar and Sangwai[190] paid primary attention to the arrangement of guest molecules in hydrate cavities and the replacement of CH_4 by CO_2 for the simultaneous development of hydrate deposits and disposal of carbon dioxide. Babakhani *et al.*[191,192] carried out a detailed study of the equilibrium compositions of hydrates formed by mixtures of hydrocarbons and carbon dioxide. The equilibrium conditions for the synthesis of the hydrate of a C_1-C_3 hydrocarbon mixture at temperatures below 0 °C were studied by Yasuda *et al.*;[193] before this study, virtually no data of this type were available.

If water contains dissolved components that do not participate in hydrate formation [salts, methanol, ethylene glycol, saccharose, propane-1,2,3-triol (glycerol) and so on], the thermodynamic activity of water in the liquid phase decreases. This leads to a decrease in the freezing temperature for these solutions and to a shift of the hydrate formation/decomposition curves towards higher pressures and lower temperatures (Fig. 11). This effect forms the basis of so-called thermodynamic inhibitors of hydrate formation, which are used to prevent GH formation during oil and gas production.[1,4]

Note that the addition of an inert diluent to the gaseous hydrate former would lead to a similar shift of the equilibrium curves of the hydrate. Examples of these inert diluents are helium and hydrogen[194,195] up to certain concentrations and pressures.[196] The addition of a liquid not involved in hydrate formation and immiscible with water [oil, dead (degassed) crude oil, *etc.*] does not affect the position of the equilibrium curves of simple GHs. If gas mixture components are redistributed between the gas and liquid (oil, crude oil) phases, the composition of the equilibrium gas phase may change; then the GH equilibrium curve also changes.[197,198] The presence of such liquid can affect the kinetic characteristics of hydrate formation/dissociation processes.

An enormous body of data on the phase equilibria of hydrates in the presence of methanol, diols and salts is summarized in monographs.[1,4] We will consider the most interesting publications on this subject. A universal (applicable to pure salts, their mixtures and dissolved nonelectrolytes) approach to predicting the effect of thermodynamic inhibitors on the equilibrium conditions of hydrate formation was reported by Hu *et al.*[199–201] The effect of high (tens of mass percent) concentrations of various metal halides and ethylene glycol on the phase equilibria of hydrates was studied at pressures up to 150 (Ref. 202) and 200 MPa.[203–206] The so high pressures were used, since at moderate pressures, hydrates in concentrated solutions are formed at extremely low temperatures, which complicates the experimental studies of hydrate formation. The inhibition of hydrate formation by ionic liquids was considered by Tariq *et al.*[207] The formation of THF hydrate in solutions of ammonia was studied by Munoz-Iglesias *et al.*[208] It was found that the melting point of the hydrate in this system decreases by tens of degrees; a mixed THF and ammonia hydrate is probably formed in this case.

For hydrates of single gases, comprehensive data on both the equilibrium curves and hydrate compositions are available (see above). However, it is almost impossible to obtain exhaustive experimental information on the hydrates formed by gas mixtures; therefore, it is necessary to use calculation methods. Quite a few engineering methods for the calculation of GH equilibrium curves and strict thermodynamic models have been developed to date; these methods allow for calculation of not only equilibrium curves, but also compositions of the hydrates and occupancy of different types of cavities by various guest molecules.[1,2,4] It is most easy and appropriate to calculate the compositions

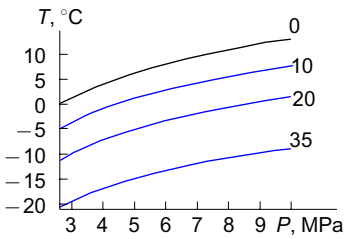


Figure 11. Equilibrium curves for the methane hydrate in methanol solutions. The methanol concentrations (mass %) in the aqueous solution occurring in equilibrium with the hydrate are indicated near the curves. The Figure was prepared by the authors using the data of Refs 1 and 4.

and properties of hydrates with several guest components using dedicated software. The calculation methods implemented in the software are based on the van der Waals – Platteeuw theory of ideal clathrate solutions [209] modified by Parrish and Prausnitz [210] and by other authors (*e.g.*, Ref. 211). In these models, GHs are considered as non-stoichiometric compounds with composition depending on the composition of hydrate-forming mixtures, temperature and pressure. The hydrate formation is split into two stages:

— transformation of ice or water into an unstable empty hydrate framework,

— sorption of guest molecules into this framework.

The energy characteristics of the transformation of ice (water) into an empty hydrate framework depend on the type of framework and the initial physical state (ice or water), but are assumed to be independent of the type of guest molecule. The unstable empty framework is stabilized *via* interactions with guest molecules that fill the cavities. This stabilization can be quantitatively characterized by the change in the chemical potential of the water molecules in the hydrate framework, which is described by the following relation:

$$\mu_{\mathrm{H}} - \mu_{\beta} = RT' \sum_{m} \left[y_m \ln\left(1 - \sum_{i} \theta_{ml}\right)\right] \quad (1)$$

Here μ_{H} and μ_{β} are the chemical potentials of water molecules in the filled and empty hydrate frameworks, respectively; R is the gas constant; T' is temperature [here and below T', K = T (°C) + 273.15]; y_m is the number of type m cavities, θ_{ml} is the occupancy of type m cavities by type l molecules (the summation involves all types of molecules that can reside in type m cavity). The θ_{ml} value is found from the relation

$$\theta_{ml}(T', P) = \frac{C_{ml}(T') f_l(T', P)}{1 + C_{ml}(T') f_l(T', P)} \quad (2)$$

where $C_{ml}(T')$ are temperature-dependent Langmuir constants, which characterize the favourability of inclusion of guest molecule l into type m cavity; $f_l(T', P)$ is the fugacity of the type l guest component.

The set of Langmuir constants $C_{ml}(T')$ characterizing the tendency of various guest molecules to occupy a particular type of cavity of the hydrate framework and a more detailed description of the calculation method can be found in the publications cited above. The $C_{ml}(T')$ values are fitted on the basis of experimental data or calculated theoretically. Using software packages (Table 2), it is possible to calculate the equilibrium curves for single hydrate formers and their mixtures and GH equilibrium curves in the presence of hydrate formation inhibitors in the aqueous phase and the compositions of coexisting phases. The software packages listed in the last three lines of Table 2 can be used to calculate the properties of fluid phases and phase equilibria (in particular, for gas hydrates) that are needed for oil and gas industry. According to Sloan *et al.*,[212] the averaged errors of calculations of the equilibrium temperatures of gas hydrates at a specified pressure carried out using various software programs are as follows: < 0.5 °C for single hydrate formers, < 0.75 °C for binary mixtures of hydrate formers and < 1.0 °C for ternary mixtures. For typical natural gas compositions, the error is < 0.75 °C; for particular gas mixtures (especially those containing exotic components), the real errors can be 3 – 4 times higher.

A separate line of research of GH phase equilibria is related to the equilibrium conditions of hydrate formation in thin micro- and mesopores of various materials, mainly adsorbents. Studies along this line were actively carried out in 1995 – 2005, mainly in relation to GH formation in sedimentary rocks. Currently, the interest in hydrate formation in porous media is mainly due to the development of gas storage methods and gas hydrate technologies. The history and the current state of studies in this area were reflected in reviews.[213, 214] In the case of mesoporous inorganic materials (silica gel, porous glasses, *etc.*), the experimental data were satisfactorily described by the Gibbs – Thomson equation for phase transitions in equally sized pores [215] with the assumption of hydrate formation inside the confining pores. This equation has the form

$$\frac{\Delta T}{T_{\mathrm{eq}} + 273.15} = -\frac{\gamma_{\mathrm{h}} \cos\theta}{\rho_{\mathrm{h}} \Delta H}\left(\frac{\alpha}{d}\right) = -K\frac{\alpha}{d} \quad (3)$$

Here ΔT is the change in the equilibrium temperature of hydrate formation, T_{eq} is the equilibrium temperature of hydrate formation at a given pressure (temperatures are in °C), γ_{h} is the specific surface energy of the hydrate and liquid water contact; θ is the contact angle between the hydrate and water at the hydrate – water – gas contact line; ρ_{h} is the hydrate density; ΔH is the enthalpy of hydrate decomposition; d is the diameter of the hydrate particles; K is the coefficient; α is the shape coefficient (four for spherical pores and two for cylindrical pores).

In recent years, numerous studies have been devoted to hydrate formation in the pores of carbon materials,[214] in particular natural coals.[216, 217] In these cases, interpretation of the results is complicated by the occurrence of several

Table 2. Program packages for the calculation of the equilibrium conditions and compositions of gas hydrates.

Program package	Developer	WEB
CSMHYD, CSMGem	Center for hydrate research of the Colorado School of Mines (Golden, USA)	http://hydrates.mines.edu/CHR/Software.html
DBRHydrate	Schlumberger	https://www.petromehras.com/petroleum-software-directory/reservoir-engineering-software/pvt-analysis-software/dbrhydrate
Multiflash	KBC Advanced Technologies (Walton on Thames, UK)	https://www.kbc.global/software/advanced-thermodynamics/
PVTsim	Calsep (Kongens Lyngby, Denmark)	https://www.pvtsimnova.com/
HydraFLASH	Heriot – Watt University (Edinburgh, UK)	http://www.hydrafact.com/index.php?page=software

parallel processes; for example, in addition to hydrate formation, adsorption of the hydrate former can take place, in some cases, by a competitive mechanism. Currently, there is no reliable conceptual model of hydrate formation in these media. The data discussed in the publications cited above suggest that GH nucleation is accelerated in the pore space of carbon materials.

Recently, interesting experimental facts and their discussion were reported by Casco *et al.*[218] The authors demonstrated that the details of hydrate formation from water adsorbed in carbon asorbents with hydrophilic and hydrophobic pore walls are substantially different. It is noteworthy that the hydrate formation in sedimentary rocks is analyzed, most often, using an approach based on the assumption of the presence of a spectrum of energy states of water in systems of this type.[55,219,220] This may be due to the occurrence of water in pores of various sizes, the presence of wetting water films on the pore walls, the presence of dissolved salts in the interstitial water, *etc.* A similar situation is observed in model finely porous media, in which properties of a liquid change in the vicinity of the pore walls. It seems appropriate to develop models for analysis of hydrate formation in model finely porous media using approaches similar to those reported by Waite *et al.*[55] and Chuvilin and co-workers.[219,220] Indeed, it was shown[221] that hydrate formation from the interstitial water can take place over a broad temperature range, the size of which cannot be explained by the effect of confining pores alone. An unusual example of the effect of porous medium on the hydrate formation was described by Buleiko *et al.*[222] The authors established that when the pore walls are not wetted by liquid propane, the propane evaporation curve shifts towards higher pressures (a phenomenon reverse to capillary condensation). In this case, it is possible to implement the metastable continuation of the univariant l_1hg curve (see Fig. 8) towards a higher temperature region, *i.e.*, it is possible to obtained a superheated hydrate.

A peculiar and poorly studied area is the formation of GHs in the interlayer space of various materials. Guggenheim and van Groos[223] reported the possibility of formation of methane hydrate between montmorillonite layers, with the 'hydrate' layer thickness being close to the unit cell parameter of the sI structure. The reported equilibrium conditions of the 'hydrate' were 1–2 °C lower than those of the bulk hydrate. Kim *et al.*[224] did not confirm the GH formation in the interlayer space. In their opinion, hydrate is formed in pores of different size formed by a random packing of bunches of montmorillonite layers. Calculations showed[225] that GHs can be formed both in the interlayer space and in the pores, but experimental results do not give clear indications of the existence of an 'interlayer' hydrate. In our opinion, the possibility of existence of 'interlayer' hydrate is currently an open question.

4. Properties of hydrates

The thermophysical properties of the hydrates, which have been intensively studied in the last quarter of the 20th century, are covered in detail in monographs.[2–4] It was found that the heat of decomposition of hydrate into the gas and water (or hydrate formation from these phases) is mainly determined by the destruction (formation) of hydrogen bonds in the water framework. At 0 °C and 0.1 MPa, the enthalpy of decomposition of methane hydrate into the gas and ice is 18.1 kJ mol^{-1}, while the enthalpy of decomposition into the gas and water is 54.2 kJ mol^{-1} (here and below, the values are referred to one mole of the gas). The same values for propane hydrate are 27.0 and 129.2 kJ mol^{-1}, respectively. The enthalpy of decomposition of the hydrate into the gas and ice includes the enthalpy of removal of guest molecules from the hydrate framework and the enthalpy of transformation of the absolutely unstable water framework into ice. Data on the heat capacity of hydrates can be found in the literature.[226–230] It was shown that in the case of weak interaction between guest molecules and the host framework, the hydrate heat capacity is additive, *i.e.*, it is virtually equal to the sum of the heat capacities of the guest component and the corresponding amount of ice I_h. Stronger host–guest interaction results in more pronounced deviation between the measured and additive values. Among the recent publications, mention should be made of a thorough investigation of the enthalpies of decomposition and heat capacities of hydrates in the isobutane–water and n-butane–isobutane–water systems.[231] A detailed review and analysis of information on thermochemical properties of hydrates were reported by Jenkins.[232,233] Data on the thermal conductivity of hydrate-containing deposits can be found in the literature.[234–237]

A characteristic feature of hydrates is abnormally low thermal conductivity.[238] At temperatures about 0 °C, the thermal conductivity of methane hydrate is close to that of water and amounts to 0.5 $W m^{-1} K^{-1}$. For the ice I_h this value at the same temperature is 2.5 $W m^{-1} K^{-1}$. The abnormally low thermal conductivity of GHs for solids is due to the presence of two weakly interacting subsystems, the guest and the host ones, the oscillations of which are largely independent. This results in phonon scattering and, hence, in a decrease in the thermal conductivity. The state of the art of the problem was discussed by English and Tse.[239–241]

Data on the mechanical properties of hydrates and their adhesion to various surfaces have been reported.[242–247] The adhesion of dry hydrate particles to one another or a dry hydrate particle to the surface is negligibly low, mainly due to imperfect structures of the contacting surfaces. If a water film is present on the particle surface (including, the film formed on the hydrate and ice surfaces in the vicinity of the melting point — so-called premelting effect), the particles can stick together due to the formation of water 'capillary bridges' between them (Fig. 12).[248–251] Water is able to wet the GH surface; therefore, on contact of two particles, water tends to fill the most narrow regions near the physical contact surface and thus binds the particles. This is the major mechanism of sticking together of hydrate particles in oil suspensions; finally, this results in the formation of hydrate plugs. The cohesion of hydrate particles can be reduced by using of anti-agglomerants (see Section 6). In recent years, the interaction forces between cyclopentane hydrate particles in mineral oil were measured in the presence of various surface active carboxylic acids[252] and

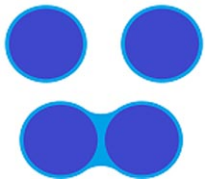


Figure 12. Illustration of the mechanism of sticking together of hydrate particles with a water layer on the surface. The dark blue colour indicates the hydrate and light blue is water. The contact of water shells of hydrate particles gives rise to liquid menisci, which ensure the particle sticking.

thermodynamic inhibitors of hydrate formation.[253] It was found that the cohesive forces between hydrate particles decrease in the presence of carboxylic acids (like in the presence of any surfactants) and increase in the presence of NaCl. The latter effect was attributed[253] to increasing amount of the aqueous phase in the system. The influence of the degree of corrosion of the metal surface and the salinity of water on the strength of interaction of a hydrate particle with this surface and with a water drop were studied by Wang *et al.*[254] and Liu *et al.*,[255] respectively. Smith *et al.*[256] demonstrated the possibility of reducing the hydrate adhesion to steel and glass surfaces by silanization and thiolation. The sintering processes of gas hydrate particles were studied by Uchida *et al.*[257]

It was found[243] that the refractive indices of methane and natural gas hydrates are close to 1.35 (638 nm, −3 °C). Note that for air hydrate, this value was found to be 1.32.[258] More detailed information on the refractive indices of GHs was presented by Bonnefoy *et al.*[259] The electrical conductivity of polycrystalline methane hydrate was investigated by Du Frane *et al.*[260] An unexpected and not ultimately clear feature is fast diffusion of methane molecules at the boundary between sI and sII hydrates found by Ranieri *et al.*[261]

Currently, spectroscopic methods are widely used for the identification of GH structural types and cavity occupancies (for spectroscopic studies of the guest and host subsystem dynamics for hydrates, see Section 2). Useful information on the characteristic bands of guest molecules located in different types of cavities in the Raman spectra was obtained by Subramanian and Sloan.[262] The effect of the environment on the positions of C–H stretching bands of methane was reported by Ohno *et al.*[263] In the authors' opinion, analysis of band positions and intensities can be used not only to determine the type of hydrate and relative cavity occupancies, but also to study finer details of the host–guest and guest–guest interactions. The temperature dependence of the positions of the totally symmetric C–H vibration bands for the methane molecule located in small cavities of various sH hydrates was studied by Fuseya *et al.*[264] The issues of using Raman spectroscopy for determining GH compositions and calibration of calculation parameters for CH_4, C_2H_6, CO_2 and N_2 were considered by Qin *et al.*[265,266] In order to study the state of methane, carbon dioxide and hydrogen sulfide on cosmic bodies, Dartois *et al.*[267–269] comprehensively investigated the low-temperature IR spectra of the hydrates of these gases. The NMR studies of gas hydrates were summarized in a review.[270] Hydrates of hydrocarbons were studied by ^{13}C NMR spectroscopy.[271–275] A review of application of spectroscopic methods for studying hydrates was published.[276] Another review[277] covers not only spectroscopic, but also other instrumental methods used to study hydrates.

5. Hydrates formed by 'non-classical' hydrate formers

Since a finite number of molecules fits into the size of cavities of known hydrate structures, the number of individual compounds that can form hydrates is limited. The vast majority of simple GHs have been studied to one or another extent in early stages of gas hydrate research. One of the few interesting examples of recent studies of this type is the formation of metastable sII hydrate of carbon monoxide during the formation of thermodynamically stable sI hydrate.[278] The formation of metastable phases with a structure differing from the structures of stable phases was previously demonstrated for nitrogen[279] and methane.[280] Meanwhile, there is an enormous number of double and mixed GHs. A group of double sII and sH hydrates formed by molecules with substantially different sizes is of particular interest. Quite a number of such hydrates were studied in the last decade; in these studies, compounds that do not form clathrate hydrates by themselves were used as larger hydrate-forming molecules. Exactly this group of hydrates is considered, first of all, in this Section.

During a long period of time, lower alcohols (up to butanols) were considered as thermodynamic inhibitors of gas hydrate formation. It was shown[281–287] that they can form sII hydrates with methane.

At positive temperatures, the equilibrium temperatures of methane + ethanol and methane + propan-2-ol double hydrates obtained from solutions with 1 : 17 molar ratio of the alcohol and water are close to those for pure methane hydrate, whereas at negative temperatures, the equilibrium temperatures are markedly higher (Fig. 13). Evidently, this is due to the fact that in the latter case, the water-rich phase remains liquid down to relatively low temperatures. The compositions of double hydrates reported in various papers are markedly different. From our point of view, the data in which the occupancies of large and small cavities by a mixture of both guests are taken to be 100% and 80–90%, respectively, are most trustworthy. For example, the spectra of the ethanol and methane double hydrate point to a composition close to the indicated one.[288] It should be noted that the formation of low-temperature sI and sII hydrates was demonstrated previously, at least, for ethanol (see references in the publications cited above). The double hydrates formed by ethanol or propan-2-ol with carbon dioxide are much less stable than those formed with methane;[289,290] furthermore, ethanol forms an sI hydrate and propan-2-ol forms an sII hydrate. It was noted[291] that methanol can be incorporated in considerable amounts into cavities of THF, xenon and hydrocarbon hydrates. The THF-based hydrate was prepared by freezing an aqueous solution containing methanol at a temperature of −40 °C; the other hydrates were obtained by low-temperature deposition of components from vapours and annealing of the resulting samples. In the double hydrate of n-propanol and methane, the propanol molecule forms a hydrogen bond with the framework at low temperatures.[292] It was shown[293] that pinacolyl and *tert*-amyl (2-methylbutan-2-ol) alcohols can form double sH hydrates with methane, but not with carbon dioxide. Apparently, this is due to the fact that location of a carbon dioxide molecule in small cavities is unfavourable. It is of interest that sII double hydrates of

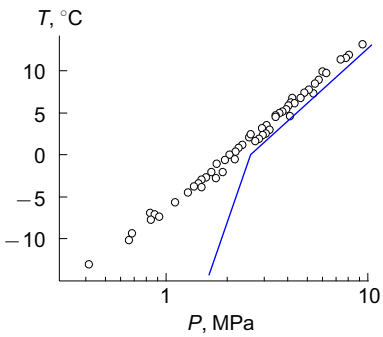


Figure 13. Equilibrium conditions for the isopropyl alcohol and methane double hydrate (dots) in comparison with the equilibrium conditions of methane hydrate (lines).[282] Adapted by the authors with the permission of Elsevier.

tert-butyl alcohol can be formed with both methane and carbon dioxide; however, the carbon dioxide double hydrate is less stable and that of methane is more stable than the hydrates of the pure gases.[294] The general tendency to form sII double hydrates with methane can also be traced for amines. It was shown [295, 296] that these hydrates can be formed for *tert*-butylamine and trimethylamine, respectively. In a pure state, these compounds form hydrates with specific structures. Similar results were obtained for methyl- and dimethylamine [297] and propylamine.[298] The double hydrate of diethylamine with methane has sH structure [298] in which large cavity is occupied by two diethylamine molecules.[299]

We will consider several more examples of double hydrates studied in recent years that deserve attention. Perhaps, the ability of ammonia to act as a guest molecule was the most unexpected discovery of the past several years. Maslakci *et al.*[300] showed that in THF and trimethylene oxide double and multicomponent hydrates, an NH_3 molecule can both occupy a hydrate framework cavity and be incorporated into the framework. As a rule, ammonia hydrates exist at temperatures much lower than 0 °C. For example, the double hydrate of methane and ammonia decomposes at −93 °C, while the pure ammonia hydrate decomposes at −123 °C.[301] The handling techniques for this type of objects imply deposition of mixtures of component vapours on a cryogenically cooled trap and hydrate formation in the resulting mixtures (other experiments will be considered below). Ammonia is not only incorporated in the hydrate, but also acts as a catalyst by destroying the system of ice hydrogen bonds, thus facilitating the hydrate formation.[302] The existence of sII double hydrates of three aldehydes (acetaldehyde, propionaldehyde and isovaleraldehyde) and methane was demonstrated by Kang *et al.*[303] Previously, it was shown that pure aldehydes also form hydrates with this structure (see the references cited in Ref. 303). In all cases, the hydrates were unstable because of aldehyde conversion to *gem*-diols taking place inside the cavity. It was shown [304] that only the *trans*-form of crotonaldehyde can be incorporated into cavities of the sII framework. Note that only few hydrates formed by aldehydes are currently known.

One more interesting group of double hydrates studied in the last decade are double hydrates of ozone with oxygen, xenon, carbon tetrachloride and carbon dioxide.[305 – 310] It was shown that ozone can be stored in the hydrate for 2 – 3 weeks at temperatures from −10 to −20 °C, with an ozone content in the hydrate being up to 2.15 mass %.[305] Kim and Seo [311] detected the first hydrate former, which was gaseous under normal conditions and capable of forming sH double hydrates with methane, that is, perfluorinated cyclobutane. Shin *et al.*[312] studied the sH double hydrates formed by isomeric methylpiperidines readily soluble in water. Previously, most of the known large guest molecules in sH hydrates were either liquids poorly soluble in water or solids. Desmedt *et al.*[313] studied the hydrate formation in the THF – perchloric acid – water ternary system. The formation of the ionic double hydrate (sII) containing up to 12.5% of the acid was demonstrated. Data indicating the possibility of incorporation of hydrogen chloride ion pairs into the THF and hydrocyanic acid hydrate were obtained.[314]

The double sII hydrates of pyrazine, pyrimidine and pyridazine with methane were studied by Lim *et al.*[315] It was shown that the enhancement of interaction between the guest molecule and water shifts the hydrate equilibrium curve towards higher pressures and lower temperatures. Similar data were obtained for several double hydrates of isomeric butanols and methane.[316] The lowest hydrate stability was found for n-butanol, which formed a hydrogen bond with the framework (isobutanol did not form a hydrate). Ahn *et al.*[317] investigated methane double hydrates with hydrate-forming molecules of the same composition (2-methylprop-2-en-1-ol and butan-2-one). It was found that double hydrates exist in these systems only below 9 – 10 °C. At higher temperatures, the co-existing phases are the sI methane hydrate and solutions of the isomers in water. In both cases, the presence of polar components leads to decreasing equilibrium temperature (increasing equilibrium pressure) of double GHs in comparison with the equilibrium curve for pure methane hydrate.

Hydrates with free radicals in the cavities studied in recent years can be considered as demonstrating a new type of guest molecules. For example, the formation of blue-coloured hydrate with a free radical in the cavity and an electron captured in the framework was detected upon γ irradiation of the *tert*-butylamine undecahydrate.[318]

Examples of application of EPR spectroscopy to study the transformations of γ-irradiated hydrates deserve attention. Kobayashi *et al.*[319] considered the transformation of the isobutyl radical to the *tert*-butyl radical accompanied by hydrogen atom transfer across the face common to two large cavities of sII hydrate. Sugahara *et al.*[320] investigated processes in the irradiated double hydrate of propane and methane. Hydrogen atom transfer from a propane molecule in a large cavity to the methyl radical in the small cavity was demonstrated. It was shown [321] that γ irradiation results in a *cis* to *trans* conformational change of methyl vinyl ketone located in the cavity of double hydrates of O_2 and CH_4; in the N_2 hydrate, this transformation does not take place. A unique example of using the muon spin spectroscopy to study free radicals in sII hydrates was reported.[322 – 324]

6. Hydrate formation kinetics ¶

6.1. Catalysts for hydrate formation

The fast and efficient preparation of gas hydrates can be accomplished using heterogeneous catalysts for hydrate formation. A significant part of studies in this field address the effect of nanoparticles of various types (metals, metal oxides, carbon materials) added to water on hydrate nucleation, the growth rate after nucleation and the attained degree of conversion of water into the hydrate. Nanoparticles are used either together with surfactants (suspension stabilizers) or without them. Relevant studies published up to 2017 inclusive were integrated in a review.[325] Analysis of the available results demonstrated that in most cases, the presence of nanoparticles leads to decreasing nucleation time and increasing rate of hydrate formation and increasing degree of water conversion to the hydrate. In the presence of surfactants, the action of nanoparticles is most often enhanced. Currently there are no generally accepted views on the mechanism of nanoparticle effect on the hydrate formation. Most likely, nanoparticles provide an additional surface for the heterogeneous nucleation of hydrates and intensify the heat and mass exchange in the

¶ The main data on the kinetics of formation and decomposition are presented in a recent review.[179] In the present review, we mainly consider new publications not included in the cited review.

liquid. Generally, analysis of the results considered in the cited review [325] indicate that the influence of nanoparticles added to water on the hydrate formation is still an intricate issue: in some cases the desired effects are absent, or characteristics are even deteriorated in comparison with pure water. For example, it was concluded [326] that graphene oxide, reduced graphene oxide, carbon nanotubes and sodium dodecyl sulfate accelerate hydrate nucleation and growth, but do not increase the degree of conversion of water to the hydrate. Other authors [327, 328] noted a promoting effect of sodium dodecyl sulfate and/or graphene oxide on all of the listed characteristics. Also, it was mentioned [329] that the hydrate formation rate increases in the presence of either hydrophobic or hydrophilic graphene in the system; however, as the graphene content in water increases, the effect becomes less pronounced due to agglomeration of particles. Grafting of the SO_3 group, similar to the hydrophilic group of sodium dodecyl sulfate, on graphene oxide markedly accelerates the nucleation and the subsequent growth of methane hydrate.[330]

Cox *et al.*[331] did not find an effect of clay particles or silicon dioxide on the nucleation and growth of methane hydrate, whereas the studies considered in the review [325] attest to acceleration of hydrate formation in the presence of silicon dioxide powders. Meanwhile, according to one more publication,[332] silicon dioxide nanopowders present in concentrations of several mass percent have an inhibitory effect on hydrate formation. The opposite effect was also observed under similar conditions.[333] The most probable cause for the observed discrepancies between the results of different authors is that they used different equipment, experimental techniques and different nanopowders. For example, opposite effects on the nucleation time were found for two samples of aluminium oxide nanopowders.[334] The observed effect depended on the state of the particle surface, but not on the nature of particles. In some cases, the presence or absence of an effect may depend on the presence of surfactants, the sample preparation procedure and insufficient amount of data for obtaining a statistically significant result.

The important role of the state of the powder surface is confirmed in some other works. It was shown [335] with certainty that hydrophobization of the surface of glass particles sharply decreases the induction period of hydrate formation; the results obtained for different hydrophobization agents can substantially differ. The state of water in the vicinity of hydrophilic particles and particles hydrophibized in different ways was studied by Raman spectroscopy.[336] It was shown that surface hydrophobization increases the structuring of adjacent water, which leads to a decrease in the induction period of hydrate formation. In the opinion of Nguyen *et al.*,[337] a more pronounced effect on the GH nucleation near hydrophobic particles is made by enrichment of the water layer adjacent to the particles with guest molecules. An interesting approach to the targeted design of a catalyst for CO_2 hydrate formation, namely, the silver salt of graphene-based polysulfonic acid, was reported.[338] The use of copper and silver complexes with oxidized carbon nanotubes proved to be rather successful; they increased the hydrate formation rate and the degree of water conversion to the hydrate.[339] A similar effect can be induced by additives of some powders of plant origin.[340] It was demonstrated [341] that the carbon steel surface and (to a higher extent) steel corrosion accelerate the methane hydrate nucleation.

6.2. Formation of hydrates from water dispersed in various media

One way to intensify the heat and mass exchange in the formation (decomposition) of GHs is dispersion of the aqueous phase. This method increases the gas – water contact area, with the medium acting as the heat conductor. The dispersion medium can also behave as a catalyst for hydrate formation, which accelerates GH nucleation and allows for conduction of the process at a lower thermodynamic supersaturation† of the system. In the outlook, studies along this line can form the basis for the design of a 'static' hydrate reactor without stirring devices, gas circulation, *etc*. An obvious drawback of using dispersing media is the decrease in the volume fraction of water and hydrate in the sample.

Below we consider publications in which the hydrate formation/decomposition took place in macroscopic pores. Li *et al.*[342] found that the hydrate formation rate and the degree of water conversion to the hydrate increase when the process is carried out in reactors filled with aluminium honeycomb. Modelling of hydrate formation in aluminium foam was reported by Fan *et al.*[343] Babu *et al.*[344] obtained a hydrate from a water-filled polyurethane foam; the GH formation (at least in early stages) took place on the surface of the foam as a result of the capillary suction of water from the foam bulk. Kumano *et al.*[345] studied the hydrate formation in a system consisting of a layer of water covered by an acrylic filter (sponge) and gaseous propane in the upper part of the reactor. The porous mass of the hydrate rapidly increased on the sponge part facing the gas, and hydrate growth also took place inside the sponge. Note that this system has an obvious similarity to water-cut sandstones.

Considerable interest was expressed in the hydrate formation in 'dry water' and 'dry foam' systems,[346 – 348] which represent aqueous dispersions stabilized by addition of $\sim$5 mass % solid particles with a hydrophobic-hydrophilic surface. It was ascertained [347, 349] that the stabilizing particles can act as catalysts for hydrate formation. After decomposition of the hydrate based on 'dry water', the disperse system is destroyed. The gel formation from dispersed water ('dry gel') allowed for conducting numerous reproducible hydrate formation – decomposition cycles.[346, 350, 351] The kinetic analysis of GH formation processes in these systems was performed by Shi *et al.*[352] In another study,[353] the obtained porous hydrogel particles were stabilized by a nanopowder. Recently,[354] repeated hydrate formation – decomposition cycles were implemented using a gel powder not stabilized by mineral particles. The features of the decomposition mechanism of GHs dispersed in 'dry water' were studied by Drachuk *et al.*[355] Podenko *et al.*[356] investigated the dependences of the rate of GH formation from 'dry water' and the efficiency of GH self-preservation on the content of the stabilizing nanopowder.

6.3. Effect of admixtures dissolved in water on the growth of gas hydrates

Surfactants that influence the GH growth were the earliest additives to be used for this purpose. In the case of pure

† Thermodynamic supersaturation is the degree of deviation of the actual thermodynamic state of a metastable system from the equilibrium state, which can be expressed in terms of pressure, temperature, concentration of hydrate former, *etc*.

water under static conditions, GH is formed as a thin film on the water surface. The film separates water and the hydrate former from each other, which sharply retards the hydrate formation. If a surfactant solution is taken instead of pure water, the mutual adhesion of GH crystallites decreases, most likely, due to the surfactant adsorption on the hydrate particles.[357, 358] The loose mass of the hydrate thus formed is pushed to the reactor walls by the crystallites newly formed on the liquid surface. This mass absorbs water due to capillary forces, which appreciably increases the contact area between water and the gas. As a consequence, a considerable part of the hydrate is formed directly inside the porous mass. It is also assumed that a surfactant added to the solution accelerates the dissolution of hydrate-forming gases. In most cases, the induction period of hydrate formation decreases in the presence of surfactants (see, *e.g.*, Ref. 359). The state-of-the-art studies along this line were reviewed in the literature.[179, 360, 361] It is of interest that hydrate formation in solution of a long known surfactant — soap (in this case, potassium oleate) — started to be studied only recently.[362] Some other compounds can act similarly to surfactants. In particular, the addition of ethylenediaminetetraacetamide markedly increases the degree of conversion of water to the hydrate.[363]

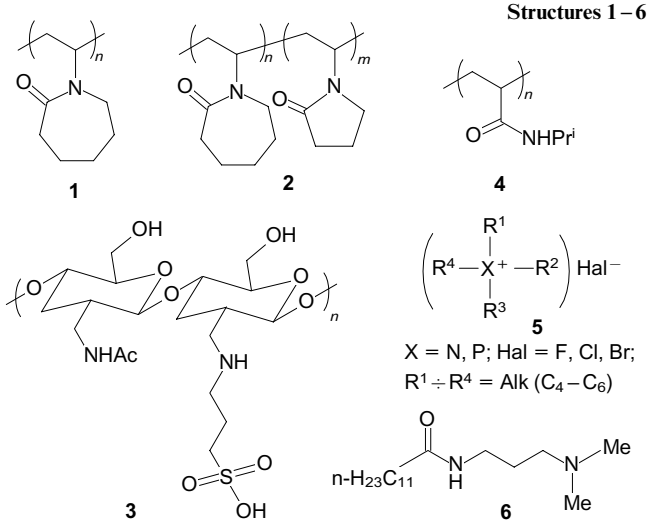
The most active studies of water-soluble additives influencing the hydrate formation addressed so-called low-dosage inhibitors — kinetic inhibitors (KIs) and anti-agglomerants (AAs). This class of inhibitors is called low-dosage because of small (up to 3 mass % relative to the mass of the aqueous phase) amounts of the inhibitors added to prevent the hydrate formation. As indicated above, thermodynamic inhibitors are normally used in markedly higher concentrations. The use of KIs and AAs decreases the environmental impact and is less expensive. Kinetic inhibitors retard the nucleation (or formation of substantial amounts of the hydrate); they are used when the supercooling is up to 10–12 °C. These inhibitors allow a multiphase flow to pass the pipeline part associated with the risk of hydrate formation before the hydrates are formed. The state-of-the-art studies in this field were reviewed in detail.[364–372] Practically, KIs are multicomponent compositions based on polymers such as poly(*N*-vinylcaprolactam) (**1**), *N*-vinylcaprolactam–*N*-vinylpyrrolidone copolymer (**2**),[366] sulfonated chitosan (**3**)[373] and poly(*N*-isopropylacrylamide) (**4**).[366] Typical AAs are quaternary ammonium or phosphonium salts (**5**)[374] or cocamidopropyl dimethylamine (**6**).[375]

Studies of KIs known to be environmentally friendly (non-modified biomolecules), *e.g.*, antifreeze proteins, starches, amino acids, chitosan and some other, have not yet met with success. The mechanism of action of KIs is not ultimately understood. Usually, the action of KIs is attributed to their adsorption on the hydrate nuclei or growing particles, which stops or retards the growth. Also, inhibitors disrupt the local structuring of water due to interaction between water molecules and inhibitor active sites.

An unusual effect related to KI (polyvinylcaprolactam) was found.[376–378] The authors ascertained that in the presence of KI, the decomposition temperature of a hydrate at a given pressure can shift towards higher values. This effect can be manifested even at rather low rates of autoclave heating (0.015 °C h^{-1}). It was shown that in the presence of KIs, several groups of separately melting hydrates can be formed from natural gas, instead of a continuous series of hydrates with regularly varying composition.[379] Kinetic inhibitors can noticeably change the occupancies of the cavities by guest molecules[380] and affect the hydrate decomposition rate.[381] The hydrate formation process that has already started can be accelerated upon the addition of KIs.[382] It was found[383] that bacterial cultures present in water can behave as KIs.

The anti-agglomerants are usually surfactants capable of being adsorbed on the GH surface and preventing hydrate particles from blocking the multiphase gas–water (brine)–crude oil flows.[374] The adsorbed surfactants endow the hydrate particle surface with hydrophobic properties; therefore, the particles are well wetted by oil and do not stick together. The surfactants that behave as AAs usually belong to quaternary ammonium or phosphonium salts or amine oxides in which one substituent is a long hydrocarbon chain, while the other substituents are selected in such a way as to ensure incorporation of molecules into incomplete cavities on the surface of a hydrate particle. Most likely, this accounts for the strong adsorption of AAs on the surface. Some AAs can also behave as KIs.[384] It was noted[385] that AAs better operate in the presence of high concentrations of dissolved salts and low content of water. Like in the case of KIs, the development of biodegradable AAs is a relevant issue (see, *e.g.*, Refs 386–388). It was shown[375] that in the presence of AAs and a minor amount of a liquid organic phase, the aqueous phase can be completely converted to the hydrate powder.

Structures 1–6



6.4. Some features of hydrate growth and morphology

Under natural conditions, hydrates are formed, most often, upon cooling of gas-saturated fluids moving in the rocks from dissolved and/or bubbling gas.[7, 54, 55] The natural hydrocarbon hydrates are polycrystalline materials, with little being known about the morphology of single crystallites. It is worth noting that large single crystals of air hydrate were found in the Greenland ice sheet.[389] Laboratory experiments are usually carried out with multiphase systems; studies in this field performed up to 2010 are summarized in a review.[390] In these systems, gas hydrates are formed at the interface between the aqueous phase and the hydrate-forming gas (organic liquid saturated with the hydrate former).[4] However, recent examples attest to hydrate formation at the contact between the wall and the aqueous solution of a hydrate former even if the interface indicated above was also present in the system.[391, 392] In the

absence of a surfactant, the contact surfaces are overgrown by a dense hydrate film. Probably, thickening of this film occurs due to diffusion of water through it.[393]

It was shown[394–397] that for water–hydrate-forming gas systems, with increasing supercooling (the driving force of hydrate formation), the crystallite size and the thickness of the formed hydrate film decrease, while the tangential film growth rate increases. When the supercooling is 4 to 8 °C, the hydrate films at the water/methane and water/cyclopentane interfaces were ~5 and ~12 μm thick immediately after their formation,[398] while after surface overgrowth, these values increased to 20–100 and 15–40 μm, respectively. The final film thickness increased with increasing supercooling. The published data on the growth rate of hydrate films at the water/methane interface as a function of system supercooling were summarized by Stoporev *et al.*[399] When the supercoolings were 2, 7 and 20 °C, the growth rates were ~0.01, 0.4 and 1 mm s^{-1}. In the case of the water/methane-saturated decane (toluene) interface, the rates were approximately the same,[400] while for the water/methane-saturated crude oil interface, the rates were somewhat lower.[401] Morrissy *et al.*[402] also detected a decrease in the growth rate of the hydrate film at the water/cyclopentane interface, caused by the presence of oil components in the system. For carbon dioxide, readily soluble in water, the growth rate of the hydrate film is approximately an order of magnitude greater.[403]

The authors of the cited publications assumed that the growth rate of the hydrate film is limited by heat transfer processes. Hence, they considered the dependence of the growth rate on the degree of supercooling of the system. The most recent data indicate that this may be incorrect. It was shown[403] that for equal supercooling, the growth rate increases with increasing temperature. According to several publications,[404–406] a more well-defined model implies that the rate-limiting step of hydrate film growth is mass transfer; correspondingly, the driving force in this case is concentration supersaturation of the hydrate former.‡ Apart from the slow film thickening due to the diffusion of water towards the gas phase, fast crystal growth from the film surface towards the bulk of water also takes place.[401,407,408] The morphology of the growing crystals varies from dendrimeric with different branching degrees at high supercooling to polygonal at low supercooling. The growth rates are <0.1 mm s^{-1}. In the authors' opinion, the growth of these crystals is provided by the hydrate former dissolved in water. Touli *et al.*[409] investigated the formation of carbon dioxide hydrate in thin capillaries. Generally, the hydrate formation features observed in these experiments are similar to those described above. The formation of a peculiar tubular crystal of the hydrate coaxial with the capillary can be considered to be the most interesting finding. The crystal wall and the capillary are separated with a gap, through which water suction towards the growing upper part of the crystal takes place. If the system contains a surfactant and a KI, the morphology of the growing hydrate changes. Since a strong film cannot be formed at the interface, the hydrate expands both towards the aqueous and gas (organic) phases.[410–414]

Karanjkar *et al.*[411] described the formation of unusual hollow conical crystal hydrates in these systems. Mitarai *et al.*[414] observed detachment of small hydrate crystals from the film and their transfer to the aqueous phase. It is known that in the presence of a surfactant, some of the hydrate crystals are squeezed out from the water–gas interface, and the porous crystal mass creeps over the reactor wall (for details, see Ref. 392). It was shown[415,416] that the hydrate formation in the presence of a hydrophilic glass surface results in creeping of the hydrate over the wall. The degree of spreading of the hydrate layer over the surface depends on the surface material (hydrophobization reduces spreading of the hydrate film). In the absence of walls (levitated droplet), formation of the hydrate shell on the droplet surface was followed by a non-uniform change in the shape of the resulting particle, which thus roughened.[417] The hydrate growth towards the gas phase was noted; this was probably caused by the presence of defects and/or pores in the hydrate film.

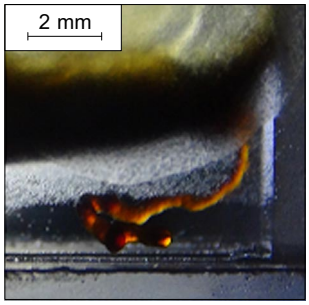


Figure 14. Photograph illustrating the unusual shape of the growing hydrate (snake) from the water/gas or water/crude oil interface towards the bulk of the aqueous phase.[401]

In conclusion, mention should be made of unusual types of growth, rather frequently encountered for hydrates: so-called whisker crystals and their colonies.[418] The length of these crystals may be thousand times greater than the thickness. The conditions determining the formation of such crystals are not entirely clear. Probably, this requires the presence of an active site — the catalyst for hydrate formation, which is freely accessed by the gas and by water *via* capillary suction. Stoporev and co-workers[399,401] observed unusual forms of hydrate growth (bubbles, snakes, see Fig. 14) from the water/gas or water/oil interface towards the bulk of water. The appearance of such forms can be attributed to either growth of a bundle of whisker crystals into the bulk of water or to specific features of the hydrate film growth.

6.5. Gas hydrate dynamics in systems containing liquid hydrocarbons

The development of efficient inhibitors and promoters of hydrate formation requires in-depth understanding of the gas hydrate nucleation and growth processes in various media, in particular in liquid hydrocarbons (crude oil). Detailed information on the modern views on the nucleation mechanism of GHs can be found in reviews.[419–422] A very interesting and poorly studied aspect is the possible multistage character of hydrate nucleation and growth. These processes can be markedly complicated by various types of nucleation taking place in the system (repeated events of primary nucleation, secondary nucleation and nucleation on various surfaces), formation of hydrates of different structures in the case of gas mixtures and even phase transitions in the nucleus according to the following possible sequence: metastable liquid–amorphous solid–metastable crystalline phase–stable crystalline phase.[179,423] The simplest case is a two-stage process of gas hydrate formation from C_1 and C_3 (in the general case,

‡ To our current knowledge, there are no studies in which a relatively large array of available experimental data is analyzed from this standpoint.

C_1-C_4) gas mixtures, which can be attributed to successive formation of hydrates with two different structures (see, *e.g.*, Ref. 424). First, a mixed sII hydrate is formed from the gas mixture. When the C_3-C_4 components are completely consumed in the hydrate formation reaction, the formation of sI hydrate starts. Multistage nucleation is probable in the systems in which repeated processes can take place (primary and/or secondary nucleation). In water-in-crude oil emulsions, a situation is possible where drop associates act as separate microreactors. In thermal curves, this can be manifested as several exothermic peaks (multiple primary nucleation).[425] If every water droplet in the emulsion acts as a microreactor, latent crystallization of the hydrate is possible, so that the exothermic peaks cannot be detected.[426,427] When secondary nucleation takes place in the system, multiple exothermic effects can be manifested in the thermal curves. The cause for the observed phenomenon is that the crystallization occurs on new nucleation sites, which are represented by the previously formed hydrate crystals. This behaviour can be due to the following factors:

— crystal growth between droplets;

— involvement of the unreacted water, for example, water covered by the hydrate crust (this can occur in water-in-crude oil emulsions when hydrate particles collide with one another).

Makogon *et al.*[428] demonstrated experimentally that the frequencies of formation of hydrate clusters on different faces of the crystal sharply differ from one another. Other possible causes for the presence of several stages of nucleation were noted above, in particular, the formation of post-critical nuclei on various surfaces present simultaneously in the system [410,429] and the formation of metastable phases.[423,430–436] The formation of metastable hydrate phases is most often observed when the driving force of the process (supercooling) is high. This can occur, for example, in the case of fast cooling under conditions where the formation of the stable phase is retarded for some reason. The formation of metastable hydrates and their subsequent recrystallization to stable polymorphs have been little studied due to obvious instrumental difficulties. The modern publications do not distinguish between the described alternatives of the multistage crystallization mechanism. Meanwhile, the mentioned details clearly indicate the complexity of this mechanism both in the early stage where phase transitions in the hydrate nucleus take place and in later stages when new crystallization sites are formed.

Thus, in the presence of a sufficient amount of hydrate former and water, the arising GH particles continue to grow and be accumulated in the system, which heavily complicates the oil and gas production. The possible mechanism of hydrate plugging of oil–water (brine)–gas multiphase flows was considered in a series of studies.[437–439] In such systems, hydrates are usually formed in the reaction of free and/or oil-dissolved associated gas with water emulsified in oil. The key stages include the heterogeneous hydrate nucleation at the water/oil interface, fast growth of the hydrate film on the surface of water droplets and slower subsequent growth of the hydrate inside the droplets. The last-mentioned process is rate-limited by gas or water diffusion into the reaction zone.[440] Despite the large contact area between water and oil saturated with hydrate-forming gas, the nucleation can also take place on the solid surfaces present in the system (vessel walls, suspended particles, phase interfaces, *etc.*);[419,441] the surface roughness and defectiveness considerably influence its ability to promote or inhibit the nucleation of the hydrate phase. We do not consider here the homogeneous nucleation, because conditions for this nucleation to proceed cannot be attained in practice,[442] except for the nucleation of tetrahydrofuran hydrate.[443,444] According to the classical nucleation theory, this process is stochastic and is described by a certain distribution function (survival function).[445] In practice, deviations from the classical theory are often observed.[446–449] The non-classical behaviour can be due to the presence of specific nucleation sites or to overestimation of the frequency of attachment of building units to a subcritical nucleus in the classical theory. The following hypotheses are currently considered to explain the mechanism of GH nucleation:[420–422]

— labile-cluster hypothesis,

— local-structuring hypothesis,

— blob hypothesis, and

— cavity-adsorption hypothesis.

The nucleation of gas hydrates can be affected by the degree of supersaturation, the presence of admixture microparticles, solid surfaces and other phases[450] (see also references given above in this Section), which attests to the multifactorial nature of this process. The addition of crude oil to a hydrate formation system leads to an avalanche increase in the number of parameters influencing GH nucleation: oil composition; emulsion composition, type, viscosity and density; the presence of mineral particles; state of the resin and asphaltene components (colloid solution or aggregates) and so on. In the case of static conditions of the experiment modelling, for example, arrest of the flow during oil production, the time dependence of the GH nucleation rate has not yet been studied. The processes such as the structuring of oil disperse systems and sedimentation of water droplets emulsified in oil may result, with time, in a change in the type and number of nucleation sites and consequently, a change in the nucleation rate. Nevertheless, some regularities of formation (and decomposition) of gas hydrates in oils were identified. The hydrate growth inside a water droplet in an emulsion obeys the contracting sphere model, although the results of some studies demonstrated that the real situation can be more complicated.[410,417,440] Some components present in oil can act as KIs and AAs.[451–453] The possibility of influence of oil components (asphaltenes) on the hydrate formation was also confirmed by the results of theoretical calculations.[441,454] The effect of asphaltenes on the hydrate nucleation and growth was studied experimentally.[197,455] Asphaltenes can either promote or inhibit GH nucleation; this depends on the type of gas (hydrocarbon, CO_2), composition of the medium; the presence, type and roughness of a substrate; and, apparently, on the characteristics of asphaltenes (chemical composition, molecule mass, degree of aggregation). To date, there is no common opinion on the influence of these compounds on the hydrate formation processes.

For attaining a stable flow of reservoir fluids, it was proposed to arrange joint transportation of oil and gas in the hydrate form.[456] Study of the rheology of hydrate slurries is important for both the development of this technology and intensification of hydrate accumulation under dynamic conditions. The modern approach to the description of dynamics of gas hydrate slurries was described in several publications.[438,457–459] For hydrate slurries in water-in-oil emulsions, the rheological model

considers rough hydrate particles of an arbitrary shape, apart from hydrate formation on water droplets. The viscosity of hydrate slurries is, as a rule, higher than the viscosity of emulsions from which they have been obtained, because of the stronger interaction between solid particles. The hydrate particles in a slurry can be combined into aggregates, the size of which is determined by two main opposing factors

— the presence of cohesive forces between the particles, promoting aggregation,

— the hydrodynamic effect of the slurry flow (shear stress), which tends to destroy the aggregates.

The accumulation of hydrates largely depends on the pipeline geometry (tilting angles, the presence of corners and bends).[460] In the presence of free water on the particle surface, the binding strength between these particles considerably increases due to the formation of capillary bridges (see Section 4); *i.e.*, the probability of agglomeration is much higher for wet particles than for dry ones.[461,462] The addition of surfactants results in adsorption of their molecules at the hydrate/oil interface, the hydrate surface is thus wetted with oil, no water capillary bridges arise, and particle agglomeration is prevented[439,463] (see also Sections 4 and 6.3). The particle agglomeration is unfavourable in this case, because the interaction forces of hydrate particles with one another and with oil are similar. The length of the hydrophobic part of the surfactant molecule, the interfacial film density and the adhesive forces between the molecules and the GH surface are considered as the key factors influencing the anti-agglomeration properties of surfactants.

When the water content is low (as a rule, $< 10-15$ vol.%), the behaviour of hydrate slurries in hydrocarbons resembles the behaviour of Newtonian liquids. In other cases (especially in the presence of free water), non-Newtonian behaviour is observed, particularly, hydrate slurries demonstrate pseudo-plasticity, *i.e.*, their viscosity decreases with increasing shear stress.[464] With other factors being the same, the absolute values of viscosity increase with increasing volume content of the hydrate in the slurry. The observed changes in the rheological properties of the slurries depend on the time and on their prehistory, *i.e.*, these systems are thixotropic. Obviously, the non-Newtonian rheological properties of hydrate slurries are caused by the possibility of aggregation of hydrate particles and formation of a three-dimensional network of aggregates. It is noteworthy that overgrowing of capillary bridges with the hydrate results in the formation of monolithic porous structures, *i.e.*, the character of interactions between hydrate particles fundamentally changes. The rheology of a hydrate slurry depending on the flow regime and composition of the medium is mainly described using the Hagen – Poiseuille law,[465] Rabinowitsh – Mooney equation,[466] extended differential effective medium theories[458] and the Herschel – Bulkley model.[464,467]

The rheological properties of hydrate slurries are studied using experimental equipment such as 'loops' (pipeline models) and rotational rheometers. An interesting modification of the rock-flow cell, in which the fluid flow is generated by cell deviation from the horizontal position, was recently proposed.[468–470] The cell can model different flow regimes and makes the inner part of the flow accessible for visual observation. The new cell is much more compact than the loop. Wang *et al.*[471] considered a model that opens up the possibility of predicting the behaviour of hydrates in systems with predominance of either oil or water. The model allows one to select the concentration of several thermodynamic inhibitors taking into account the addition of AAs. It was noted that the presence of crude oil components (paraffins) may lead to the loss of effectiveness of several AAs,[472] whereas in the presence of salt ions (Na^+ and Cl^-), the minimum effective AA dose may decrease.[473] As the hydrate is being formed in a pipeline, the pressure drop along the metering section increases, while the flow rate decreases, *i.e.*, the apparent viscosity of the slurry increases. The apparent viscosity of the slurry increases with increasing content of the hydrate and decreases with increasing shear rate (see, for example, Ref. 467). When the flow is stopped (shut-in scenario in the pipeline), it can be restored in the presence of anti-agglomerants in > 1 mass % concentration. At lower concentrations, the cohesive force between the hydrate particles may increase, and if the shut-in period is long, pipeline plugging may occur.[473]

Measurements using rotational rheometers provide more accurate rheological characteristics of the suspensions than the loop data; however, the metering conditions are far from field experiments. Webb *et al.*[474–476] investigated the rheological properties of hydrate slurries in crude oil, dodecane and mineral oil (in particular, in the presence of surfactants). It is noteworthy that on heating slurries with a high water content, the viscosity first decreases due to a decrease in the viscosity of the dispersion medium; when the hydrate starts to decompose, the viscosity increases, due to agglomeration of the melting hydrate particles as free water appears in the system, and passes through a maximum. Analysis of a large array of data demonstrated that the highest viscosity values are found for samples with a degree of conversion of 40 – 70%.

A large array of numerical information on the rheological properties of hydrate slurries in oil and comparison of experimental and calculated values have been reported.[477,478] Majid *et al.*[478] found a nearly exponential dependence of the apparent viscosity of slurries on the hydrate content. A study of the rheological properties of hydrate slurries depending on the type of stabilizing agents was reported by Lv *et al.*[479] The effect of paraffins on the formation and rheological characteristics of GH slurries was reported.[452,480] Note that the addition of paraffins to the system did not affect the pseudo-plastic behaviour of the slurry, although the viscosity increased with increasing concentration of the additive. The growth of the hydrate with paraffins occurred in two stages at a lower rate. The authors attributed this finding to deposition of paraffins, which hampered mass transfer and, hence, prevented further growth of the hydrate.

A number of studies[467,481–483] describe the effect of hydrates on the flow of multiphase gas – water – oil – hydrate systems in pipelines. It is known that, depending on the number of phases, their properties and character of interaction, the following main flow regimes are possible in these systems:

— stratified flow (layer by layer flow of gas and liquid phases),

— slug flow (flow of large bubbles separated by continuous liquid),

— bubble flow (liquid flow with gas bubbles),

— annular flow (flow of the liquid phase along the pipe walls with the gas being at the centre).

In the cited studies, it was shown experimentally that the presence of the hydrate may lead to a change in the flow regime, *e.g.*, a turbulent flow changes to a laminar flow.[467] In general, it can be stated that the rheology of hydrate slurries is now being actively studied. The knowledge gained in this area often makes it possible to avoid flow blockage by hydrate deposits. Nevertheless, hydrate plugs are still formed. The methods used to detect them were described by Longo *et al.*[484]

The final stage of the hydrate life cycle is decomposition. Depending on the GH decomposition temperature, two groups of systems can be clearly differentiated: those decomposing above and below 0 °C (some features of hydrate behaviour below the melting point of ice were covered in reviews[485,486]). Most often, at temperatures above zero, gas hydrate decomposition takes place at equilibrium temperatures (an exception is provided by the abnormal influence of KIs). However, in some cases, it is possible to obtain superheated GHs (see Sections 3 and 6.3 and Refs 222, 376–378) and influence the rate of hydrate decomposition. For example, it was shown that the addition of 0.1 mass % polyvinylpyrrolidone (typical KI) and 0.5 mass % lecithin to the drilling mud considerably retarded hydrate dissociation in the hydrate-containing rocks at 2 °C.[487] One more interesting way of suppressing the hydrate decomposition at positive temperatures is forced preservation attained by coating of the hydrate by another, more stable hydrate, *e.g.*, coating of the THF hydrate by a layer of cyclopentane hydrate.[488–490] To the best of our knowledge, except for the examples described above, there are no more methods for suppressing the hydrate decomposition at positive temperatures (this implies the occurrence of a hydrate outside its stability region).

At temperatures below 0 °C, the rate of hydrate decomposition often sharply decreases (down to almost complete termination) due to the self-preservation effect related to the formation of an ice film on the surface of hydrate particles.[491–493] A detailed study of the hydrate decomposition demonstrated that in a particular temperature range, the surface decomposition of a hydrate particle gives a gas and supercooled water (see, *e.g.*, Ref. 180). The formation of a pseudo-liquid interfacial transition layer between the hydrate and ice was demonstrated by Nguyen *et al.*[494] In addition, it was shown[495] that a pseudo-liquid layer of water can be formed on hydrate particles due to the premelting effect, which influences their agglomeration. This effect can be responsible for the self-preservation of hydrates in oils.[496]

The possibility of controlling the decomposition of gas hydrates by choosing an appropriate host medium was discussed by Takeya *et al.*[497] It was also shown[221] that decomposition of methane hydrate in the pristine and modified halloysite nanotubes at temperatures below 0 °C occurs in different ways. In the former case, the reaction rate decreases after a part of the hydrate has decomposed, and some of the hydrate survives almost to 0 °C. Clay modification (unification of the surface, closure of large pores) results in one-step hydrate decomposition in the vicinity of the equilibrium temperature (−80 °C). It was found that sea water (2.7 mass % NaCl) also gives rise to self-preservation of methane hydrate.[498] A mixture of ice and hydrohalite ($NaCl \cdot 2H_2O$) serves as the preserving layer in this case. However, this process is possible only at temperatures below the eutectic temperature (−20 °C) of the water–sodium chloride system. Melting of hydrohalite results in hydrate decomposition. A similar conclusion was drawn earlier.[282,499] In a study[282] considering a non-salt system, melting of an alcohol solution induced dissolution of the protective ice shell, and self-preserved mixed hydrate of methane and propan-2-ol decomposed at temperatures above −20 °C.

For oil-containing systems, decomposition of hydrate slurries was studied in a model environment (diesel fuel) with both low (10–30 vol.%) and high (95–100 vol.%) water contents.[500,501] It should be noted that self-preservation was observed in these systems only upon the formation of the bulk hydrate. In the case of GH slurries obtained from water-in-oil emulsions, efficient self-preservation took place even when the size of hydrate particles was about a few tens of micrometres.[496,502,503]

Mixing of a pure methane hydrate powder with oil fractions such as resins, asphaltenes, saturated hydrocarbons, aromatics and polar compounds under conditions of hydrate stability and subsequent decomposition demonstrated that the branched saturated hydrocarbon fraction of crude oil is responsible for efficient self-preservation. In addition, it was shown that the diffusion of the methane molecule is hampered in the presence of crude oil. It can be assumed that the gas released upon decomposition forms a local supersaturation, thus creating a sort of 'as buffer vessel' around the hydrate particle. Alternatively, the specific hydrophobic environment provides better conditions for the formation of the protective layer. The dynamics of decomposition of methane hydrates obtained in different crude oils and in different ways (synthesis from emulsions and mixing of pure hydrate with crude oil) at a constant temperature (−20 °C) is depicted in Fig. 15. The hydrate decomposition rate barely depended on variable parameters, being equal to ~ 0.02 mL g^{-1} min^{-1}. However, it should be noted that the particle size in the slurry (with an invariable size of hydrate particles) often affected the proportion of GH that decomposed below −20 °C. Currently, it is unclear why self-preservation of hydrate slurries is observed in complex mixtures of isoalkanes (for example, in transformer oil), but does not occur in suspensions based on linear alkanes.

In conclusion, it can be stated that studying physicochemical processes of hydrate interaction with components of the medium during the GH formation, growth and dissociation (especially below 0 °C) provides more in-depth understanding of their mechanisms and, hence, would not only help to avoid emergency situations in oil fields, but would also contribute to the development of scientific grounds for application of hydrates in some modern technologies.

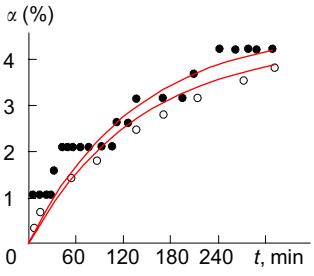


Figure 15. Dynamics of decomposition of methane hydrate slurries in various crude oils at −20 °C. α is the fraction of the total gas content of the hydrate. The Figure was prepared by the authors using the data of Refs 504, 505: dark and light dots, respectively; lines are approximations of these data.

7. Technological applications of gas hydrates

7.1. Natural gas storage and transportation

Natural gas transportation is mainly accomplished by three methods: gas pipeline transport, transportation of liquefied natural gas (LNG) at a temperature of approximately −160 °C and of compressed natural gas (CNG) at a pressure of 20 – 25 MPa by special tankers. A currently considered alternative to these methods is natural gas storage and transportation as natural gas hydrates (NGH) or solidified natural gas (SNG). Regarding the specific gravity of the stored gas, this method is inferior to LNG and CNG technologies by factors of ~3.5 and ~1.7, respectively. The major part of the cargo in the NGH/SNG technology is water. Benefits of the gas hydrate method are simple storage design (thermally insulated vessels) and mild storage conditions (atmospheric pressure, slight negative temperatures, see below). The absence of high pressure and cryogenic temperature, and also slow release of the gas upon destruction of the storage vessel makes this transportation and storage technique the safest among the considered ones. Furthermore, since only gas and water participate in the process, the technique can be regarded as environmentally friendly.

According to feasibility study, the use of the NGH/SNG method is most promising for gas supply to small household and industrial consumers not connected to long distance pipelines,[506] for the design of stationary gas storage in which the gas specific gravity in the tank is not critical, and for the development of small fields.[507, 508] The delay in the implementation of gas transportation and storage as gas hydrates can be attributed to a low rate of GH accumulation. A highly promising approach to increasing rate of formation of gas hydrates and attainable degree of conversion of water to the hydrate is the use for hydrate formation promoters (see Section 7.4). It is noteworthy that under certain conditions, the safety of hydrate gas storage may become the crucial factor determining the expediency of using this technique. The engineering and economic aspects of the NGH/SNG technology were considered in a review.[486] An interesting modification of this technology may be the 'direct' combustion of gas hydrates (combining the stages of hydrate decomposition and released gas combustion); studies of processes taking place in this case have been reported.[509 – 511]

It is currently believed that for hydrate storage and transportation, it is possible to use pipeline transportation of slurries of hydrate powder in hydrocarbons thermodynamically stable under transportation conditions (see below) or pellets consisting of gas hydrate and ice with a size from a few millimetres to a few centimetres. In these pellets, gas hydrate occurs in the self-preserved state. According to a number of publications,[512 – 514] by joint packing of elliptical pellets of various sizes, it is possible to fill up to 78% of the storage volume; if the pellets have equal size, the degree of filling of the storage markedly decreases. It is noteworthy that large blocks shaped as rectangular parallelepipeds would be most favourable for hydrate storage. However, currently there are no ways for producing such blocks. The temperature dependence of the decomposition rate of the pellets under atmospheric pressure has the lowest minimum at a temperature of −20 °C, which accounts for the choice of this temperature for hydrate transportation. At −5 °C, the rate of gas loss from the pellets increases by more than an order of magnitude. The rate of gas loss from the pellets depends on the method of their production and the storage period. Initially, it amounts to ~0.7% and then it decreases down to ~0.1% per day.[515 – 517]

The feasibility study of the possibility of sea transportation of natural gas as GHs was carried out by specialists from Japan, Germany and South Korea.[515 – 518] In particular, Japanese researchers considered the issue of natural gas hydrate transportation from small and medium gas pools in Indonesia (currently, their development is not economically viable). For shipping of field-produced gas hydrates, it was proposed to build a fleet of eight specially designed vessels with a displacement tonnage of > 50 000 tons. Studies demonstrated that this method could be implemented, but under existing conditions, it is not economically feasible. It is of interest that one of the engineering problems found during the research was associated with the caking of hydrate pellets during transportation. For solving this problem, it was proposed to rotate the GH vessels during the trip.

A demonstration project on gas supply to small domestic and industrial consumers using the gas hydrate technology reached the practical implementation stage.[519, 520] The project included the construction of an industrial unit for the production of 5 tons of hydrate pellets per day and manufacture of transportable containers for gas delivery (Fig. 16). The hydrates were produced using the cold from liquefied natural gas discharge terminal. A 280 kW industrial power generator and a residential complex for 10 families were taken as the consumers in the project. Note that in Japan, pipeline transportation is used most often for gas delivery. Meanwhile, there are some industrial and household consumers to whom it is difficult or not economically feasible to lay pipelines.

This project was meant for gas supply to exactly these consumers. The pellets with the initial hydrate content of 70 – 80% were transported in a polyurethane foam-insulated container holding up to 7.5 tons of hydrates (up to 650 m^3 of the gas) for the industrial consumer and two containers delivering 400 kg of hydrates (~50 m^3 of the gas) for household use. The transportation time of the hydrates was ~2 h (the distance was 100 km). It was found that after completion of the self-preservation process, the gas content in the pellet changed little over a week,

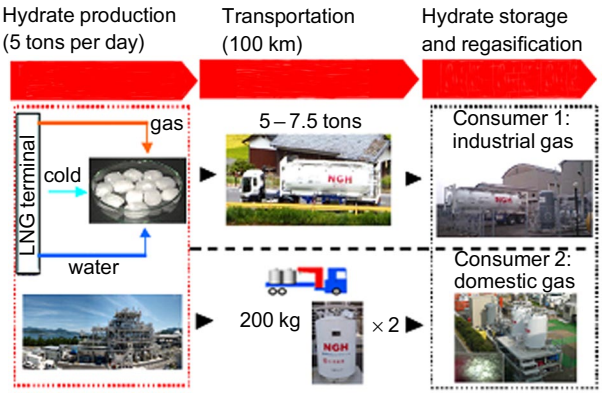


Figure 16. Demonstration project on gas supply to small domestic and industrial consumers using the NGH (SNG) hydrate technology. The Figure was adapted from Ref. 20 with the permission of copyright holders.

whereas the gas loss during this process reached 10%. The gas working pressure in the containers was up to 0.8 MPa. Hydrates decomposed as warm water was circulated across the container bottom; the amount of the obtained gas was controlled by varying the intensity of circulation. The implementation of the demonstration project showed the possibility of transportation (with acceptable loss) and use of natural gas supplied as gas hydrate.

It is beyond doubt that gas hydrate technologies for natural gas delivery and storage have good prospects for the northern regions of Russia and countries with similar climatic conditions.[521 – 523] It should be noted that the use of hydrates is also intended for the disposal of CO_2 (see, *e.g.*, Refs 524, 525) and N_2O.[526] The use of gas hydrate technology for the construction of underground hydrogen storage was also considered in the literature;[527] however, the probability of practical implementation of this project is relatively low.

Examples of joint crude oil and natural gas transportation as gas hydrates are currently represented by Cold Flow[528] and HYDRAFLOW[529] processes. The Cold Flow process implies pipeline transportation of slurries of hydrate particles in crude oil; the particles do not tend to stick together or to pipeline walls.[456] Low particle sticking to pipeline walls and to other hydrate particle is ensured in this case by the absence of a free water film on the particle surface, as water is completely converted to the hydrate. In this flow, all phases are in thermodynamic equilibrium; therefore, the composition and amounts of flow components do not change during the transportation. To ensure complete conversion of water to the hydrate, it was proposed to inject a large amount of fine hydrate particles (seeds) into the turbulent multiphase crude oil – water – gas flow; naturally, the $P-T$ conditions in the flow should correspond to the hydrate stability zone. This technology is considered to be applicable to multiphase flows with an initial water content of up to 20 vol.%. The use of this method may decrease the wax deposits on the pipeline walls, probably due to the partial wax deposition on the hydrate particles and abrasive action of these particles. For fast and most complete conversion of water to the hydrate, it was proposed to inject a large number of fine hydrate particles (seeds) into the multiphase flow and provide for vigorous stirring of the flow using static stirring devices located in the pipeline.

The HYDRAFLOW process implies free formation of the hydrate in the multiphase flow.[530] In this case, hydrates should be formed before the possible complete disappearance of the gas phase, and this requires an excess amount of water compared with the amount of the gas. The stability of the obtained hydrate slurry in a mixture of hydrocarbons and water is provided by adding AAs. In the case of crude oils containing a sufficient amount of natural AAs, no additives are required. The content of hydrates in the multiphase flow can reach 30 vol.%; the viscosity of the pumped mixture can be adjusted by changing the content of oil, water or hydrate. The state of the art and prospects of development of the above-mentioned processes are discussed in a review of Straume *et al.*[531]

7.2. Separation of mixtures using gas hydrates

When GH is formed from a mixture of gases, the concentration of each gas in the hydrate differs from its concentration in the gas phase occurring in equilibrium with the hydrate (see Section 3). This phenomenon can be used to separate gas mixtures; this issue was discussed in detail in the literature.[6, 532, 533] As a rule, all hydrate-forming components present in the initial mixture can be found in the hydrate, but the components with better hydrate-forming properties (low equilibrium pressure and higher equilibrium temperature of the corresponding single-component hydrates) are present in higher amounts. In this regard, it is more reasonable to use hydrate formation (usually, in several stages) for the rough separation of large amounts of a gas mixture into several constituents and further purify each of them by other methods. Xu *et al.*[534] described a continuously operating two-stage pilot unit for the separation of synthesis gas (40% CO_2 + 60% H_2). As a result of hydrate formation, the hydrogen concentration in the mixture increased to ~85%; then the degree of hydrogen purity was brought to >99% as a result of adsorption purification. The energy consumption for the separation proved to be 30% lower than that for the cryogenic process.

Combined hydrate and membrane separation of multicomponent gas mixtures containing heavy hydrocarbons and hydrogen sulfide has been described.[532, 535] In this method, hydrate formation is used for preliminary removal of the indicated components prior to the membrane separation of light gases (CH_4, CO_2, N_2). It is clear from general considerations that the gas hydrate separation would be the most efficient if the equilibrium $P-T$ conditions of hydrate formation for the gases to be separated are considerably different (the presence of impurities may significantly affect the separation[536, 537]). It was shown[538] that in the general case, the separating capacity of the hydrates depends on the driving force (supercooling), the presence (or absence) of promoters and even the occupancy of cavities; also the effect of various promoters on the degree of gas separation was discussed. This process is determined (with contents of the components being similar) by the rate of conversion of various gases to the hydrate form.

2-Naphthyl-substituted sulfonate and lignin with a low sugar content (with no promoter properties) proved to be effective for the separation of methane and CO_2 mixtures. Reagents of this type should facilitate capture of one gas and prevent the hydrate formation for the other gas. The most pronounced effect is observed when the driving force is moderate (near the equilibrium curve). n-Hexyl polyglucoside and octyldecyl polyglucoside were found to be efficient for the hydrate separation of CH_4 and N_2 (the percentage of methane in the hydrate form increased by 10%). Tetra-n-butylammonium bromide (TBAB) is inefficient for the separation of CH_4 and N_2 mixtures.[539] In the TBAB hydrate, only small cavities are vacant, and the affinities of methane and nitrogen molecules for these cavities differ little. Conversely, methane – CO_2 and nitrogen – CO_2 mixtures can be efficiently separated using ionic clathrate hydrates.[540, 541] The addition of sodium dodecyl sulfate, which is a typical kinetic promoter of hydrate formation, somewhat improves the separation of CH_4 and N_2 mixtures.[542] The authors[542] believe that the desired degree of separation can be attained by increasing the number of hydrate formation cycles. In the THF hydrate, all large cavities are also occupied. However, this hydrate can be used as a molecular sieve for the separation of methane + hydrogen or carbon dioxide + hydrogen[543] gas mixtures (nitrogen-containing mixtures were not studied in the cited work). It was shown[544] that for a nitrogen content of 25 vol.% in the gas phase, only 3% of nitrogen passes to the hydrate if the hydrate is formed from a 40% aqueous

solution of methanol (thermodynamic inhibitor). A combination of the hydrate and absorption methods for the separation of a mixture of methane, ethane, ethylene and nitrogen was described by Liu *et al.*[545] In this case, the hydrate formation was carried out in a water-in-diesel fuel emulsion. The initial gas (15% of ethane and ethylene) was separated into two streams containing 2 and ~50% of these components.

In connection with the task of reducing the atmospheric emission of carbon dioxide, many studies address the separation of various CO_2-containing gas mixtures. Studies in this field are considered in detail in a number of reviews.[546 – 548] Numerous experiments were carried out for the isolation of CO_2 and CH_4 from their mixtures with air (or nitrogen as model air) and with nitrogen and sulfur oxides.[549] The methods of separation of these gas mixtures *via* GH formation were described in recent patents (see, *e.g.*, patents [550 – 552]). The authors classify these studies as being directed towards the development of methods for the extraction of greenhouse gases from the flue and mine gases (mixtures of methane released from coal with air used for mine ventilation).

In most cases, attempts are made to withdraw CO_2 and CH_4 from gas mixtures by capturing them in a double hydrate with some auxiliary hydrate-forming component. In view of the huge volumes of gases to be separated and the need to put them under pressure for hydrate formation, the prospects of this trend of research are not obvious. It seems more promising to use hydrate methods in those cases where the initial gas is already under a pressure high enough for hydrate formation (separation of synthesis gas, isolation of noble gases from natural gas), or in the case of gases that form hydrates at moderate pressures (sulfur hexafluoride, Freons). Ahn *et al.*[553] described a continuous laboratory setup for the separation of SF_6 contaminated with air. An increase in the sulfur hexafluoride concentration from 81 to 93% was attained. Development of gas hydrate processes for SF_6 purification and collection is in progress.[554] The hydrate separation of synthesis gas was covered in reviews.[555, 556] In this case, carbon dioxide is trapped *via* the formation of double hydrates with a variety of auxiliary components such as THF, cyclopentane, quaternary ammonium salts, *etc*. The above-mentioned attempt to use THF hydrate as a molecular sieve for the isolation of H_2 is also of interest.[543]

Analysis of the literature demonstrated that the following techniques appear promising for the separation of gas mixtures *via* hydrate formation:

— hydrate formation at a low driving force (near the equilibrium) without additives (formation of the most stable hydrate);

— hydrate formation at a low driving force (near the equilibrium) using the water memory effect (acceleration of hydrate accumulation);

— molecular design of the reagents facilitating capture of one of the gases and hampering the hydrate formation by the other gas; development of additive formulations;

— hydrate formation from ice in the thermal cycling regime (above and below the melting point of ice);

— hydrate formation in a porous medium (see, for example, Ref. 557);

— addition of an organic liquid that would increase the methane content at the water/organic liquid interface (hydrate formation from emulsion);

— combination of the above techniques.

The possible application of hydrate-based separation techniques is associated not only with the separation of gas mixtures. A gas hydrate process of gas condensate stabilization is described in a patent.[558] Furthermore, the use of GH formation for drying liquid chlorine was proposed.[559] One of the separation processes that may be accomplished using gas hydrate technology is desalination of water. None of the salts usually present in natural brines can be incorporated into the gas hydrate framework. Therefore, upon hydrate formation, the dissolved salts are concentrated in the residual liquid (brine). If the hydrate is completely separated from brine, then hydrate decomposition will give pure water. The gas hydrate desalination processes were first tested in the 1960s – 1970s. These methods were inferior in efficiency to conventional methods, first of all, due to high energy consumption for the compression of gases and cooling of the reactor, complexity of separation of GHs from brine and a low rate of hydrate formation. In recent years, it was proposed to combine the gasification processes of liquefied natural gas delivered by tankers (cold generation) with water desalination.[560] This combination undoubtedly increases the energy efficiency of the process and makes it competitive compared to well-developed distillation and reverse osmosis techniques.[561] Meanwhile, the problems of increasing the efficiency of GH separation from brine and the GH formation rate remain relevant. The current state of research in this field is reflected in reviews.[562, 563]

7.3. Other gas hydrate technologies

A potentially possible application of hydrates is the application as a working medium in cold storage devices in centralized air conditioning systems for buildings. The need to use these devices is associated with the difference in the cost of electricity during the day and at night, which is typical of many countries. It appears to be more appropriate to accumulate the working medium at night when the electricity is cheaper and to consume the cold during the day. From the efficiency standpoint, it is cost-efficient not only to cool the working medium of the storage device, but also to select compounds in which the phase transition is accompanied by heat absorption.

Currently, hydrates of tetraalkylammonium salts are considered to be most promising among the hydrate inclusion compounds. Also, the possibility of using gas hydrates of Freons and carbon dioxide for this purpose is considered. The state-of-the-art studies in this field are described in detail in a paper [564] and in a review.[565] Certain researchers' attention is now paid to studying the applicability of gas hydrates in the food industry to concentrate juices, for long-term food preservation and even for dough leavening during bread baking.[566] Note that advantages of the hydrate method for juice concentration over evaporation include lower energy expenditure and the absence of heating or boiling of solutions, which can result in the loss of consumer properties (taste, colour and so on) at high degree of water removal (in the case of hydrate formation with CH_3F and CH_3Br to concentrate apple, tomato and orange juice, it is possible to remove up to 75% of water they contain). The use of this technique is held up due to the absence of methods for fast generation of GHs and sophisticated separation of GHs from the solution.

Thus, there are quite a few practical applications of GHs and gas hydrate technologies that have been implemented at experimental industrial, pilot or laboratory level or

described in patents. It is beyond doubt that some of the proposed techniques will be brought to practical use. Also, it should be noted that most of engineering solutions proposed in the new literature are rooted in the early stages of gas hydrate studies,[3] and the current interest in them is the return to old solutions at a new technological level and in new economic circumstances.

7.4. Preparation methods of gas hydrates

The presence of a fast and economically viable method for the preparation of hydrates is a necessary condition for implementation of any gas hydrate technology; therefore, we will briefly consider the current situation in this field. According to the classification proposed by Yakushev *et al.*,[567] methods for hydrate preparation can be classified in terms of the method used to mix the components:

— gas injection into water,
— water injection into compressed gas,
— mixed methods.

Methods used both on a large scale and in laboratory production of hydrates mainly correspond to this classification. An exception is provided by the method in which the hydrate is formed on melting of crushed ice under a pressure of hydrate-forming gas. On a laboratory scale, it is a convenient and simple method that provides high degrees of conversion of water to hydrates in simple autoclaves without a mechanical stirrer. A sharp acceleration of the hydrate formation reaction under these conditions is an established fact, although the chemical essence of the involved processes is yet unknown.

Most often, hydrates are prepared by gas injection into water, which is implemented in a particular design using a conventional stirred reactor. A lot of laboratory experiments were carried out using bubble reactors — columns filled with water or an aqueous solution of an auxiliary component — through which the gas is bubbled.[568, 569] Exactly this method was used to obtain the hydrate in the demonstration project described above (see, *e.g.*, Refs 519, 520). A hydrate slurry in water ($\sim$20%) was accumulated in a stirred reactor with gas bubbling and then it was routed to the water separation column.[570] Then the hydrate-rich suspension could be delivered to pellet formation or to the second-stage fluidized-bed reactor in which the remaining portions of water were converted to the hydrate. Some of the suspension was recycled to the reactor in order to maintain the presence of crystallization sites and hydrate growth in the reactor.

According to some of the proposed reactor designs, both the hydrate formation and hydrate separation from the liquid took place in the same vessel. In all cases, separation of the hydrate from water was induced by the difference between their densities. A patented process [571] differs from the process described above by the presence of a second-stage screw reactor (or another reactor with a similar operation principle) in which the thick hydrate slurry was crushed, vigorously stirred and moved along the reactor. Examples of laboratory studies of hydrate formation processes in stirred reactors as functions of the stirring velocity and the shape of the stirrer were reported by Douieb *et al.*[572] In a patented process,[573] the stages of gas and liquid mixing and initial hydrate formation proceeded in an ejector type mixer. The subsequent hydrate formation took place as the resulting slurry was pumped through a heat exchanger reactor. It was shown [574, 575] that this process design is the most promising for the use on a large scale. This method was implemented in a continuous pilot unit for the separation of synthesis gas.[534] Laboratory experiments with a reactor of this type were also described by Yang *et al.*[576] It was noted above that the addition of minor amounts of surfactants makes it possible to avoid sticking together of hydrate crystals and to accelerate the hydrate growth; therefore, in some cases, solutions of surfactants were used for GH production (see, for example, Ref. 577).

As an example of a method that implies dispersion of water in a gas, consider the patented [578] process of injecting a gas/water mixture into a vessel containing a compressed hydrate former. Spraying of the mixture into a low-pressure zone results in cooling of the gas due to the Joule–Thomson effect, which serves for the withdrawal of heat released upon the hydrate formation. Experiments with this type of reactor were described by Brown *et al.*[579] Alternatively, it is possible to consider a reactor in which the sprayed water is cooled on a porous metal plate, while a liquid coolant is pumped through the plate, entrains the hydrate and dissipates the released heat.[580] There are variants of this method that imply the use of a fluidized bed. A reactor of this type was designed, manufactured and tested.[581] It is a long (12.2 m) vertical pipe with a cooling shell. A gas and water flow mixed with a part of hydrate slurry recycled to the reactor is fed to the lower part of the pipe. The upward flow of the slurry maintains the beads in the reactor in the suspended state. The chaotic movement of the beads gives rise to a large gas–water contact surface area, the hydrate deposits are scraped away from the walls and the laminar flow of the liquid near the wall is destroyed, which intensifies the heat exchange. The capacity of this reactor, which steadily operated for a long time, was $>$750 kg per day. The process can easily be scaled up by designing a reactor with a large number of heat exchanger pipes of the same type.

Currently, considerable interest is expressed in the development of column type reactors with a filler containing dispersed water (see, *e.g.*, Refs 582–584). In these reactors, GHs are formed when the gas is pumped through the reactor at a relatively high pressure, while decomposition takes place when pressure is decreased. A variant of this method is the formation of GHs as a hydrate cap through capillary suction of water from the porous medium.[2, 585]

In conclusion, we will briefly consider some hydrate formation processes that cannot be assigned to the methods mentioned above. Bai *et al.*[586] prepared carbon dioxide hydrate by mixing the downward helical flows of water and gas in a vessel resembling cyclone in the design. A patent [587] proposed the use of surfactant solutions for accumulation of gas hydrates in storage reactors with no moving parts. The storage reactor contained a large number of vertical plates the lower parts of which were immersed into a surfactant solution. The hydrate formed at the gas–water interface was displaced from the liquid surface to these plates and uniformly filled the vessel bulk. An interesting application of surfactants for hydrate preparation is the method for hydrate synthesis from water emulsions in organic liquids proposed in a patent.[588]

The hydrate formation reaction can be accelerated not only by using surfactants and stirring, but also by acoustic and shock wave impact.[589] In a medium containing bubbles of hydrate-forming gas, shock waves with amplitudes of up to hundreds of atmospheres are generated in the hydrate stability zone, induce fragmentation of gas bubbles, inten-

sify gas exchange, increase the metastability of the medium and, as a consequence, enhance the hydrate formation. A patent [590] describes an ideologically similar method for accelerating the hydrate formation at the gas – water interface by acoustic vibrations with a frequency of 1 – 20 kHz (see also Ref. 591). Some ideas are based on the employment of unusual physical states of the reactants. For example, it was proposed [592] to prepare the hydrate of carbon dioxide (and other compressible gases) at elevated pressures in the reaction between the liquid hydrate former and water. The preparation of hydrates on boiling the hydrate former under a layer of a liquid (water) was described.[591, 593] Xiao *et al.*[594] considered an original method for accelerating the hydrate formation, which implied activation of the reaction mixture by reciprocating impact. The formed hydrates were compacted in this case.

7.5. Formation of hydrates from amorphous layers under cryogenic conditions

Numerous studies are now available on the formation of GHs during recrystallization of amorphous layers obtained by co-deposition of water vapour and a gaseous hydrate former occurring at low pressure onto a substrate cooled to a cryogenic temperature. The interest in these studies is associated, to a large extent, with elucidation of the possibility of GH existence in outer space. The initially obtained layers are, most often, amorphous; as they are heated, crystalline ice and hydrates are formed.

Numerous studies dealing with crystallization of amorphous mixtures of water with various gases using predominantly thermal methods were carried out by Faizullin's research group (see, for example, Refs 595, 596). Nakayama *et al.*[597] obtained an amorphous layer of water and xenon at −263 °C. Crystallization of xenon hydrate took place at temperatures above −133 °C. Using NMR spectroscopy, it was shown that at lower temperatures, the geometry of the xenon atom surrounded by water molecules may be similar to small *D* cavity. In another study,[598] the amorphous layers $CO_2 + H_2O$ were obtained at −233 °C. The crystallization of CO_2 hydrate took place at temperatures above −173 °C. The authors found out that in the temperature range from −193 to −173 °C, the CO_2 equilibrium pressure for this hydrate is 10^{-3}–10^{-4} Pa. Crystallization of the layers obtained in this way under external mechanical compression was studied by Mitterdorfer *et al.*[599] Ghosh *et al.*[600, 601] demonstrated fast crystallization of amorphous mixtures of water with THF, methane and carbon dioxide at temperatures above −173 °C and pressure of $\sim 10^{-5}$ Pa. It was also shown that the last-mentioned two hydrates can slowly crystallize even at much lower temperatures (approximately −133°C).

8. Note added in proof

Recently, several important publications with new results appeared in the gas hydrate chemistry and technological applications. For example, new phases were identified for hydrogen [602] and TBAB [603] hydrates. Therefore, it is necessary to consider the recent studies in brief.

First, as we repeatedly noted in the review, the control over the nucleation process of gas hydrates is a key to development of technologies for gas storage in the hydrate form, separation of mixtures (in gas separation and water desalination processes), cold storage systems and prevention of the hydrate formation during oil and gas production. In this connection, Ma *et al.*[604] demonstrated an effect of solid surfaces on the hydrate nucleation. It was found that the activity of nucleation sites of methane hydrate in a water-in-crude oil emulsion is a function of time.[605] It is obvious that under static conditions, so sophisticated systems continuously change, inducing the formation and activation of new crystallization sites. New reagents were obtained for both acceleration and retardation of hydrate nucleation and growth;[606, 607] the effect of molecular structure of anti-agglomerants on their efficiency depending on the hydrocarbon medium and salinity was studied.[608]

Second, mention should be made of the rapidly developing combined approaches to accelerating the hydrate formation:

— combined use of thermodynamic and kinetic promoters (shift of the equilibrium towards milder conditions with simultaneous increase in the rate of gas binding to the hydrate state);[609]

— further development of microdroplet systems in which the hydrate formation is accelerated due to generation of an extended water – gas interfacial area.[610]

Podenko *et al.*[610] attained a high stability of proposed systems after a hydrate formation – decomposition cycle, which allows for decreasing the cost of their regeneration. Zeng *et al.*[611] reported a simple and elegant approach to suppression of methane hydrate dissociation by mixing the hydrate with liquid hydrate formers the hydrates of which are stable at atmospheric pressure and temperatures slightly above 0 °C. This method may increase the hydrate stability during storage and transportation. The combined approach also proved to be efficient in gas mixture separation [612] and hydrate gas production [613] processes. The possibility of using self-preservation effect of gas hydrates in a porous medium to increase the efficiency of methane replacement by carbon dioxide is being actively studied.[614, 615]

Third, particular attention should be paid to studies of the effect of process parameters on the efficiency of kinetic inhibitors.[616, 617] Although catastrophic agglomeration of hydrate particles took place in the alkaline medium, the gas consumption rate considerably increased. In our opinion, pH variation is a promising trend for the control of the hydrate growth rate. Finally, we would like to mention an important study [618] in which the optimal solution was proposed for the search for recommendations for preventing hydrate complications in the oil and gas production on the basis of laboratory tests.

9. Conclusion

Currently, studying of GHs is a relevant and vigorously developing line of research. This interdisciplinary area combines the studies at the boundary of geology, engineering, physics, chemistry and biology. Exploration works of the last decades, which were supported by the governments of many countries, confirmed the global occurrence of natural hydrates and the conceptual possibility of natural gas production from the hydrates. It became clear that hydrates represent a significant and dynamic (on the geological time scale) component of the ecosystem affecting the climate and global processes in the Earth's crust.

In the GH-related fields of chemistry and engineering, the greatest progress was made in the last decade in the study of kinetics of hydrate formation and decomposition, development of low-dosage inhibitors of hydrate formation and investigations of properties of hydrate dispersions in

crude oils and hydrocarbon liquids. The development of these areas was primarily due to the need to ensure the flow assurance of oil and natural gas production processes. The potentials of gas hydrate technology for gas storage and transportation, separation of gas mixtures and desalination of water are being actively studied. Note that the papers and patents published in the 1960s – 1980s widely consider these subjects, which is not always mentioned in recent studies.

In the field of fundamental studies of gas hydrates, the possibility of hydrate formation by highly polar molecules, including alcohols, amines and ammonia, is of considerable interest. High-pressure studies formed a new part of the structural chemistry of hydrates. We tried to reflect all these issues in the present review.

This review was written with the financial support of the Russian Foundation for Basic Research (Project No. 19-18-50165).

10. List of acronyms and designations

AA — anti-agglomerant,
CNG — compressed natural gas for transportation,
GH — gas hydrate,
HSZ —hydrate stability zone,
KI — kinetic inhibitor,
LNG — liquefied natural gas for transportation,
NGH, SNG — natural gas hydrate, solidified natural gas for transportation,
sI — cubic structure I,
sII — cubic structure II,
sH — hexagonal structure III,
TBAB — tetra-n-butylammonium bromide,
THF — tetrahydrofuran,
C, $C_{ml}(T)$ — Langmuir constants,
d — diameter of hydrate particles,
D (D') cavity — dodecahedral cavity,
E cavity — icosahedral cavity,
$f_l(T,P)$ — fugacity of the guest component of type l,
g — water vapour-saturated gas,
h — gas hydrate,
H cavity — hexadecahedral cavity,
i — ice I_h,
l_1 — saturated or unsaturated solution of hydrate-forming gas in water,
l_2 — water-saturated liquid hydrate former,
n — hydrate number,
P — pressure,
Q_1, Q_2 — quadruple points,
R — gas constant,
T — temperature,
T cavity — tetradecahedral cavity,
T_{eq} — equilibrium temperature of hydrate formation at a given pressure,
V — unit cell volume at a given pressure,
V_0 — unit cell volume at a 'zero' pressure,
X — mole fraction of hydrate former,
α — shape coefficient,
γ_h — surface energy at the hydrate/water interface,
ΔH — enthalpy of hydrate decomposition,
ΔT — change in the equilibrium temperature of hydrate formation,
θ — contact angle at the hydrate – water – gas interface,
θ_{ml} — occupancy of type m cavities by type l molecules,
μ_H and μ_β — chemical potentials of a water molecule in occupied and empty hydrate frameworks, respectively,
y_m — number of type m cavities,
ρ_h — hydrate density.

References

1. V.A.Istomin, V.G.Kvon. *Preduprezhdenie i Likvidatsiya Gazovykh Hidratov v Sistemakh Dobychi Gaza*. (Prevention and Elimination of Gas Hydrates in Gas Production Systems). (Moscow: OOO 'IPTS GAZPROM', 2004)
2. V.I.Istomin, V.S.Yakushev. *Gazovye Gidraty v Prirodnykh Usloviyakh*. (Natural Gas Hydrates). (Moscow: Nedra, 1992)
3. S.Sh.Byk, Yu.F. Makogon, V.I.Fomina. *Gazovye Gidraty*. (Gas Hydrates). (Moscow: Khimiya, 1980)
4. E.D.Sloan, C.A.Koh. *Clathrate Hydrates of Natural Gases*. (3rd. Ed). (London, New York, Boca Raton, FL: CRC Press, 2008)
5. V.M.Vorotyntsev, V.M.Malyshev. *Russ. Chem. Rev.*, **67**, 81 (1998)
6. V.M.Vorotyntsev, V.M.Malyshev. *Russ. Chem. Rev.*, **80**, 971 (2011)
7. V.S.Yakushev. *Prirodnyi Gaz i Gazovye Gidraty v Kriolitozone*. (Natural Gas and Gas Hydrates in the Cryolithozone). (Moscow: GAZPROM-VNIIGAZ, 2009)
8. T.V.Matveeva. In *Mirovoi Okean*. (World Ocean). Vol. III. L.I.Lobkovskii, G.A.Cherkashev). (Moscow: Nauchnyi Mir, 2020). P. 586
9. D.W.Davidson. In *Water. A Comprehensive Treaties*. Vol. 2. (Ed. F.Franks). (New York, London: Plenum Press, 1973). P. 115
10. Y.A.Dyadin, I.S.Terekhova, T.V.Rodionova, D.V.Soldatov. *J. Struct. Chem.*, **40**, 645 (1999)
11. Y.F.Makogon. *J. Nat. Gas Sci. Eng.*, **2**, 49 (2010)
12. A.Y.Manakov, V.I.Kosyakov, S.F.Solodovnikov. In *Comprehensive Supramolecular Chemistry II*. Vol. 7. (Eds J.L.Atwood, G.W.Gokel, L.J.Barbour). (Oxford: Elsevier, 2017). P. 161
13. S.Vorobyev, A.Bychkov, V.Khilimonyuk, S.Buldovicz, E.Ospennikov, E.Chuvilin. *Geosciences*, **9**, 10 (2019)
14. A.V.Milkov. *Earth Sci. Rev.*, **66**, 183 (2004)
15. M.D.Max, A.H.Johnson, W.P.Dillon. *Naturall Gas Hydrate — Arctic Ocean Deepwater Resource Potential. (Springer, Briefs in Energy)*, (Springer, 2013)
16. L.P.Liu, Z.L.Sun, L.Zhang, N.Y.Wu, Y.C.Qin, Z.Z.Jiang, W.Geng, H.Cao, X.L.Zhang, B.Zhai, C.L.Xu, Z.C.Shen, Y.G.Jia. *Acta Geol. Sin., Engl. Ed.*, **93**, 731 (2019)
17. Z.R.Chong, S.H.B.Yang, P.Babu, P.Linga, X.-S.Li. *Appl. Energy*, **162**, 1633 (2016)
18. T.A.Minshull, H.Marin-Moreno, P.Betlem, J.Bialas, S. Bunz, E.Burwicz, A.L.Cameselle, G.Cifcig, M.Giustiniani, J.I.T.Hillman, S.Holz, J.R.Hopper, G.Ion, R.Leon, V.Magalhaes, Y.Makovsky, M.P.Mata, M.D.Max, T.Nielsen, S.Okay, I.Ostrovsky, N.O'Neill, L.M.Pinheiro, A.A.Plaza-Faverola, D.Rey, S.Roy, K.Schwalenberg, K.Senger, S.Vadakkepuliyambatta, A.Vasilev, J.T.Vazquez. *Marine Petrol. Geol.*, **111**, 735 (2020)
19. O.Khlystov, M.De Batist, H.Shoji, A.Hachikubo, S.Nishio, L.Naudts, J.Poort, A.Khabuev, O.Belousov, A.Manakov, G.Kalmychkov. *J. Asian Earth Sci.*, **62**, 162 (2013)
20. V.A.Soloviev. *Russ. Geol. Geophys.*, **43**, 648 (2002)
21. C.Ruppel. *J. Chem. Eng. Data*, **60**, 429 (2015)
22. I.A.Zinchenko, B.I.Sharipov, A.A.Krutoi, E.V.Perlova, S.A.Leonov. *The J. Oil Gas Geol.*, 87 (2018)
23. T.V.Matveeva, A.A.Semenova, N.A.Shchur, E.A.Logvina, O.V.Nazarova. *J. Mining Inst.*, **226**, 387 (2017)
24. V.A.Akulichev, A.I.Obzhirov, R.B.Shakirov, E.V.Maltseva, A.I.Gresov, Y.A.Telegin. *Dokl. Earth Sci.*, **454**, 94 (2014)

25. V.I.Bogoyavlenskii, A.S.Yanchevskaya, I.V.Bogoyavlenskii, A.V.Kishankov. *Arktika: Ekologiya i Ekonomika*, **3**, 42 (2018)
26. X.-S.Li, C.-G.Xu, Y.Zhang, X.-K.Ruan, G.Li, Y.Wang. *Appl. Energy*, **172**, 286 (2016)
27. L.Yang, Y.L.Liu, H.Q.Zhang, B.Xiao, X.W.Guo, R.P.Wei, L.Xu, L.J.Sun, B.Yu, S.D.Leng, Y.H.Li. *Chin. J. Chem. Eng.*, **27**, 2133 (2019)
28. Z.Kong, Q.Jiang, X.Dong, J.Wang, X.Wan. *J. Clean. Product.*, **203**, 1 (2018)
29. Y.Konno, T.Fujii, A.Sato, K.Akamine, M.Naiki, Y.Masuda, K.Yamamoto, J.Nagao. *Energy Fuels*, **31**, 2607 (2017)
30. S.Sakurai, I.Nishioka, M.Matsuzawa, B.Matzain, A.Goto, J.E.Lee. *SPE Product. Operat.*, **32**, 500 (2017)
31. T.Yu, G.Q.Guan, A.Abudula. *Appl. Energy*, **251**, 113338 (2019)
32. K.Yamamoto, X.X.Wang, M.Tamaki, K.Suzuki. *RSC Adv.*, **9**, 25987 (2019)
33. O.M.Khlystov, S.Nishio, A.Y.Manakov, H.Sugiyama, A.V.Khabuev, O.V.Belousov, M.A.Grachev. *Russ. Geol. Geophys.*, **55**, 1122 (2014)
34. P.Kumar, T.S.Collett, K.M.Shukla, U.S.Yadav, M.V.Lall, K.Vishwanath, N.-E.S.Party. *Mar. Petrol. Geol.*, **108**, 3 (2019)
35. V.Y.Lipenkov. In *Physics of Ice Core Records*. (Ed. T.Hondoh), Hokkaido University Press, Sapporo, 2000, P. 327
36. C.Weikusat, S.Kipfstuhl, I.Weikusat. *J. Glaciol.*, **61**, 923 (2015)
37. A.N.Salamatin, V.Y.Lipenkov, T.Hondoh. *J. Cryst. Growth*, **257**, 412 (2003)
38. O.Mousis, E.Chassefiere, N.G.Holm, A.Bouquet, J.H.Waite, W.D.Geppert, S.Picaud, Y.Aikawa, M.Ali-Dib, J.-L.Charlou, P.Rousselot. *Astrobiology*, **15**, 308 (2015)
39. E.Chassefiere, E.Dartois, J.M.Herri, F.Tian, F.Schmidt, O.Mousis, A.Lakhlifi. *Icarus*, **223**, 878 (2013)
40. D.Gautier, F.Hersant. *Space Sci. Rev.*, **116**, 25 (2005)
41. U.Marboeuf, O.Mousis, J.M.Petit, B.Schmitt, A.L.Cochran, H.A.Weaver. *Astron. Astrophys.*, **525**, A144 (2011)
42. F.M.O'Connor, O.Boucher, N.Gedney, C.D.Jones, G.A.Folberth, R.Coppell, P.Friedlingstein, W.J.Collins, J.Chappellaz, J.Ridley, C.E.Johnson. *Rev. Geophys.*, **48**, RG4005 (2010)
43. C.D.Ruppel, J.D.Kessler. *Rev. Geophys.*, **55**, 126 (2017)
44. F.Wang, B.Zhao, G.Li. *Energies*, **11**, 2384 (2018)
45. N.J.English, J.M.D.MacElroy. *Chem. Eng. Sci.*, **121**, 133 (2015)
46. J.S.Tse. In *Reviews in Computational Chemistry*. Vol. 28. (Eds A.L.Parrill, K.B.Lipkowitz). (Wiley and Sons, 2015). P. 315
47. B.C.Barnes, A.K.Sum. *Curr. Opin. Chem. Eng.*, **2**, 184 (2013)
48. I.N.Tsimpanogiannis, I.G.Economou. *J. Supercrit. Fluids*, **134**, 51 (2018)
49. R.V.Belosludov, O.S.Subbotin, H.Mizuseki, Y.Kawazoe, V.R.Belosludov. *J. Chem. Phys.*, **131**, 12 (2009)
50. J.B.Klauda, S.I.Sandler. *Ind. Eng. Chem. Res.*, **40**, 4197 (2001)
51. L.E.Zerpa, J.-L.Salager, C.A.Koh, E.D.Sloan, A.K.Sum. *Ind. Eng. Chem. Res.*, **50**, 188 (2011)
52. L.E.Zerpa, E.D.Sloan, A.K.Sum, C.A.Koh. *J. Petrol. Sci. Eng.*, **98 – 99**, 122 (2012)
53. A.Y.Manakov, A.D.Duchkov. *Russ. Geol. Geophys.*, **58**, 240 (2017)
54. K.You, P.B.Flemings, A.Malinverno, T.S.Collett, K.Darnell. *Rev. Geophys.*, **57**, 1146 (2019)
55. W.F.Waite, J.C.Santamarina, D.D.Cortes, B.Dugan, D.N.Espinoza, J.Germaine, J.Jang, J.W.Jung, T.J.Kneafsey, H.Shin, K.Soga, W.J.Winter, T.-S.Yun. *Rev. Geophys.*, **47**, RG4003 (2009)
56. L.Yang, A.Falenty, M.Chaouachi, D.Haberthur, W.F.Kuhs. *Geochem. Geophys. Geosyst.*, **17**, 3717 (2016)
57. Y.Zhao, J.Zhao, D.Shi, Z.Feng, W.Liang, D.Yang. *J. Nat. Gas Sci. Eng.*, **31**, 139 (2016)
58. K.Shin, J.H.Cha, Y.Seo, H.Lee. *Chem. – Asian J.*, **5**, 22 (2010)
59. G.A.Jeffrey. In *Comprehensive Supramolecular Chemistry*. Vol. 6. (Eds J.L.Atwood, D.D.MacNicol, F.Vogtle). (Oxford: Elsevier, 1996). P. 757
60. S.M.Everett, C.J.Rawn, B.C.Chakoumakos, D.J.Keefer, A.Huq, T.J.Phelps. *Am. Miner.*, **100**, 1203 (2015)
61. S.Subramanian, A.L.Ballard, R.A.Kini, S.F.Dec, E.D.Sloan. *Chem. Eng. Sci.*, **55**, 5763 (2000)
62. S.Subramanian, R.A.Kini, S.F.Dec, E.D.Sloan. *Chem. Eng. Sci.*, **55**, 1981 (2000)
63. S.Subramanian, R.A.Kini, S.F.Dec, E.D.Sloan. *Ann. NY Acad. Sci.*, **912**, 873 (2000)
64. S.F.Dec. *J. Phys. Chem. C*, **116**, 9660 (2012)
65. C.Petuya, A.Desmedt. *J. Phys. Chem. C*, **123**, 4871 (2019)
66. A.Y.Manakov, A.Y.Likhacheva, V.A.Potemkin, A.G.Ogienko, A.V.Kurnosov, A.I.Ancharov. *ChemPhysChem*, **12**, 2475 (2011)
67. K.C.Hester, Z.Huo, A.L.Ballard, C.A.Koh, K.T.Miller, E.D.Sloan. *J. Phys. Chem. B*, **111**, 8830 (2007)
68. T.C.Hansen, A.Falenty, W.F.Kuhs. *J. Chem. Phys.*, **144**, 054301 (2016)
69. S.Takeya, S.Alavi, S.Hashimoto, K.Yasuda, Y.Yamauchi, R.Ohmura. *J. Phys. Chem. C*, **122**, 18134 (2018)
70. K.A.Udachin, C.I.Ratcliffe, J.A.Ripmeester. *Angew. Chem., Int. Ed.*, **40**, 1303 (2001)
71. S.Alavi, K.Udachin, C.I.Ratcliffe, J.A.Ripmeester. In *Supramolecular Chemistry: from Molecules to Nanomaterials*. Vol. 6. (Wiley, 2012)
72. L.Dobrzycki, P.Taraszewska, R.Boese, M.K.Cyranski, S.A.Cirkel. *Angew. Chem., Int. Ed.*, **54**, 10138 (2015)
73. K.A.Udachin, G.D.Enright, C.I.Ratcliffe, J.A.Ripmeester. *J. Am. Chem. Soc.*, **119**, 11481 (1997)
74. I.U.Goldschleger, G.Kerenskaya, K.C.Janda, V.A.Apkarian. *J. Phys. Chem. A*, **112**, 787 (2008)
75. H.Dureckova, T.K.Woo, K.A.Udachin, J.A.Ripmeester, S.Alavi. *Faraday Discuss.*, **203**, 61 (2017)
76. K.A.Udachin, S.Alavi, J.A.Ripmeester. *J. Phys. Chem. C*, **117**, 14176 (2013)
77. K.A.Udachin, C.I.Ratcliffe, G.D.Enright, J.A.Ripmeester. *Angew. Chem., Int. Ed.,* **47**, 9704 (2008)
78. S.Takeya, H.Fujihisa, H.Yamawaki, Y.Gotoh, R.Ohmura, S.Alavi, J.A.Ripmeester. *Angew. Chem., Int. Ed.*, **55**, 9287 (2016)
79. K.Shin, I.L.Moudrakovski, M.D.Davari, S.Alavi, C.I.Ratcliffe, J.A.Ripmeester. *CrystEngComm*, **16**, 7209 (2014)
80. K.Shin, I.L.Moudrakovski, C.I.Ratcliffe, J.A.Ripmeester. *Angew. Chem., Int. Ed.*, **56**, 6171 (2017)
81. L.S.Aladko, Y.A.Dyadin. *Mendeleev Commun.*, 67 (1994)
82. S.Park, D.Lim, Y.Seo, H.Lee. *Chem. Commun.*, **51**, 8761 (2015)
83. T.Bando, T.Sugahara. *Fluid Phase Equilib.*, **413**, 36 (2016)
84. J.Seol, W.Shin, D.Y.Koh, H.Kang, B.Sung, H.Lee. *J. Phys. Chem. C*, **116**, 1439 (2012)
85. Y.Ba, J.A.Ripmeester, C.I.Ratcliffe. *Can. J. Chem.*, **89**, 1055 (2011)
86. O.Yamamuro, H.Suga. *J. Therm. Anal.*, **35**, 2025 (1989)
87. D.H.Lee, C.H.Choi, T.H.Choi, B.J.Sung, H.Kang. *J. Phys. Chem. Lett.*, **5**, 2568 (2014)
88. O.Yamamuro, T.Matsuo, H.Suga, W.I.F.David, R.M.Ibberson, A.J.Leadbetter. *Physica B*, **213**, 405 (1995)
89. C.Y.Jones, I.Peral. *Am. Miner.*, **89**, 1176 (2004)
90. S.Alavi, K.Udachin, J.A.Ripmeester. *Chem. – Eur. J.*, **16**, 1017 (2010)
91. C.Gutt, B.Asmussen, W.Press, M.R.Johnson, Y.P.Handa, J.S.Tse. *J. Chem. Phys.*, **113**, 4713 (2000)
92. E.Pefoute, M.Prager, M.Russina, A.Desmedt. *Fluid Phase Equilib.*, **413**, 116 (2016)
93. K.A.Udachin, C.I.Ratcliffe, J.A.Ripmeester. *J. Phys. Chem. B*, **105**, 4200 (2001)

94. S.Takeya, K.A.Udachin, I.L.Moudrakovski, R.Ohmura, J.A.Ripmeester. *Chem. – Eur. J.*, **22**, 7567 (2016)
95. J.A.Ripmeester, C.I.Ratcliffe, I.G.Cameron. *J. Phys. Chem. B*, **108**, 929 (2004)
96. H.Nelson, A.Ihrig, R.Kahlau, P.Kibies, S.M.Kast, R.Bohmer. *J. Non-Cryst. Solids*, **407**, 431 (2015)
97. Y.H.Ahn, B.Lee, K.Shin. *Crystals*, **8,** 328 (2018)
98. S.Alavi, S.Takeya, R.Ohmura, T.K.Woo, J.A.Ripmeester. *J. Chem. Phys.*, **133**, 074505 (2010)
99. A.T.Trueba, M.C.Kroon, C.J.Peters, I.L.Moudrakovski, C.I.Ratcliffe, S.Alavi, J.A.Ripmeester. *J. Chem. Phys.*, **140**, 214703 (2014)
100. I.A.Monreal, L.Cwiklik, B.Jagoda-Cwiklik, J.P.Devlin. *J. Phys. Chem. Lett.*, **1**, 290 (2010)
101. Y.A.Dyadin. *Supramol. Chem.*, **6**, 59 (1995)
102. M.J.Collins, C.I.Ratcliffe, J.A.Ripmeester. *J. Phys. Chem.*, **94**, 157 (1990)
103. C.Petuya, F.Damay, D.Talaga, A.Desmedt. *J. Phys. Chem. C*, **121**, 13798 (2017)
104. G.H.Cady. *J. Phys. Chem.*, **85**, 3225 (1981)
105. G.H.Cady. *J. Phys. Chem.*, **87**, 4437 (1983)
106. L.Kotai, S.Balint, I.Gacs, G.Lakatos, A.Angyal, R.N.Mehrotra. *Z. Anorg. Allg. Chem.*, **638**, 279 (2012)
107. Z.X.Huo, M.D.Jager, K.T.Miller, E.D.Sloan. *Chem. Eng. Sci.*, **57**, 705 (2002)
108. Z.X.Huo, K.Hester, E.D.Sloan, K.T.Miller. *AIChE J.*, **49**, 1300 (2003)
109. T.Uchida, S.Takeya, Y.Kamata, I.Y.Ikeda, J.Nagao, T.Ebinuma, H.Narita, O.Zatsepina, B.A Buffett. *J. Phys. Chem. B*, **106**, 12426 (2002)
110. Y.-P.Seo, D.Y.Kim, H.Lee, J.-W.Lee, I.L.Moudrakowski, J.A.Ripmeester. In *Proceedings of 5th International Conference on Gas Hydrates 2005(ICGH 2005)*. Vol. 1. (Trondheim, Norway: Tapir Academic Press, 2005), P. 567
111. H.J.Ng. *Ann. NY Acad. Sci.*, **912**, 1034 (2000)
112. A.Hoshikawa, T.Matsukawa, T.Ishigaki. *Physica B: Condens. Matter*, **551**, 274 (2018)
113. D.Le Quang, D.L.Quang, B.Bouillot, J.-M.Herri, P.Glenat, P.Duchet-Suchaux. *Fluid Phase Equilib.*, **413**, 10 (2016)
114. S.M.Babakhani, B.Bouillot, S.Ho-Van, J.Douzet, J.-M.Herri. *Fluid Phase Equilib.*, **472**, 22 (2018)
115. C.H.Yu, L.T.Chen, B.J.Sun. *Chin. J. Chem. Eng.*, **27**, 2189 (2019)
116. V.Y.Komarov, S.F.Solodovnikov, E.V.Grachev, V.I.Kosyakov, A.Y.Manakov, A.V.Kurnosov, V.A.Shestakov. *Crystallogr. Rev.*, **13**, 257 (2007)
117. A.Y.Manakov, Yu. A. Dyadin. *Ros. Khim. Zh.*, **47** (3), 28 (2003)
118. J.S.Loveday, R.J.Nelmes. *Phys. Chem. Chem. Phys.*, **10**, 937 (2008)
119. B.Chazallon, W.F.Kuhs. *J. Chem. Phys.*, **117**, 308 (2002)
120. A.Y.Manakov, V.I.Voronin, A.V.Kurnosov, A.E.Teplykh, V.Y.Komarov, Y.A.Dyadin. *J. Inclusion Phenom. Macrocycl. Chem.*, **48**, 11 (2004)
121. E.Y.Aladko, A.I.Ancharov, S.V.Goryainov, A.V.Kurnosov, E.G.Larionov, A.Y.Likhacheva, A.Y.Manakov, V.A.Potemkin, M.A.Sheromov, A.E.Teplykh, V.I.Voronin, F.V.Zhurko. *J. Phys. Chem. B*, **110**, 21371 (2006)
122. C.A.Tulk, D.D.Klug, A.M.dos Santos, G.Karotis, M.Guthrie, J.J.Molaison, N.Pradhan. *J. Chem. Phys.*, **136**, 054502 (2012)
123. A.V.Kurnosov, V.Y.Komarov, V.I.Voronin, A.E.Teplykh, A.Y.Manakov. *Angew. Chem., Int. Ed.*, **43**, 2922 (2004)
124. A.Y.Manakov, V.I.Voronin, A.V.Kurnosov, A.E.Teplykh, E.G.Larionov, Y.A.Dyadin. *Dokl. Phys. Chem.*, **378**, 148 (2001)
125. A.G.Ogienko, M.Tkacz, A.Y.Manakov, J.Lipkowski. *J. Phys. Chem. B*, **111**, 12795 (2007)
126. A.Y.Manakov, A.G.Ogienko, M.Tkacz, J.Lipkowski, A.S.Stoporev, N.V.Kutaev. *J. Phys. Chem. B*, **115**, 9564 (2011)
127. J.S.Loveday, R.J.Nelmes, M.Guthrie, D.D.Klug, J.S.Tse. *Phys. Rev. Lett.*, **87**, 215501 (2001)
128. L.Yang, C.A.Tulk, D.D.Klug, B.C. Chakoumakos, L.Ehm, J.J.Molaison, J.B.Parise, J.M.Simonson. *Chem. Phys. Lett.*, **485**, 104 (2010)
129. A.Rasoolzadeh, A.Shariati. *Fluid Phase Equilib.*, **494**, 8 (2019)
130. S.Alavi, J.A.Ripmeester. *Chem. Phys. Lett.*, **479**, 234 (2009)
131. S.Alavi, J.A.Ripmeester. *Angew. Chem., Int. Ed.*, **46**, 6102 (2007)
132. A.Falenty, T.C.Hansen, W.F.Kuhs. *Nature (London)*, **516**, 231 (2014)
133. W.F.Kuhs, T.C.Hansen, A.Falenty. *J. Phys. Chem. Lett.*, **9**, 3194 (2018)
134. D.M.Amos, M.-E.Donnelly, P.Teeratchanan, C.L.Bull, A.Falenty, W.F.Kuhs, A.Hermann, J.S.Loveday. *J. Phys. Chem. Lett.*, **8**, 4295 (2017)
135. R.Kumar, D.D.Klug, C.I.Ratcliffe, C.A.Tulk, J.A.Ripmeester. *Angew. Chem., Int. Ed.*, **52**, 1531 (2013)
136. L.del Rosso, M.Celli, L.Ulivi. *Nat. Commun.*, **7**, 13394 (2016)
137. L.del Rosso, F.Grazzi, M.Celli, D.Colognesi, V.Garcia-Sakai, L.Ulivi. *J. Phys. Chem. C*, **120**, 26955 (2016)
138. M.Catti, L.del Rosso, L.Ulivi, M.Celli, F.Grazzi, T.C.Hansen. *Phys. Chem. Chem. Phys.*, **21**, 14671 (2019)
139. B.Massani, L.J.Conway, A.Hermann, J.Loveday. *J. Chem. Phys.*, **151**, 104305 (2019)
140. O.Bollengier, M.Choukroun, O.Grasset, E.Le Menn, G.Bellino, Y.Morizet, L.Bezacier, A.Oancea, C.Taffin, G.Tobie. *Geochim. Cosmochim. Acta*, **119**, 322 (2013)
141. G.S.Smirnov, V.V.Stegailov. *J. Phys. Chem. Lett.*, **4**, 3560 (2013)
142. T.A.Strobel, M.Somayazulu, S.V.Sinogeikin, P.Dera, R.J.Hemley. *J. Am. Chem. Soc.*, **138**, 13786 (2016)
143. L.E.Bove, U.Ranieri. *Philos. Trans. R. Soc. A: Mathem. Phys. Eng. Sci.*, **377**, 25 (2019)
144. Y.Matsumoto, Y.Katsuta, F.Kamo, T.Bando, T.Makino, T.Sugahara, K.Ohgaki. *J. Phys. Chem. B*, **118**, 13404 (2014)
145. D.Y.Koh, H.Kang, J.Jeon, Y.H.Ahn, Y.Park, H.Kim, H.Lee. *J. Phys. Chem. C*, **118**, 3324 (2014)
146. H.L.Lu, J.W.Wang, C.L.Liu, C.I.Ratcliffe, U.Becker, R.Kumar, J.Ripmeester. *J. Am. Chem. Soc.*, **134**, 9160 (2012)
147. S.Park, D.Y.Koh, H.Kang, J.W.Lee, H.Lee. *J. Phys. Chem. C*, **118**, 20203 (2014)
148. H.P.Veluswamy, R.Kumar, P.Linga. *Appl. Energy*, **122**, 112 (2014)
149. T.Nakayama, S.Tomura, M.Ozaki, R.Ohmura, Y.H.Mori. *Energy Fuels*, **24**, 2576 (2010)
150. M.Ozaki, S.Tomura, R.Ohmura, Y.H.Mori. *Int. J. Hydrogen Energy*, **39**, 3327 (2014)
151. V.P.Mel'nikov, A.N.Nesterov, L.S.Podenko, A.M.Reshetnikov. *Dokl. Earth Sci.*, **459**, 1353 (2014)
152. N.Fray, U.Marboeuf, O.Brissaud, B.Schmitt. *J. Chem. Eng. Data*, **55**, 5101 (2010)
153. U.Marboeuf, N.Fray, O.Brissaud, B.Schmitt, D.Bockelee-Morvan, D.Gautier. *J. Chem. Eng. Data*, **57**, 3408 (2012)
154. H.D.Nagashima, N.Fukushima, R.Ohmura. *Fluid Phase Equilib.*, **413**, 53 (2016)
155. H.D.Nagashima, K.Nemoto, R.Ohmura. *J. Chem. Thermodyn.*, **127**, 86 (2018)
156. H.D.Nagashima, R.Ohmura. *J. Chem. Thermodyn.*, **102**, 252 (2016)
157. Y.Jin, K.Matsumoto, J.Nagao, W.Shimada. *J. Chem. Eng. Data*, **56**, 58 (2011)
158. A.H.Mohammadi, D.Richon. *Ind. Eng. Chem. Res.*, **49**, 3976 (2010)
159. K.Yasuda, Y.Oto, R.K.Shen, T.Uchida, R.Ohmura. *J. Chem. Thermodyn.*, **67**, 143 (2013)
160. M.Kida, M.Watanabe, Y.Jin, J.Nagao. *J. Chem. Eng. Data*, **60**, 1939 (2015)
161. T.Ozeki, Y.Kikuchi, S.Takeya, A.Hachikubo. *J. Chem. Eng. Data*, **63**, 2266 (2018)

162. A.H.Mohammadi, A.Chapoy, D.Richon, B.Tohidi. *Ind. Eng. Chem. Res.*, **43**, 7148 (2004)
163. H.S.Truong-Lam, S.J.Cho, J.D.Lee. *Appl. Energy*, **255**, 9 (2019)
164. A.Chapoy, H.Haghighi, R.Burgass, B.Tohidi. *J. Chem. Thermodyn.*, **47**, 6 (2012)
165. A.H.Mohammadi, D.Richon. *AIChE J.*, **53**, 1601 (2007)
166. W.J.Ou, W.J.Lu, F.L.Ning, X.G.Wu. *Mar. Chem.*, **212**, 74 (2019)
167. S.Someya, S.Bando, B.X.Chen, Y.C.Song, M.Nishio. *Int. J. Heat Mass Trans.*, **48**, 2503 (2005)
168. L.Geng, K.Qu, W.Lu, L.Jiang, I.M.Chou. *Fluid Phase Equilib.*, **438**, 37 (2017)
169. Q.Sun, H.Tian, X.Guo, A.Liu, L.Yang. *Canad. J. Chem. Eng.*, **96**, 620 (2018)
170. Q.Sun, H.Tian, Z.Z.Li, X.Q.Guo, A.X.Liu, L.Y.Yang. *Fluid Phase Equilib.*, **409**, 131 (2016)
171. F.Lang, P.Servio. *J. Nat. Gas Sci. Eng.*, **26**, 130 (2015)
172. J.Abdi, V.Mohebbi, R.M.Behbahani. *J. Nat. Gas Sci. Eng.*, **45**, 307 (2017)
173. H.Bruusgaard, P.Servio. *Fluid Phase Equilib.*, **305**, 97 (2011)
174. J.Gaudette, P.Servio. *J. Chem. Eng. Data*, **52**, 1449 (2007)
175. F.Lang, P.Servio. *J. Chem. Eng. Data*, **59**, 2547 (2014)
176. T.Makino, T.Sugahara, K.Ohgaki. *J. Chem. Eng. Data*, **50**, 2058 (2005)
177. B.Strauch, J.M.Schicks, M.Luzi-Helbing, R.Naumann, M.Herbst. *J. Chem. Thermodyn.*, **117**, 193 (2018)
178. Y.A.Dyadin, I.V.Bondaryuk, F.V.Zhurko. In *Inclusion Compound. Vol. 5*. Academic Press, London, 1984. P. 213
179. A.Y.Manakov, N.V.Penkov, T.V.Rodionova, A.N.Nesterov, E.E.Fesenko. *Russ. Chem. Rev.*, **86**, 845 (2017)
180. M.S.Madygulov, A.N.Nesterov, A.M.Reshetnikov, V.A.Vlasov, A.G. Zavodovsky. *Chem. Eng. Sci.*, **137**, 287 (2015)
181. V.P.Melnikov, A.N.Nesterov, A.M.Reshetnikov, V.A.Istomin, V.G.Kwon. *Chem. Eng. Sci.*, **65**, 906 (2010)
182. K.A.Khaldoyanidi. *Russ. J. Inorg. Chem.*, **56**, 450 (2011)
183. A.L.Ballard, E.D.Sloan. *Chem. Eng. Sci.*, **56**, 6883 (2001)
184. P.Kastanidis, I.N.Tsimpanogiannis, I.E.Romanos, A.K.Stubos, I.G. Economou. *J. Chem. Eng. Data*, **64**, 4991 (2019)
185. M.N.Khan, P.Warrier, C.J.Peters, C.A.Koh. *J. Nat. Gas Sci. Eng.*, **35**, 1388 (2016)
186. S.Shahnazar, N.Hasan. *Fluid Phase Equilib.*, **379**, 72 (2014)
187. V.Belandria, A.Eslamimanesh, A.H.Mohammadi, D.Richon. *Ind. Eng. Chem. Res.*, **50**, 6455 (2011)
188. V.Belandria, A.Eslamimanesh, A.H.Mohammadi, D.Richon. *Ind. Eng. Chem. Res.*, **50**, 4722 (2011)
189. V.Belandria, A.Eslamimanesh, A.H.Mohammadi, P.Theveneau, H.Legendre, D.Richon. *Ind. Eng. Chem. Res.*, **50**, 5783 (2011)
190. D.R.Bhawangirkar, J.S.Sangwai. *Ind. Eng. Chem. Res.*, **58**, 14462 (2019)
191. S.M.Babakhani, B.Bouillot, J.Douzet, S.Ho-Van, J.M.Herri. *J. Chem. Thermodyn.*, **122**, 73 (2018)
192. S.M.Babakhani, B.Bouillot, J.Douzet, S.Ho-Van, J.M.Herri. *Chem. Eng. Sci.*, **179**, 150 (2018)
193. K.Yasuda, H.Ogawa, R.Ohmura. *J. Chem. Eng. Data*, **55**, 358 (2010)
194. A.V.Ildyakov, A.Y.Manakov, A.P.Zavjalov, S.P.Bardakhanov. *Chem. Eng. Technol.*, **34**, 1733 (2011)
195. S.S.Skiba, E.G.Larionov, A.Y.Manakov, B.A.Kolesov, V.I.Kosyakov. *J. Phys. Chem. B*, **111**, 11214 (2007)
196. R.G.Grim, P.B.Kerkar, M.Shebowich, M.Arias, E.D.Sloan, C.A.Koh, A.K.Sum. *J. Phys. Chem. C*, **116**, 18557 (2012)
197. A.S.Stoporev, A.P.Semenov, V.I.Medvedev, R.I.Mendgaziev, V.A.Istomin, D.V.Sergeeva, A.Y.Manakov, V.A.Vinokurov. *J. Petrol. Sci. Eng.*, **176**, 952 (2019)
198. V.Koryakina, I.Ivanova, M.Semenov, I.Rozhin, A.Fedorova, E.Y.Shits. *Russ. J. Appl. Chem.*, **90**, 1258 (2017)
199. Y.Hu, B.R.Lee, A.K.Sum. *AIChE J.*, **64**, 2240 (2018)
200. Y.Hu, J.-H.Sa, B.R.Lee, A.K.Sum. *AIChE J.*, **64**, 4097 (2018)
201. Y.Hu, B.R.Lee, A.K.Sum. *AIChE J.*, **63**, 5111 (2017)
202. R.Burgass, A.Chapoy, X.Li. *J. Chem. Thermodyn.*, **118**, 193 (2018)
203. Y.Hu, K.-H.Lee, B.R.Lee, A.K.Sum. *J. Ind. Eng. Chem.*, **50**, 142 (2017)
204. Y.Hu, T.Y.Makogon, P.Karanjkar, K.-H.Lee, B.R.Lee, A.K.Sum. *J. Chem. Eng. Data*, **62**, 1910 (2017)
205. Y.Hu, T.Y.Makogon, P.Karanjkar, K.-H.Lee, B.R.Lee, A.K.Sum. *J. Chem. Thermodyn.*, **117**, 27 (2018)
206. D.Z.Huang, S.S.Fan, D.Q.Liang, Z.P.Feng. *Chin. J. Geophys., Chin. Ed.*, **48**, 1125 (2005)
207. M.Tariq, D.Rooney, E.Othman, S.Aparicio, M.Atilhan, M.Khraisheh. *Ind. Eng. Chem. Res.*, **53**, 17855 (2014)
208. V.Munoz-Iglesias, M.Choukroun, T.H.Vu, R.Hodyss, A.Mahjoub, W.D.Smythe, C.Sotin. *ACS Earth Space Chem.*, **2**, 135 (2018)
209. J.H.van-der-Waals, J.C.Platteeuw. In *Advances in Chemical Physics*. Vol. 2. (Ed. I.Prigogine). (NewYork: Interscience, 1959). P. 1
210. W.R.Parrish, J.M.Prausnitz. *Ind. Eng. Chem. Proc. Des. Dev.*, **11**, 26 (1972)
211. J.B.Klauda, S.I.Sandler. *Chem. Eng. Sci.*, **58**, 27 (2003)
212. E.D.Sloan, C.A.Koh, A.K.Sum, A.L.Ballard, G.J.Shoup, N.McMullen, J.L.Creek, T.Palermo. *J. Petrol. Technol., Soc. Petrol. Eng.*, **61**, SPE118534JPT (2009)
213. D.Kim, H.Lee. *Korean J. Chem. Eng.*, **33**, 1977 (2016)
214. L.Borchardt, M.E.Casco, J.Silvestre-Albero. *ChemPhysChem*, **19**, 1298 (2018)
215. H.K.Christenson. *J. Phys.: Condens. Matter*, **13**, R95 (2001)
216. V.G.Smirnov, A.Y.Manakov, V.V.Dyrdin, Z.R.Ismagilov, E.S.Mikhailova, T.V.Rodionova, G.V.Villevald, V.Y.Malysheva. *Fuel*, **228**, 123 (2018)
217. V.G.Smirnov, A.Y.Manakov, E.A.Ukraintseva, G.V.Villevald, T.D.Karpova, V.V.Dyrdin, S.Y.Lyrshchikov, Z.R.Ismagilov, I.S.Terekhova, A.G.Ogienko. *Fuel*, **166**, 188 (2016)
218. M.E.Casco, E.Zhang, S.Gratz, S.Krause, V.Bon, D.Wallacher, N.Grimm, D.M.Tobbens, T.Hauss, L.Borchardt. *J. Phys. Chem. C*, **123**, 24071 (2019)
219. E.M.Chuvilin, V.A.Istomin, S.S.Safonov. *Cold Reg. Sci. Technol.*, **68**, 68 (2011)
220. V.Istomin, E.Chuvilin, B.Bukhanov, T.Uchida. *Cold Reg. Sci. Technol.*, **137**, 60 (2017)
221. Y.Em, A.Stoporev, A.Semenov, A.Glotov, E.Smirnova, G.Villevald, V.Vinokurov, A.Manakov, Y.Lvov. *ACS Sust. Chem. Eng.*, **8**, 7860 (2020)
222. V.M.Buleiko, B.A.Grigoriev, V.A.Istomin. *Fluid Phase Equilib.*, **441**, 64 (2017)
223. S.Guggenheim, A.F.K.van Groos. *Geology*, **31**, 653 (2003)
224. D.Kim, Y.-H.Ahn, S.-J.Kim, J.Y.Lee, J.Lee, Y.-J.Seo, H.Lee. *J. Phys. Chem. C*, **119**, 22148 (2015)
225. K.F.Yan, X.S.Li, Z.Y.Chen, Y.Zhang, C.G.Xu, Z.M.Xia. *Chin. J. Chem. Eng*, **27**, 1212 (2019)
226. Y.P Handa. *J. Chem. Thermodyn.*, **18**, 915 (1986)
227. Y.P.Handa. *J. Chem. Thermodyn.*, **17**, 201 (1985)
228. Y.P.Handa, O.Yamamuro, M.Oguni, H.Suga. *J. Chem. Thermodyn.*, **21**, 1249 (1989)
229. S.P.Kang, H.Lee, B.J.Ryu. *J. Chem. Thermodyn.*, **33**, 513 (2001)
230. J.Zhao, S.Sun, C.Liu, Q.Meng. *Heat Mass Transfer*, **54**, 3287 (2018)
231. V.M.Buleiko, B.A.Grigoriev, J.Mendoza. *Fluid Phase Equilib.*, **462**, 14 (2018)
232. H.D.B.Jenkins. *J. Chem. Thermodyn.*, **117**, 236 (2018)
233. H.D.B.Jenkins. *J. Chem. Thermodyn.*, **117**, 242 (2018)
234. B.Wang, Z.Fan, P.Lv, J.Zhao, Y.Song. *Int. J. Heat Mass Transfer*, **110**, 142 (2017)

235. E.Chuvilin, B.Bukhanov, V.Cheverev, R.Motenko, E.Grechishcheva. In *Impact of Thermal Conductivity on Energy Technologies*. (Ed. A.Shahzad). (London: IntechOpen, 2018). P. 115
236. S.Sun, J.Zhao, J.Zhao, Y.Hao, J.Yang. *J. Chem. Thermodyn.*, **132**, 423 (2019)
237. E.Chuvilin, B.Bukhanov. *Energy Fuels*, **31**, 5246 (2017)
238. P.Andersson, R.G.Ross. *J. Phys. C: Solid State Phys.*, **16**, 1423 (1983)
239. N.J.English, J.S.Tse. *Energies*, **3**, 1934 (2010)
240. N.J.English, J.S.Tse. *Phys. Rev. Lett.*, **103**, 015901 (2009)
241. N.J.English, J.S.Tse, D.J.Carey. *Phys. Rev. B*, **80**, 134306 (2009)
242. F.Ning, Y.Yu, S.Kjelstrup, T.J.H.Vlugt, K.Glavatskiy. *Energy Environ. Sci.*, **5**, 6779 (2012)
243. J.F.Gabitto, C.Tsouris. *J. Thermodyn.*, 1 (2010)
244. J.W.Jung, J.C.Santamarina. *Geochem. Geophys. Geosyst.*, **12**, Q08003 (2011)
245. J.Yang, A.Hassanpouryouzband, B.Tohidi, E.Chuvilin, B.Bukhanov, V.Istomin, A.Cheremisin. *J. Geophys. Res.: Solid Earth*, **124**, 2551 (2019)
246. E.Chuvilin, B.Bukhanov, S.Grebenkin, V.Doroshin, A.Iospa. *Cold Reg. Sci. Technol.*, **153**, 101 (2018)
247. P.Wu, Y.Li, W.Liu, Y.Liu, D.Wang, Y.Song. *J. Geophys. Res.: Solid Earth*, **125**, e2019JB019103 (2020)
248. Z.M.Aman, E.P.Brown, E.D.Sloan, A.K.Sum, C.A.Koh. *Phys. Chem. Chem. Phys.*, **13**, 19796 (2011)
249. Z.M.Aman, W.J.Leith, G.A.Grasso, E.D.Sloan, A.K.Sum, C.A.Koh. *Langmuir*, **29**, 15551 (2013)
250. E.Brown, M.N.Khan, D.Salmin, J.Wells, S.Wang, C.J.Peters, C.A.Koh. *J. Nat. Gas Sci. Eng.*, **35**, 1435 (2016)
251. S.Hu, C.A.Koh. *Langmuir*, **33**, 11299 (2017)
252. Z.M.Aman, E.D.Sloan, A.K.Sum, C.A.Koh. *Energy Fuels*, **26**, 5102 (2012)
253. B.R.Lee, C.A.Koh, A.K.Sum. *Ind. Eng. Chem. Res.*, **53**, 18189 (2014)
254. S.Wang, S.Hu, E.P.Brown, M.A.Nakatsuka, J.Zhao, M.Yang, Y.Song, C.A.Koh. *Phys. Chem. Chem. Phys.*, **19**, 13307 (2017)
255. C.W.Liu, M.Z.Li, C.T.Liu, K.L.Geng, Y.X.Li. *Energy Fuels*, **30**, 6240 (2016)
256. J.D.Smith, A.J.Meuler, H.L.Bralower, R.Venkatesan, S.Subramanian, R.E.Cohen, G.H.McKinley, K.K.Varanasi. *Phys. Chem. Chem. Phys.*, **14**, 6013(2012)
257. T.Uchida, D.Kishi, T.Shiga, M.Nagayama, K.Gohara. *J. Chem. Eng. Data*, **60**, 284 (2015)
258. T.Uchida, W.Shimada, T.Hondoh, S.Mae, N.I.Barkov. *Appl. Opt.*, **34**, 5746 (1995)
259. O.Bonnefoy, F.Gruy, J.M.Herri. *Mater. Chem. Phys.*, **89**, 336 (2005)
260. W.L.Du Frane, L.A.Stern, K.A.Weitemeyer, S.Constable, J.C.Pinkston, J.J.Roberts. *Geophys. Res. Lett.*, **38**, L09313 (2011)
261. U.Ranieri, M.M.Koza, W.F.Kuhs, S.Klotz, A.Falenty, P.Gillet, L.E.Bove. *Nat. Commun.*, **8**, 1076 (2017)
262. S.Subramanian, E.D.Sloan. *J. Phys. Chem. B*, **106**, 4348 (2002)
263. H.Ohno, M.Kida, T.Sakurai, Y.Iizuka, T.Hondoh, H.Narita, J.Nagao. *ChemPhysChem*, **11**, 3070 (2010)
264. G.Fuseya, S.Takeya, A.Hachikubo. *RSC Adv.*, **10**, 17473 (2020)
265. J.Qin, W.F.Kuhs. *AIChE J.*, **59**, 2155 (2013)
266. J.Qin, W.F.Kuhs. *J. Chem. Eng. Data*, **60**, 369 (2015)
267. E.Dartois, B.Schmitt, D.Deboffle, M.Bouzit. *Proceedings of the International Astronomical Union*. Vol. 5 (S263). (Cambridge, UK: Cambridge University Press, 2009). P. 33
268. E.Dartois, D.Deboffle, M.Bouzit. *Astron. Astrophys.*, **514**, A49 (2010)
269. E.Dartois, P.Duret, U.Marboeuf, B.Schmitt. *Icarus*, **220**, 427 (2012)
270. M.Yang, Z.R.Chong, J.Zheng, Y.Song, P.Linga. *Renew. Sust. Energy Rev.*, **74**, 1346 (2017)
271. M.Kida, A.Hori, H.Sakagami, S.Takeya, Y.Kamata, N.Takahashi, T.Ebinuma, H.Narita. *J. Phys. Chem. A*, **115**, 643 (2011)
272. M.Kida, H.Sakagami, N.Takahashi, A.Hachikubo, H.Shoji, Y.Kamata, T.Ebinuma, H.Narita, S.Takeya. *J. Jpn. Petrol. Inst.*, **50**, 132 (2007)
273. M.Kida, H.Sakagami, N.Takahashi, J.Nagao. *J. Phys. Chem. A*, **117**, 4108 (2013)
274. M.Kida, H.Sakagami, M.Watanabe, Y.Jin, N.Takahashi, J.Nagao. *Chem. Eng. Sci.*, **140**, 10 (2016)
275. J.W.Lee, H.L.Lu, I.L.Moudrakovski, C.I.Ratcliffe, R.Ohmura, S.Alavi, J.A.Ripmeester. *J. Phys. Chem. A*, **115**, 1650 (2011)
276. F.Rauh, B.Mizaikoff. *Anal. Bioanal. Chem.*, **402**, 163 (2012)
277. Y.Rojas, X.Lou. *Asia-Pacific J. Chem. Eng.*, **5**, 310 (2010)
278. J.Zhu, S.Du, X.Yu, J.Zhang, H.Xu, S.C.Vogel, T.C.Germann, J.S.Francisco, F.Izumi, K.Momma, Y.Kawamura, C.Jin, Y.Zhao. *Nat. Commun.*, **5**, 4128 (2014)
279. W.F.Kuhs, B.Chazallon, P.G.Radaelli, F.Pauer. *J. Inclusion Phenom. Mol. Recog. Chem.*, **29**, 65 (1997)
280. J.M.Schicks, J.A.Ripmeester. *Angew. Chem., Int. Ed.*, **43**, 3310 (2004)
281. R.Anderson, A.Chapoy, H.Haghighi, B.Tohidi. *J. Phys. Chem. C*, **113**, 12602 (2009)
282. A.A.Sizikov, A.Y.Manakov. *Fluid Phase Equilib.*, **371**, 75 (2014)
283. A.A.Sizikov, A.Y.Manakov, E.Y.Aladko. *Fluid Phase Equilib.*, **425**, 351 (2016)
284. Y.Lee, S.Lee, Y.K.Jin, Y.Seo. *Chem. Eng. J.*, **258**, 427 (2014)
285. Y.Lee, S.Lee, S.Park, Y.Kim, J.W.Lee, Y.Seo. *J. Phys. Chem. B*, **117**, 2449 (2013)
286. K.Yasuda, S.Takeya, M.Sakashita, H.Yamawaki, R.Ohmura. *Ind. Eng. Chem. Res.*, **48**, 9335 (2009)
287. K.Yasuda, S.Takeya, M.Sakashita, H.Yamawaki, R.Ohmura. *J. Phys. Chem. C*, **113**, 12598 (2009)
288. J.-W.Lee, S.-P.Kang. *J. Phys. Chem. B*, **116**, 332 (2012)
289. T.Makiya, T.Murakami, S.Takeya, A.K.Sum, S.Alavi, R.Ohmura. *Phys. Chem. Chem. Phys.*, **12**, 9927 (2010)
290. N.Fukushima, S.Shiratori, T.Makiya, T.Murakami, R.Ohmura. *J. Chem. Thermodyn.*, **115**, 114 (2017)
291. K.Shin, K.A.Udachin, I.L.Moudrakovski, D.M.Leek, S.Alavi, C.I.Ratcliffe, J.A.Ripmeester. *Proc. Natl. Acad. Sci. USA*, **110**, 8437 (2013)
292. K.Udachin, S.Alavi, J.A.Ripmeester. *J. Chem. Phys.*, **134**, 121104 (2011)
293. E.Kim, Y.K. Jin, Y.Seo. *Fluid Phase Equilib.*, **393**, 85 (2015)
294. E.Kim, S.Lee, J.D.Lee, Y.Seo. *Fuel*, **164**, 237 (2016)
295. P.S.R.Prasad, T.Sugahara, E.D.Sloan, A.K.Sum, C.A.Koh. *J. Phys. Chem. A*, **113**, 11311 (2009)
296. Y.Youn, M.Cha, H.Lee. *Fluid Phase Equilib.*, **413**, 123 (2016)
297. Y.Youn, J.Seol, M.Cha, Y.H.Ahn, H.Lee. *J. Chem. Eng. Data*, **59**, 2004 (2014)
298. W.Shin, S.Park, J.-W.Lee, Y.Seo, D.-Y.Koh, J.Seol, H.Lee. *J. Phys. Chem. C*, **116**, 16352 (2012)
299. D.D.Chashchin, A.Y.Manakov, A.S.Yunoshev. *Struct. Chem.*, **31**, 1113 (2020)
300. Z.Maslakci, J.P.Devlin, N.Uras-Aytemiz. *J. Chem. Phys.*, **146**, 234508 (2017)
301. K.Shin, R.Kumar, K.A.Udachin, S.Alavi, J.A.Ripmeester. *Proc. Natl. Acad. Sci. USA*, **109**, 14785 (2012)
302. M.Kilic, J.P.Devlin, N.Uras-Aytemiz. *J. Chem. Phys.*, **148**, 234501 (2018)
303. H.Kang, Y.H.Ahn, D.Y.Koh, H.Lee. *Korean J. Chem. Eng.*, **33**, 1897 (2016)
304. Y.H.Ahn, Y.Youn, M.Cha, H.Lee. *RSC Adv.*, **7**, 12359 (2017)
305. K.Shishido, S.Muromachi, R.Nakamura, S.Takeya, R.Ohmura. *New J. Chem.*, **38**, 3160 (2014)

306. S.Muromachi, T.Nakajima, R.Ohmura, Y.H.Mori. *Fluid Phase Equilib.*, **305**, 145 (2011)
307. S.Muromachi, R.Ohmura, Y.H.Mori. *J. Chem. Thermodyn.*, **49**, 1 (2012)
308. S.Muromachi, R.Ohmura, S.Takeya, Y.H.Mori. *J. Phys. Chem. B*, **114**, 11430 (2010)
309. T.Nakajima, S.Akatsu, R.Ohmura, S.Takeya, Y.H.Mori. *Angew. Chem., Int. Ed.*, **50**, 10340 (2011)
310. T.Nakajima, T.Kudo, R.Ohmura, S.Takeya, Y.H.Mori. *PLOS One*, **7**, e48563 (2012)
311. E.Kim, Y.Seo. *Chem. Eng. J.*, **359**, 775 (2019)
312. W.Shin, S.Park, D.Y.Koh, J.Seol, H.Ro, H.Lee. *J. Phys. Chem. C*, **115**, 18885 (2011)
313. A.Desmedt, L.Martin-Gondre, T.T.Nguyen, C.Petuya, L.Barandiaran, O.Babot, T.Toupance, R.G.Grim, A.K.Sum. *J. Phys. Chem. C*, **119**, 8904 (2015)
314. N.Uras-Aytemiz, F.M.Balci, Z.Maslakci, H.Ozsoy, J.P.Devlin. *J. Phys. Chem. A*, **119**, 9018 (2015)
315. D.Lim, S.Park, H.Ro, K.Shin, H.Lee. *J. Phys. Chem. C*, **119**, 10218 (2015)
316. Y.Youn, M.Cha, H.Lee. *ChemPhysChem*, **16**, 2876 (2015)
317. Y.H.Ahn, S.Baek, J.Min, M.Cha, J.W.Lee. *ChemPhysChem*, **20**, 429 (2019)
318. A.Tani, S.Koyama, Y.Urabe, K.Takato, T.Sugahara, K.Ohgaki. *J. Phys. Chem. B*, **118**, 13409 (2014)
319. N.Kobayashi, T.Minami, A.Tani, M.Nakagoshi, T.Sugahara, K.Takeya, K.Ohgaki. *Energies*, **5**, 1705 (2012)
320. T.Sugahara, Y.Kobayashi, A.Tani, T.Inoue, K.Ohgaki. *J. Phys. Chem. A*, **116**, 2405 (2012)
321. Y.H.Ahn, H.Kang, M.Cha, K.Shin, H.Lee. *ACS Omega*, **2**, 1601 (2017)
322. M.Mozafari, L.Chandrasena, I.McKenzie, K.Samedov, P.W.Percival. *Can. J. Chem.*, **96**, 217 (2018)
323. P.W.Percival, M.Mozafari, J.C.Brodovitch, L.Chandrasena. *J. Phys. Chem. A*, **118**, 1162 (2014)
324. M.Mozafari, L.Chandrasena, I.McKenzie, K.Samedov, P.W.Percival. *Radiat. Phys. Chem.*, **168**, 7 (2020)
325. O.Nashed, B.Partoon, B.Lal, K.M.Sabil, A.M.Shariff. *J. Nat. Gas Sci. Eng.*, **55**, 452 (2018)
326. S.Abedi-Farizhendi, M.Rahmati-Abkenar, M.Manteghian, J.S.Yekshaveh, V.Zahmatkeshan. *J. Petrol. Sci. Eng.*, **172**, 636 (2019)
327. H.Pahlavanzadeh, M.Khanlarkhani, S.Rezaei, A.H.Mohammadi. *Fuel*, **253**, 1392 (2019)
328. E.Rezaei, M.Manteghian, M.Tamaddondar. *J. Petrol. Sci. Eng.*, **147**, 857 (2016)
329. A.McElligott, H.Uddin, J.L.Meunier, P.Servio. *Energy Fuels*, **33**, 11705 (2019)
330. F.Wang, H.-L.Meng, G.Guo, S.-J.Luo, R.-B.Guo. *ACS Sust. Chem. Eng.*, **5**, 6597 (2017)
331. S.J.Cox, D.J.F.Taylor, T.G.A.Youngs, A.K.Soper, T.S.Totton, R.G.Chapman, M.Arjmandi, M.G.Hodges, N.T.Skipper, A.Mich. *J. Am. Chem. Soc.*, **140**, 3277 (2018)
332. R.Wang, T.L.Liu, F.L.Ning, W.J.Ou, L.Zhang, Z.Wang, L.Peng, J.X.Sun, Z.C.Liu, T.S.Li, H.C.Sun, G.S.Jiang. *J. Energy Chem.*, **30**, 90 (2019)
333. R.Wang, H.Sun, X.Xu, J.Zhang, J.Wang, Z.Yang, Z.Zhang, X.Lai, T.Liu, G.Jiang. *Energy Sources, Part A*, **40**, 2257 (2018)
334. A.N.Nesterov, A.M.Reshetnikov, A.Y.Manakov, T.V.Rodionova, E.A. Paukshtis, I.P.Asanov, S.P.Bardakhanov, A.I.Bulavchenko. *J. Mol. Liq.*, **204**, 118 (2015)
335. H.J.Li, L.G.Wang. *Fuel*, **140**, 440 (2015)
336. H.J.Li, P.Stanwix, Z.Aman, M.Johns, E.May, L.G.Wang. *J. Phys. Chem. A*, **120**, 417 (2016)
337. N.N.Nguyen, A.V.Nguyen, K.M.Steel, L.X.Dang, M.Galib. *J. Phys. Chem. C*, **121**, 3830 (2017)
338. Y.He, F.Wang. *J. Mater. Chem. A*, **6**, 22619 (2018)
339. Y.-M.Song, F.Wang, G.Guo, S.-J.Luo, R.-B.Guo. *Appl. Energy*, **224**, 175 (2018)
340. B.S.Kiran, P.S.R.Prasad. *ACS Omega*, **3**, 18984 (2018)
341. P.Hu, D.Chen, M.Zi, G.Wu. *Fuel*, **230**, 126 (2018)
342. R.L.Li, D.P.Liu, L.Yang, G.M.Cui, J.Wang, X.Wang, Z.Z.Liu. *Fuel*, **252**, 574 (2019)
343. S.Fan, L.Yang, X.Lang, Y.Wang, D.Xie. *Chem. Eng. Sci.*, **82**, 185 (2012)
344. P.Babu, R.Kumar, P.Linga. *Environmen. Sci. Technol.*, **47**, 13191 (2013)
345. H.Kumano, T.Asaoka, K.Sugaya, Y.Mochizuki, M.Okada. *Int. J. Air-Condit. Refrigerat.*, **23**, 1550030 (2015)
346. B.O.Carter, W.X.Wang, D.J.Adams, A.I.Cooper. *Langmuir*, **26**, 3186 (2010)
347. F.Farhang, A.V.Nguyen, K.B.Sewell. *Energy Fuels*, **28**, 7025 (2014)
348. J.Park, K.Shin, J.Kim, H.Lee, Y.Seo, N.Maeda, W.Tian, C.D.Wood. *J. Phys. Chem. C*, **119**, 1690 (2015)
349. J.Wang, R.Wang, R.-H.Yoon, Y.Seol. *J. Chem. Eng. Data*, **60**, 383 (2015)
350. B.-H.Shi, L.Yang, S.-S.Fan, X.Lou. *Fuel*, **194**, 395 (2017)
351. L.Yang, G.M.Cui, D.P.Liu, S.S.Fan, Y.M.Xie, J.Chen. *Chem. Eng. Sci.*, **146**, 10 (2016)
352. B.H.Shi, S.S.Fan, X.Lou. *Chem. Eng. Sci.*, **109**, 315 (2014)
353. A.Ding, L.Yang, S.Fan, X.Lou. *Chem. Eng. Sci.*, **96**, 124 (2013)
354. L.Yang, X.Lan, D.P.Liu, G.M.Cui, B.L.Dou, J.Wang. *Chem. Eng. J.*, **374**, 802 (2019)
355. A.Drachuk, V.P.Melnikov, N.S.Molokitina, A.N.Nesterov, L.S.Podenko, A.M.Reshetnikov, A.Y.Manakov. *J. Energy Chem.*, **24**, 309 (2015)
356. L.S.Podenko, A.O.Drachuk, N.S.Molokitina, A.N.Nesterov. *Russ. J. Phys. Chem. A*, **92**, 255 (2018)
357. C.Lo, J.S.Zhang, A.Couzis, P.Somasundaran, J.W.Lee. *J. Phys. Chem. C*, **114**, 13385 (2010)
358. O.Salako, C.Lo, A.Couzis, P.Somasundaran, J.W.Lee. *J. Colloid Interface Sci.*, **412**, 1 (2013)
359. Y.Luzinova, G.T.Dobbs, Y.Raichlin, A.Katzir, B.Mizaikoff. *Chem. Eng. Sci.*, **66**, 5497 (2011)
360. A.Kumar, G.Bhattacharjee, B.D.Kulkarni, R.Kumar. *Ind. Eng. Chem. Res.*, **54**, 12217 (2015)
361. Y.He, M.T.Sun, C.Chen, G.D.Zhang, K.Chao, Y.Lin, F.Wang. *J. Mater. Chem. A*, **7**, 21634 (2019)
362. J.Chen, T.Wang, Z.Zeng, J.H.Jiang, B.Deng, C.Z.Chen, J.Y.Li, C.H.Li, L.M.Tao, X.Li, S.X.Xiao. *Chem. Eng. J.*, **363**, 349 (2019)
363. A.Farhadian, M.A.Varfolomeev, Z.Abdelhay, D.Emelianov, A.Delaunay, D.Dalmazzone. *Ind. Eng. Chem. Res.*, **58**, 7752 (2019)
364. M.S.Kamal, I.A.Hussein, A.S.Sultan, N.von Solms. *Renew. Sust. Energy Rev.*, **60**, 206 (2016)
365. W.Ke, D.Y.Chen. *Chin. J. Chem. Eng.*, **27**, 2049 (2019)
366. M.A.Kelland. *Energy Fuels*, **32**, 12001 (2018)
367. R.N.Shakhmaev, A.Sh.Sunagatullina, V.V.Zorin. *Neftegazovoe Delo*, **15**, 147 (2016)
368. S.Shahnazar, S.Bagheri, A.Termeh Yousefi, J.Mehrmashhadi, M.S. Abd Karim, N.A. Kadri. *Rev. Inorg. Chem.*, **38**, 1 (2018)
369. C.P.Tang, D.Q.Liang. *Chin. J. Chem. Eng*, **27**, 2107 (2019)
370. S.Yaqub, B.Lal, B.Partoon, N.B.Mellon. *Fluid Phase Equilib.*, **477**, 40 (2018)
371. A.Y.Zhukov, M.A.Stolov, M.A.Varfolomeev. *Chem. Technol. Fuels Oil*, **53**, 377 (2017)
372. C.B.Bavoh, B.Lal, H.Osei, K.M.Sabil, H.Mukhtar. *J. Nat. Gas Sci. Eng.*, **64**, 52 (2019)
373. A.Farhadian, M.A.Varfolomeev, A.Shaabani, S.Nasiri, I.Vakhitov, Y.F.Zaripova, V.V.Yarkovoi, A.V.Sukhov. *Carbohydr. Polym.*, **236**, 116035 (2020)
374. M.Kelland. *Production Chemicals for the Oil and Gas Industry*. (2nd Edn.). (Boca Raton, FL, 2014)
375. M.Sun, A.Firoozabadi. *Fuel*, **146**, 1 (2015)

376. A.C.Gulbrandsen, T.M.Svartaas. *Energy Fuels*, **31**, 8505 (2017)
377. A.C.Gulbrandsen, T.M.Svartas. *Energy Fuels*, **31**, 9863 (2017)
378. H.Sharifi, J.Ripmeester, P.Englezos. *J. Nat. Gas Sci. Eng.*, **35**, 1573 (2016)
379. N.Daraboina, J.Ripmeester, V.K.Walker, P.Englezos. *Energy Fuels*, **25**, 4392 (2011)
380. N.Daraboina, J.Ripmeester, V.K.Walker, P.Englezos. *Energy Fuels*, **25**, 4398 (2011)
381. N.Daraboina, P.Linga, J.Ripmeester, V.K.Walker, P.Englezos. *Energy Fuels*, **25**, 4384 (2011)
382. H.Sharifi, P.Englezos. *J. Chem. Eng. Data*, **60**, 336 (2015)
383. I.Townson, V.K.Walker, J.A.Ripmeester, P.Englezos. *Energy Fuels*, **26**, 7170 (2012)
384. P.C.Chua, M.A.Kelland. *Energy Fuels*, **32**, 1674 (2018)
385. S.K.Nagappayya, R.M.Lucente-Schultz, V.M.Nace, V.M.Ho. *J. Chem. Eng. Data*, **60**, 351 (2015)
386. A.Farhadian, M.A.Varfolomeev, A.Kudbanov, S.R.Gallyamova. *Chem. Eng. Sci.*, **206**, 507 (2019)
387. H.Kim, Y.H.Ahn, Y.Seo, C.D.Wood. *Fuel*, **257**, 12 (2019)
388. W.Lee, Y.Choi, Y.Kim, J.S.Lim, S.P.Kang. *J. Petrol. Sci. Eng.*, **183**, 9 (2019)
389. T.Hondoh, H.Anzai, A.Goto, S.Mae, A.Higashi, C.C.Langway. *J. Inclusion Phenom. Mol. Recog. Chem.*, **8**, 17 (1990)
390. C.Y.Sun, B.Z.Peng, A.Dandekar, Q.L.Ma, G.J.Chen. *Annu. Rep. Prog. Chem., Sect. C*, **106**, 77 (2010)
391. T.P.Adamova, A.Y.Manakov, A.S.Stoporev. *Russ. J. Appl. Chem.*, **92**, 607 (2019)
392. N.S.Molokitina, A.N.Nesterov, L.S.Podenko, A.M.Reshetnikov. *Fuel*, **235**, 1400 (2019)
393. S.R.Davies, E.D.Sloan, A.K.Sum, C.A.Koh. *J. Phys. Chem. C*, **114**, 1173 (2010)
394. S.L.Li, C.Y.Sun, B.Liu, Z.Y.Li, G.J.Chen, A.K.Sum. *Sci. Rep.*, **4**, 4129 (2014)
395. K.Saito, M.Kishimoto, R.Tanaka, R.Ohmura. *Cryst. Growth Des.*, **11**, 295 (2011)
396. R.Tanaka, R.Sakemoto, R.Ohmura. *Cryst Growth Des.*, **9**, 2529 (2009)
397. S.L.Li, C.Y.Sun, B.Liu, X.J.Feng, F.G.Li, L.T.Chen, G.J.Chen. *AIChE J.*, **59**, 2145 (2013)
398. C.J.Taylor, K.T.Miller, C.A.Koh, E.D.Sloan. *Chem. Eng. Sci.*, **62**, 6524 (2007)
399. A.S.Stoporev, T.P.Adamova, A.Y.Manakov. *Cryst. Growth Des.*, **20**, 1927 (2020)
400. K.Imasato, H.Tokutomi, R.Ohmura. *Cryst. Growth Des.* , **15**, 428 (2015)
401. T.P.Adamova, A.S.Stoporev, A.Y.Manakov. *Cryst. Growth Des.*, **18**, 6713 (2018)
402. S.A.Morrissy, A.J.McKenzie, B.F.Graham, M.L.Johns, E.F.May, Z.M.Aman. *Energy Fuels*, **31**, 5798 (2017)
403. B.Z.Peng, A.Dandekar, C.Y.Suin, H.Luo, Q.L.Ma, W.X.Pang, G.J.Chen. *J. Phys. Chem. B*, **111**, 12485 (2007)
404. S.L.Li, Y.F.Wang, C.Y.Sun, G.J.Chen, B.Liu, Z.Y.Li, Q.L.Ma. *Chem. Eng. Sci.*, **135**, 412 (2015)
405. V.A.Vlasov. *Heat Mass Trans.*, **55**, 3537 (2019)
406. T.Mochizuki, Y.H.Mori. *Chem. Eng. Sci.*, **171**, 61 (2017)
407. M.Aifaa, T.Kodama, R.Ohmura. *Cryst. Growth Des.*, **15**, 559 (2015)
408. S.Watanabe, K.Saito, R.Ohmura. *Cryst. Growth Des.*, **11**, 3235 (2011)
409. A.Touil, D.Broseta, A.Desmedt. *Langmuir*, **35**, 12569 (2019)
410. A.S.Stoporev, A.P.Semenov, V.I.Medvedev, A.A.Sizikov, P.A.Gushchin, V.A.Vinokurov, A.Y.Manakov. *J. Cryst. Growth*, **485**, 54 (2018)
411. P.U.Karanjkar, J.W.Lee, J.F.Morris. *Cryst. Growth Des.*, **12**, 3817 (2012)
412. H.Hayama, M.Mitarai, H.Mori, J.Verrett, P.Servio, R.Ohmura. *Cryst. Growth Des.*, **16**, 6084 (2016)
413. H.Bruusgaard, L.D.Lessard, P.Servio. *Cryst. Growth Des.*, **9**, 3014(2009)
414. M.Mitarai, M.Kishimoto, D.Suh, R.Ohmura. *Cryst. Growth Des.*, **15**, 812 (2015)
415. F.Wang, L.Wang, C.Wang, G.Guo, G.Liu, S.Luo, R.Guo. *Cryst. Growth Des.*, **15**, 5112 (2015)
416. S.Esmail, J.G.Beltran. *J. Nat. Gas Sci. Eng.*, **35**, 1535 (2016)
417. K.Jeong, P.J.Metaxas, J.Chan, T.O.Kuteyi, Z.M.Aman, P.L.Stanwix, M.L.Johns, E.F.May. *Phys. Chem. Chem. Phys.*, **21**, 21685 (2019)
418. Yu.F.Makogon, J.S.Holsti. *Ros. Khim. Zh.*, **47** (3), 43 (2003)
419. N.N.Nguyen, M.Galib, A.V.Nguyen. *Energy Fuels*, **34**, 6751 (2020)
420. A.Hassanpouryouzband, E.Joonaki, M.V.Farahani, S.Takeya, C.Ruppel, J.Yang, N.J.English, J.M.Schicks, K.Edlmann, H.Mehrabian. *Chem. Soc. Rev.*, **49**, 5225 (2020)
421. M.Khurana, Z.Yin, P.Linga. *ACS Sust. Chem. Eng.*, **5**, 11176 (2017)
422. W.Ke, T.M.Svartaas, D.Y.Chen. *J. Nat. Gas Sci. Eng.*, **61**, 169 (2019)
423. Y.F.Bi, A.Porras, T.S.Li. *J. Chem. Phys.*, **145**, 211909 (2016)
424. R.Kumar, P.Linga, I.Moudrakovski, J.A.Ripmeester, P.Englezos. *AIChE J.*, **54**, 2132 (2008)
425. M.E.Semenov, A.Y.Manakov, E.Y.Shitz, A.S.Stoporev, L.K.Altunina, L.A.Strelets, S.Y.Misyura, V.E.Nakoryakov. *J. Therm. Anal. Calorim.*, **119**, 757 (2015)
426. D.Clausse, E.Wardhono, J.-L.Lanoiselle. *Colloids Surf. A*, **460**, 519 (2014)
427. A.S.Stoporev, L.I.Svarovskaya, L.A.Strelets, L.K.Altunina, G.V.Villevald, T.D.Karpova, T.V.Rodionova, A.Y.Manakov. *Chin. J. Chem. Eng.*, **27**, 668 (2019)
428. Y.F.Makogon, I.Melikhov, E.Kozlovskaya, V.Bozhevol'nov. *Russ. J. Phys. Chem. A*, **81**, 1645 (2007)
429. A.S.Stoporev, A.P.Semenov, V.I.Medvedev, B.I.Kidyarov, A.Y.Manakov, V.A.Vinokurov. *J. Therm. Anal. Calorim.*, **134**, 783 (2018)
430. A.H.Nguyen, V.Molinero. *J. Chem. Phys.*, **140**, 084506 (2014)
431. J.M.Schicks, M.Luzi-Helbing. *J. Chem. Eng. Data*, **60**, 269 (2015)
432. T.Dong, J.-F.Lin, J.T.Gu, P.J.Polito, J.O'Connell, P.B.Flemings. *Am. Geophys. Union Fall Meeting*, OS53B (2017)
433. A.S.Stoporev, A.G.Ogienko, A.A.Sizikov, A.P.Semenov, D.S.Kopitsyn, V.A.Vinokurov, L.I.Svarovskaya, L.K.Altunina, A.Y.Manakov. *J. Nat. Gas Sci. Eng.*, **60**, 284 (2018)
434. S.Ovalle, C.Martinez, L.Bonilla, A.Lara, J.G.Beltran. *Can. J. Chem. Eng.*, **97**, 2818 (2019)
435. M.Aminnaji, R.Anderson, B.Tohidi. *J. Petrol. Sci. Eng.*, **178**, 1044 (2019)
436. D.E.S.de Menezes, A.K.Sum, A.Desmedt, P.D.Pessoa, M.D.R.Fuentes. *Chem. Eng. Sci.*, **208**, 11 (2019)
437. A.K.Sum, C.A.Koh, E.D.Sloan. *Energy Fuels*, **26**, 4046 (2012)
438. C.L.Bassani, A.K.Sum, J.-M.Herri, R.E.Morales, A.Cameirão. *Ind. Eng. Chem. Res.*, **59**, 2123 (2020)
439. C.L.Bassani, A.M.Melchuna, A.Cameirao, J.M.Herri, R.E.M.Morales, A.K.Sum. *Ind. Eng. Chem. Res.,* **58**, 14446 (2019)
440. Y.H.Sun, S.H.Jiang, S.L.Li, G.B.Zhang, W.Guo. *Chin. J. Chem. Eng*, **27**, 2164 (2019)
441. I.N.Tsimpanogiannis, J.Costandy, P.Kastanidis, S.El Meragawi, V.K.Michalis, N.I.Papadimitriou, S.N.Karozis, N.I.Diamantonis, O.A.Moultos, G.E.Romanos, A.K.Stubos, I.G.Economou. *Mol. Phys.*, **116**, 2041 (2018)
442. B.C.Knott, V.Molinero, M.F.Doherty, B.Peters. *J. Am. Chem. Soc.*, **134**, 19544 (2012)
443. W.Zhang, J.L.Creek, C.A.Koh. *Meas. Sci. Technol.*, **12**, 1620 (2001)

444. R.S.DeFever, S.Sarupria. *J. Chem. Phys.*, **147**, 204503 (2017)
445. D.Kashchiev, A.Firoozabadi. *J. Cryst. Growth*, **243**, 476 (2002)
446. E.F.May, V.W.Lim, P.J.Metaxas, J.Du, P.L.Stanwix, D.Rowland, M.L.Johns, G.Haandrikman, D.Crosby, Z.M.Aman. *Langmuir*, **34**, 3186 (2018)
447. P.J.Metaxas, V.W.S.Lim, C.Booth, J.Zhen, P.L.Stanwix, M.L.Johns, Z.M.Aman, G.Haandrikman, D.Crosby, E.F.May. *Fuel*, **252**, 448 (2019)
448. V.W.S.Lim, P.J.Metaxas, M.L.Johns, G.Haandrikman, D.Crosby, Z.M.Aman, E.F.Maya. *Chem. Eng. J.*, **388**, 124177 (2020)
449. V.A.Shestakov, V.I.Kosyakov, A.Y.Manakov, A.S.Stoporev, E.V.Grachev. *Russ. J. Phys. Chem. A*, **92**, 1293 (2018)
450. G.A.Mali, A.Chapoy, B.Tohidi. *J. Chem. Thermodyn.*, **117**, 91 (2018)
451. K.Erstad, S.Hoiland, P.Fotland, T.Bartw. *Energy Fuels*, **23**, 2213 (2009)
452. D.X.Zhang, Q.Y.Huang, H.M.Zheng, W.Wang, X.W.Cheng, R.B.Li, W.D.Li. *Energy Fuels*, **33**, 5081 (2019)
453. W.Lee, J.Min, Y.-H.Ahn, S.Baek, C.A.Koh, J.W.Lee. *Ind. Eng. Chem. Res.*, **58**, 5064 (2019)
454. M.Zi, D.Chen, H.Ji, G.Wu. *Energy Fuels*, **30**, 5643 (2016)
455. G.A.B.Sandoval, R.L.Thompson, C.M.S.Sad, A.Teixeira, E.J.Soares. *Energy Fuels*, **33**, 7138 (2019)
456. E.O.Straume, R.E.M.Morales, A.K.Sum. In *Proceedings of the 8th International Conference on Gas Hydrates (ICGH8-2014)*. (Beijing, China, 2014). Art. T5-56
457. A.A.A.Majid, D.T.Wu, C.A.Koh. *Engineering*, **4**, 321 (2018)
458. Y.Qin, P.F.Pickering, M.L.Johns, E.F.May, Z.M.Aman. *Energy Fuels*, **34**, 7955 (2020)
459. L.Ding, B.H.Shi, Y.Liu, S.F.Song, W.Wang, H.H.Wu, J.Gong. *Fuel*, **239**, 126 (2019)
460. J.-H.Sa, X.Zhang, A.K.Sum. *Fuel*, **269**, 117440 (2020)
461. S.Wang, S.Fan, X.Lang, Y.Wang, P.Wang. *Fuel*, **259**, 116201 (2020)
462. C.Liu, C.Zhang, C.Zhou, Y.Mi, Z.Wang. *Energy Fuels*, **34**, 4525 (2020)
463. P.M.Naullage, A.A.Bertolazzo, V.Molinero. *ACS Centr. Sci.*, **5**, 428 (2019)
464. W.Fu, Z.Wang, J.Zhang, Y.Cao, B.Sun. *J. Petrol. Sci. Eng.*, **184**, 106504 (2020)
465. A.Sinquin, I.Palermo, Y.Peysson. *Oil Gas Sci. Technol. Rev. Inst. Franc. Petrol.*, **59**, 41 (2004)
466. B.-H.Shi, S.Chai, L.-Y.Wang, X.Lv, H.-S.Liu, H.-H.Wu, W.Wang, D.Yu, J.Gong. *Fuel*, **185**, 323 (2016)
467. X.-D.Shen, G.-D.Hou, J.-X.Ding, X.-B.Zhou, C.-P.Tang, Y.He, J.-S.Lu, D.-Q.Liang. *J. Nat. Gas Sci. Eng.*, **55**, 64 (2018)
468. J.-H.Sa, A.Melchuna, X.Zhang, R.Morales, A.Cameirao, J.-M.Herri, A.K.Sum. *Ind. Eng. Chem. Res.*, **58**, 8544 (2019)
469. X.Zhang, A.Melchuna, J.-H.Sa, A.K.Sum. *J. Nat. Gas Sci. Eng.*, **79**, 103340 (2020)
470. A.Melchuna, X.Zhang, J.-H.Sa, E.Abadie, P.Glénat, A.K.Sum. *Energy Fuels*, **34**, 9371 (2020)
471. Y.Wang, C.A.Koh, J.White, Z.Patel, L.E.Zerpa. *Fuel*, **252**, 458 (2019)
472. E.P.Brown, D.Turner, G.Grasso, C.A.Koh. *Fuel*, **264**, 116573 (2020)
473. S.Hu, C.A.Koh. *Fuel*, **269**, 117208 (2020)
474. E.B.Webb, P.J.Rensing, C.A.Koh, E.D.Sloan, A.K.Sum, M.W.Liberatore. *Rev. Sci. Instrum.*, **83**, 015106 (2012)
475. E.B.Webb, C.A.Koh, M.W.Liberatore. *Langmuir*, **29**, 10997 (2013)
476. E.B.Webb, C.A.Koh, M.W.Liberatore. *Ind. Eng. Chem. Res.*, **53**, 6998 (2014)
477. Y.Qin, Z.M.Aman, P.F.Pickering, M.L.Johns, E.F.May. *J. Non-Newton. Fluid Mech.*, **248**, 40 (2017)
478. A.A.A.Majid, D.T.Wu, C.A.Koh. *Langmuir*, **33**, 11436 (2017)
479. Y.Lv, Y.Guan, S.Guo, Q.Ma, J.Gong, G.Chen, C.Sun, K.Guo, L.Yang, B.Shi, W.Qin, Y.Qiao. *Energies*, **10**, 1105 (2017)
480. Y.Chen, B.Shi, Y.Liu, Q.Ma, S.Song, L.Ding, X.Lv, H.Wu, W.Wang, H.Yao. *Energy Fuels*, **33**, 2915 (2019)
481. L.Ding, B.Shi, X.Lv, Y.Liu, H.Wu, W.Wang, J.Gong. *Chem. Eng. Sci.*, **146**, 199 (2016)
482. X.Zhang, E.O.Straume, G.A.Grasso, R.E.Morales, A.K.Sum. *Fuel*, **262**, 116558 (2020)
483. C.Ruan, L.Ding, B.Shi, Q.Huang, J.Gong. *RSC Adv.*, **7**, 48127 (2017)
484. J.P.Longo, J.R.Galvão, T.Antes, E.N.dos Santos, J.C.da Silva, C.Martelli, A.K.Sum, R.E.Morales, M.J.da Silva. *IEEE Sens. J.*, **20**, 5012 (2020)
485. H.D.Nagashima, T.Miyagi, K.Yasuda, R.Ohmura. *Fluid Phase Equilib.,* **517**, 112610 (2020)
486. H.P.Veluswamy, A.Kumar, Y.Seo, J.D.Lee, P.Linga. *Appl. Energy*, **216**, 262 (2018)
487. X.Zhao, Z.Qiu, C.Zhao, J.Xu, Y.Zhang. *Chem. Eng. Sci.*, **199**, 113 (2019)
488. H.Sharifi, A.Yoneyama, S.Takeya, J.Ripmeester, P.Englezos. *J. Phys. Chem. C*, **122**, 17019 (2018)
489. P.Naeiji, T.K.Woo, S.Alavi, J.A.Ripmeester. *J. Phys. Chem. C*, **123**, 28715 (2019)
490. V.A.Istomin. *Russ. J. Phys. Chem.*, **73**, 188(1999)
491. A.Falenty, W.F.Kuhs. *J. Phys. Chem. B*, **113**, 15975 (2009)
492. V.S.Yakushev, V.A.Istomin. *Geokhimiya*, (6), 899 (1990)
493. E.D.Yershov, Y.P.Lebedenko, Y.M.Chuvilin, V.A.Istomin, V.S.Yakushev. *Dokl. Akad. Nauk*, **321**, 788 (1991)
494. A.H.Nguyen, M.A.Koc, T.D.Shepherd, V.Molinero. *J. Phys. Chem. C*, **119**, 4104 (2015)
495. N.N.Nguyen, R.D.Berger, H.-J.Butt. *ACS Appl. Mater. Interfaces*, **12**, 14599 (2020)
496. A.S.Stoporev, A.A.Sizikov, T.V.Cheshkova, A.O.Loskutova, A.A.Grinko, E.A.Yarkova, A.P.Semenov, A.Y.Manakov, V.A.Vinokurov. *Energy Fuels*, **32**, 11279 (2018)
497. S.Takeya, H.Fujihisa, Y.Gotoh, V.Istomin, E.Chuvilin, H.Sakagami, A.Hachikubo. *J. Phys. Chem. C*, **117**, 7081 (2013)
498. S.Takeya, H.Mimachi, T.Murayama. *Appl. Energy*, **230**, 86 (2018)
499. H.Sato, H.Sakamoto, S.Ogino, H.Mimachi, T.Kinoshita, T.Iwasaki, K.Sano, K.Ohgaki. *Chem. Eng. Sci.*, **91**, 86 (2013)
500. Y.-N.Lv, M.-L.Jia, J.Chen, C.-Y.Sun, J.Gong, G.-J.Chen, B.Liu, N.Ren, S.-D.Guo, Q.-P.Li. *Energy Fuels*, **29**, 5563 (2015)
501. G.Song, Y.Li, W.Wang, K.Jiang, Z.Shi, X.Ye, P.Zhao. *J. Nat. Gas Sci. Eng.*, **45**, 26 (2017)
502. A.A.Sizikov, V.A.Vlasov, A.S.Stoporev, A.Y.Manakov. *Energy Fuels*, **33**, 12353 (2019)
503. A.S.Stoporev, T.V.Cheshkova, A.P.Semenov, A.Y.Manakov, V.A.Vinokurov. *Mendeleev Commun.*, **28**, 533 (2018)
504. A.S.Stoporev, A.Y.Manakov, L.K.Altunina, A.V.Bogoslovsky, L.A.Strelets, E.Y.Aladko. *Energy Fuels*, **28**, 794 (2014)
505. A.S.Stoporev, A.Y.Manakov, L.K.Altunina, L.A.Strelets. *Energy Fuels*, **30**, 9014 (2016)
506. S.I.Dolgaev, V.G.Kvon, V.I.Istomin, Yu.A.Gerasimov, A.A.Troinikova. *Nauchno-tekhnicheskii Sbornik — Vesti Gazovoi Nauki*, **33**, 100 (2018)
507. V.S.Yakushev, V.G.Kvon, S.I.Dolgaev, V.I.Istomon. *Analiz Konkurentnykh Preimushchestv Gidratnykh Tekhnologii v Gazovoi Promyshlennosti*. (Moscow: Gazprom VNIIGAZ, 2010)
508. H.J.Kang, Y.Yang, M.S.Ki, M.S.Shin, J.Choi, J.-H.Cha, D.Lee. *Ocean Eng.*, **113**, 162 (2016)
509. Y.C.Chien, D.Dunn-Rankin. *Energies*, **12**, 1939 (2019)
510. S.Y.Misyura. *Energy*, **181**, 589 (2019)
511. S.Y.Misyura, V.E Nakoryakov. *Energy Fuels*, **27**, 7089 (2013)

512. H.Shirota, S.Ota. In *Proceedings of the 7th International Conference on Gas Hydrates (ICGH 2011)*. (Edinburgh, Scotland, UK, 2011). Art. 539
513. S.Tanaka, S.Hanasaki. In *Proceedings of the 8th International Conference on Gas Hydrates (ICGH8-2014)*. (Beijing, China, 2014). Art. T3-73
514. T.Takaoki, T.Iwasaki, Y.Katoh, T.Arai, K.Horiguchi. In *Proceedings of the 4th International Conference on Gas Hydrates*. (Yokohama, Japan, 2002). P. 982
515. G.Rehder, R.Eckl, M.Elfgen, A.Falenty, R.Hamann, N.Kaehler, W.F.Kuhs, H.Osterkamp, C.Windmeier. *Energies*, **5**, 2499 (2012)
516. H.-K.Kang, Y.-T.Kim, K.-P.Kim, D.-H.Kim, T.-B.Ha. In *Proceedings of the 8th International Conference on Gas Hydrates (ICGH8-2014)*. (Beijing, China, 2014). Art. T4-4
517. K.Kim, D.Kim, T.Ha, H.Kang, Y.Kim. In *Proceedings of the 8th International Conference on Gas Hydrates (ICGH8-2014)*. (Beijing, China, 2014). Art. T3-22
518. S.Ota, H.Shirota, T.Nakata, S.Yuasa. In *Proceedings of the 7th International Conference on Gas Hydrates (ICGH 2011)*. (Edinburgh, Scotland, UK, 2011). Art. 63
519. S.Watanabe, S.Takahashi, H.Mizubayashi, S.Murata, H.Murakami. In *Proceedings of the 6th International Conference on Gas Hydrates*. (Vancouver, Canada, 2008). Art. 5442
520. K.Horiguchi, S.Watanabe, H.Moriya, S.Nakai, A.Yoshimitsu, A.Taoda. In *Proceedings of the 7th International Conference on Gas Hydrates (ICGH 2011)*. (Edinburgh, Scotland, UK, 2011). Art. 371
521. V.S.Yakushev. *Nauka i Tekhnika v Gazovoi Promyshlennosti*, **21**, 10 (2005)
522. V.S.Yakushev, V.G.Kvon, S.I.Dolgaev, S.E.Podenok, V.I.istomin. *Gazovaya Promyshlennost.' (Spetsvypusk 'Gazofikatsiya i Gazoraspredelenie'*), S(**640**), 75 (2009)
523. S.Y.Obara, Y.Kikuchi, K.Ishikawa, M.Kawai, Y.Kashiwaya. *Energy*, **74**, 810 (2014)
524. A.Hassanpouryouzband, J.Yang, B.Tohidi, E.Chuvilin, V.Istomin, B.Bukhanov. *ACS Sust. Chem. Eng.*, **7**, 5338 (2019)
525. S.Y.Misyura, I.G.Donskoy. *J. CO_2 Util.*, **34**, 313 (2019)
526. J.Zhao, X.Guo, M.Sun, Y.Zhao, L.Yang, Y.Song. *Chem. Eng. J.*, **361**, 12 (2019)
527. T.Shibata, H.Yamachi, R.Ohmura, Y.H.Mori. *Int. J. Hydrogen Energy*, **37**, 7612 (2012)
528. Patent US 6774276 (2004)
529. Patent US 20090124520 (2009)
530. R.Azarinezhad, A.Chapoy, R.Anderson, B.Tohidi. In *Proceedings of the 6th International Conference on Gas Hydrates*. (Vancouver, Canada, 2008). Art. 5322
531. E.O.Straume, R.E.M.Morales, A.K.Sum. *Energy Fuels*, **33**, 1 (2019)
532. P.Warrier, M.N.Khan, M.A.Carreon, C.J.Peters, C.A.Koh. *J. Renew. Sust. Energy*, **10**, 034701 (2018)
533. V.M.Vorotyntsev, V.M.Malyshev, I.V.Vorotyntsev. *Gazovye Gidraty v Protsessakh Razdeleniya Gazovykh Smesei*. (N.Novgorod: R.E.Alekseev Nizhegorodskii State University, 2014)
534. C.G.Xu, Y.S.Yu, W.J.Xie, Z.M.Xia, Z.Y.Chen, X.S.Li. *Appl. Energy*, **255**, 12 (2019)
535. V.M.Vorotyntsev, V.M.Malyshev, I.V.Vorotyntsev. *Petrol. Chem.*, **54**, 491 (2014)
536. M.Sergeeva, A.Petukhov, I.Vorotyntsev, V.Malyshev, V.Vorotyntsev. *Petrol. Sci. Technol.*, **37**, 86 (2019)
537. M.S.Sergeeva, A.N.Petukhov, D.N.Shablykin, V.M.Malyshev, V.M.Vorotyntsev. *Russ. J. Phys. Chem. A*, **93**, 2297 (2019)
538. P.Di Profio, V.Canale, N.D'Alessandro, R.Germani, A.Di Crescenzo, A.Fontana. *ACS Sust. Chem. Eng.*, **5**, 1990 (2017)
539. Y.Kamata, H.Oyama, W.Shimada, T.Ebinuma, S.Takeya, T.Uchida, J.Nagao, H.Narita. *Jpn. J. Appl. Phys., P. 1*, **43**, 362 (2004)
540. F.Ahmadloo, G.Mali, A.Chapoy, B.Tohid. In *Proceedings of the 6th International Conference on Gas Hydrates (ICGH 2008)*. (Vancouver, Canada, 2008); https://www.pet.hw.ac.uk/research/hydrate/abstracts/ab158.cfm.html (last access 10.01.2021)
541. H.Hashimoto, T.Yamaguchi, H.Ozeki, S.Muromachi. *Sci. Rep.*, **7**, 1 (2017)
542. Q.Sun, X.Guo, A.Liu, B.Liu, Y.Huo, G.Chen. *Ind. Eng. Chem. Res.*, **50**, 2284 (2011)
543. J.-R.Zhong, L.-T.Chen, T.-C.Liu, X.-Y.Zeng, Y.-F.Sun, C.-Y.Sun, B.Liu, G.-J.Chen, J.A.Ripmeester. *J. Phys. Chem. C*, **121**, 27822 (2017)
544. Patent US 5434330A (1995)
545. H.Liu, L.Mu, B.Liu, X.Zhang, J.Wang, B.Wang, C.Sun, L.Yang, H.Wang, P.Xiao, G.Chen. *Ind. Eng. Chem. Res.*, **52**, 2707 (2013)
546. Z.W.Ma, P.Zhang, H.S.Bao, S.Deng. *Renew. Sust. Energy Rev.*, **53**, 1273 (2016)
547. Q.Sun, Y.T.Kang. *Renew. Sust. Energy Rev.*, **62**, 478 (2016)
548. A.Eslamimanesh, A.H.Mohammadi, D.Richon, P.Naidoo, D.Ramjugernath. *J. Chem. Thermodyn.*, **46**, 62 (2012)
549. M.Yang, H.Zhou, P.Wang, Y.Song. *Appl. Energy*, **221**, 374 (2018)
550. Patent US 9550144 (2014)
551. Patent WO 2018118623 (2018)
552. Patent US 20180178161 (2018)
553. C.K.Ahn, G.H.Kim, J.E.Lee, K.S.Kim, K.Kim. *Sep. Purif. Technol.*, **217**, 221 (2019)
554. K.Kim, K.S.Kim, J.E.Lee, S.Park, C.-K.Ahn, G.-H.Kim. *Sep. Purif. Technol.*, **200**, 29 (2018)
555. P.Babu, P.Linga, R.Kumar, P.Englezos. *Energy*, **85**, 261 (2015)
556. H.Dashti, L.Z.Yew, X.Lou. *J. Nat. Gas Sci. Eng.*, **23**, 195 (2015)
557. J.Liu, Y.Wei, W.Meng, P.-Z.Li, Y.Zhao, R.Zou. *Research*, 3206024 (2019)
558. Patent RU 2195994 (2003)
559. S.Jovic, J.T.F.Keurentjes, J.C.Schouten, J.van der Schaaf. *Chem. Eng. Res. Des.*, **115**, 423 (2016)
560. T.B.He, S.K.Nair, P.Babu, P.Linga, I.A.Karimi. *Appl. Energy*, **222**, 13 (2018)
561. Z.R.Chong, T.B.He, P.Babu, J.N.Zheng, P.Linga. *Desalination*, **463**, 69 (2019)
562. P.Babu, A.Nambiar, T.He, I.A.Karimi, J.D.Lee, P.Englezos, P.Linga. *ACS Sust. Chem. Eng.*, **6**, 8093 (2018)
563. J.N.Zheng, F.B.Cheng, Y.P.Li, X.Lu, M.J.Yang. *Chin. J. Chem. Eng.*, **27**, 2037 (2019)
564. X.Wang, M.Dennis, L.Hou. *Renew. Sust. Energy Rev.*, **36**, 34 (2014)
565. C.X.Cheng, F.Wang, Y.J.Tian, X.H.Wu, J.L.Zheng, J.Zhang, L.W.Li, P.L.Yang, J.F.Zhao. *Renew. Sust. Energy Rev.*, **117**, 109492 (2020)
566. T.Classen, P.Seidl, S.Loekman, B.Gatternig, C.Rauh, A.Delgado. *Curr. Opin. Food Sci.*, **29**, 48 (2019)
567. V.S.Yakushev, V.G.Kvon, Yu.A.Gerasimov, V.A.Istomin. *Sovremennoe Sostoyanie Gazogidratnykh Tekhnologii. Obzornaya Informatsiya*. (The Current State of Gas Hydrate Technologies. Overview Information) (Moscow: OOO 'IRTs Gazprom', 2008)
568. J.Cai, C.-G.Xu, Z.-M.Xia, Z.-Y.Chen, X.-S.Li. *Appl. Energy*, **204**, 1526 (2017)
569. T.Shimizu, Y.Yamamoto, N.Tenma. *SPE J.*, **22**, 746 (2017)
570. Patent US 8043579B2 (2011)
571. Patent EP 1956071A1 (2008)
572. S.Douieb, L.Fradette, F.Bertrand, B.Haut. *AIChE J.*, **61**, 4387 (2015)

573. Patent EP 2196521A1 (2010)
574. Y.H.Mori. *Chem. Eng. Res. Des.*, **117**, 715 (2017)
575. Y.H.Mori. *Energies*, **8**, 1317 (2015)
576. D.L.Yang, L.A.A.Le, R.J.Martinez, R.P.Currier, D.F.Spencer. *Chem. Eng. J.*, **172**, 144 (2011)
577. J.Du, H.Li, L.Wang. *Fuel*, **230**, 134 (2018)
578. Patent US 8354565 (20013)
579. T.D.Brown, C.E.Taylor, M.P.Bernardo. *Energies*, **3**, 1154 (2010)
580. S.Fujita, K.Watanabe, Y.H.Mori. *AIChE J.*, **55**, 1056 (2009)
581. J.Waycuilis, H.Sirajuddin, P.Rensing. In *Proceedings of the 7th International Conference on Gas Hydrates (ICGH 2011)*. (Edinburgh, Scotland, UK, 2011). Art. 652
582. A.Kumar, D.Khatri, J.D.Lee, R.Kumar. *Korean J. Chem. Eng.*, **33**, 1922 (2016)
583. P.Linga, M.A.Clarke. *Energy Fuels*, **31**, 1 (2017)
584. X.W.Liu, L.Q.Tian, D.Y.Chen, G.Z.Wu. *Fuel*, **257**, 9 (2019)
585. F.Filarsky, C.Schmuck, H.J.Schultz. *Ind. Eng. Chem. Res.*, **58**, 16687 (2019)
586. J.Bai, D.Q.Liang, D.L.Li, S.S.Fan, J.W.Du, X.X.Dai, Z.Long. *Energy Fuels*, **24**, 1207 (2010)
587. Patent RU 2293907C2 (2004)
588. Patent US 20070203374 (2007)
589. V.E.Nakoryakov, V.E.Dontsov, A.A.Chernov. *Dokl. Phys.*, **51**, 621 (2006)
590. Patent US 20060272805 (2006)
591. A.A.Chernov, A.A.Pil'nik, D.S.Elistratov, I.V.Mezentsev, A.V.Meleshkin, M.V.Bartashevich, M.G.Vlasenko. *Sci. Rep.*, **7**, 40809 (2017)
592. Patent CA 2140549 (1994)
593. A.V.Meleshkin, M.V.Bartashevich, V.V.Glezer. *Appl. Surface Sci.*, **493**, 84(2019)
594. P.Xiao, X.-M.Yang, C.-Y.Sun, J.-L.Cui, N.Li, G.-J.Chen. *Chem. Eng. J.*, **336**, 647 (2018)
595. M.Z.Faizullin, A.V.Vinogradov, V.P.Koverda. *Chem. Eng. Sci.*, **130**, 135 (2015)
596. M.Z.Faizullin, A.V.Vinogradov, A.S.Tomin, V.P.Koverda. *Int. J. Heat Mass Transfer*, **143**, 7 (2019)
597. H.Nakayama, D.D.Klug, C.I.Ratcliffe, J.A.Ripmeester. *Chem. – Eur. J.*, **9**, 2969 (2003)
598. R.Netsu, T.Ikeda-Fukazawa. *Chem. Phys. Lett.*, **716**, 22 (2019)
599. C.Mitterdorfer, M.Bauer, T.Loerting. *Phys. Chem. Chem. Phys.*, **13**, 19765 (2011)
600. J.Ghosh, R.G.Bhuin, G.Ragupathy, T.Pradeep. *J. Phys. Chem. C*, **123**, 16300 (2019)
601. J.Ghosh, R.R.J.Methikkalam, R.G.Bhuin, G.Ragupathy, N.Choudhary, R.Kumar, T.Pradeep. *Proc. Natl. Acad. Sci. USA*, **116**, 1526 (2019)
602. Y. Wang, K. Glazyrin, V. Roizen, A.R. Oganov, I.Chernyshov, X.Zhang, E.Greenberg, V.B.Prakapenka, X.Yang, S.-q.Jiang. *Phys. Rev. Lett.*, **125**, 255702 (2020)
603. A.S.Stoporev, A.G.Kiiamov, M.A.Varfolomeev, T.V.Rodionova, A.Y.Manakov. *Mendeleev Commun.*, **31**, 17 (2021)
604. R.Ma, H.Zhong, L.Li, J.Zhong, Y.Yan, J.Zhang, J.Liu. *J. Phys. Chem. C*, **124**, 2664 (2020)
605. V.Shestakov, A.Sagidullin, A.Stoporev, E.Grachev, A.Y.Manakov. *J. Mol. Liq.*, **318**, 114018 (2020)
606. F.Asadi, P.J.Metaxas, V.W.Lim, T.A.Nguyen, Z.M.Aman, E.F.May, A.V.Nguyen. *Chem. Eng. J.*, 127932 (2020); https://doi.org/10.1016/j.cej.2020.127932
607. Q.Zhang, L.Limmer, H.Frey, M.A.Kelland. *Energy Fuels* (2021); https://doi.org/10.1021/acs.energyfuels.0c04333
608. S.Hu, L.Vo, D.Monteiro, S.Bodnar, P.Prince, C.A.Koh. *Langmuir* (2021); https://doi.org/10.1021/acs.langmuir.0c02503
609. G.Bhattacharjee, M.N.Goh, S.E.Arumuganainar, Y.Zhang, P.Linga. *Energy Environ. Sci.*, **13**, 4946 (2020)
610. L.S.Podenko, A.O.Drachuk, N.S.Molokitina, A.N.Nesterov. *J. Nat. Gas Sci. Eng.*, **88**, 103811 (2021); https://doi.org/10.1016/j.jngse.2021.103811
611. Y.Zeng, J.Chen, X.Yu, T.Wang, B.Deng, F.Zeng, J.Li. *Fuel*, **277**, 118222 (2020)
612. M.S.Sergeeva, N.A.Mokhnachev, D.N.Shablykin, A.V.Vorotyntsev, D.M.Zarubin, A.A.Atlaskin, M.M.Trubyanov, I.V.Vorotyntsev, V.M.Vorotyntsev, A.N.Petukhov. *J. Nat. Gas Sci. Eng.*, **86**, 103740 (2021)
613. Y.Wang, X.Lang, S.Fan, S.Wang, C.Yu, G.Li. *Energy Fuels* (2021); https://doi.org/10.1021/acs.energyfuels.0c04138
614. Y.Xie, T.Zheng, J.-R.Zhong, Y.-J.Zhu, Y.-F.Wang, Y.Zhang, R.Li, Q.Yuan, C.-Y.Sun, G.-J.Chen. *Appl. Energy*, **268**, 115008 (2020)
615. Y.Xie, Y.-J.Zhu, T.Zheng, Q.Yuan, C.-Y.Sun, L.-Y.Yang, G.-J.Chen. *Chem. Eng. J.*, **403**, 126283 (2021)
616. M.A.Kelland, Q.Zhang, E.G.Dirdal, M.F.Mady. *Energy Fuels*; https://doi.org/10.1021/acs.energyfuels.0c03519
617. M.Park, Y.Sohn, H.Kim, K.-H.Park, M.Ryu, Y.Seo. *Energy Fuels* (2021); https://doi.org/10.1021/acs.energyfuels.0c04159
618. Y.Wang, S.Subramanian, D.Estanga, A.A.Majid, S.Hu, D.C.Salmin, C.A.Koh, L.E.Zerpa. *Energy Fuels*, **34**, 13523 (2020)